Die approbierte gedruckte Originalversion dieser Diplomarbeit ist an der TU Wien Bibliothek verfügbar
The approved original version of this thesis is available in print at TU Wien Bibliothek.

Diploma thesis

Flexible Tiling

Custom fabrication method for double curved active textiles

Submitted in satisfaction of the requirements for the degree of
Diplom-Ingenieur / Diplom- Ingenieurin
at the TU Wien, Faculty of Architecture and Planning
von

Sebastian Baumfried
01609397

Supervisor: Senior Artist Dr.in techn. Efstathia Eleni Baseta
Co-Supervisor: Univ.Ass. Dott.mag. Marco Palma
Institute of Art and Design E264
Research Unit of Three-Dimensional Design and Model Making E264/2
Technische Universität Wien,
Karlsplatz 13, 1040 Wien, Österreich

Wien, am

Die approbierte gedruckte Originalversion dieser Diplomarbeit ist an der TU Wien Bibliothek verfügbar
The approved original version of this thesis is available in print at TU Wien Bibliothek.

Abstract

The fabrication of double curved geometries is a topic of interest across various fields and especially in architecture, with traditional methods often relying on molds and formwork, making the process resource intensive. Recent material-driven research into programmable matter and active materials— characterized for example by their ability to self-transform from 2D to 3D geometries—has aimed to address these challenges, but not yet achieved precise curvature control and scalability.

This thesis investigates a material-centered approach for fabricating double curved surfaces using "Active Textiles," a composite material system formed by 3D printing plastics on pre-stretched fabric. Upon tension release, the fabric transitions from a flat 2D state into a double curved 3D configuration.

Initially, this study focused on systematic material experiments to examine fabrication parameters such as pre-stretching patterns and 3D printed cross-section thickness on individual tiles. A custom-built digital fabrication setup was developed to ensure precision and repeatability in producing double curved tiles. These experiments uncovered key relationships between material properties, fabrication methods, and resulting tile geometries.

Building on the insights gained from the material experiments for individual tiles, the research explores the innovative approach of tiling these active textile components. It examines the interactions between individual tiles and their collective influence on the overall surface geometry. This enabled the fabrication of a larger digitally designed surface, demonstrating potential for scalability and enhanced curvature control.

By focusing on material-driven methods, this research highlights the potential of programmable materials in fabricating intricate double curved surfaces rapidly. Despite identified limitations in scalability and material rigidity, the findings pave the way for future advancements in active textile fabrication techniques and programmable matter applications.

Die approbierte gedruckte Originalversion dieser Diplomarbeit ist an der TU Wien Bibliothek verfügbar
The approved original version of this thesis is available in print at TU Wien Bibliothek.

Abstrakt

In verschiedenen Bereichen, insbesondere aber in der Architektur, ist die Herstellung von doppelt gekrümmten Flächen ein relevantes Thema. Traditionelle Methoden greifen dabei oft auf die Verwendung von Formen und Schalungen zurück, welche diesen Prozess ressourcenintensiv und zeitintensiv machen. Aktuelle materialbasierte Forschung zu “programmable matter” und “active materials”, die sich beispielsweise durch ihre Fähigkeit sich von einer 2D- in eine 3D-Form zu transformieren auszeichnen, zielt darauf ab, sich diesen Herausforderungen zu stellen. Jedoch wurde bislang keine präzise Steuerung der Flächenkrümmung oder Skalierbarkeit erreicht.

Diese Diplomarbeit untersucht einen materialzentrierten Ansatz zur Herstellung doppelt gekrümmter Flächen mithilfe von „Active Textiles“, einem Verbundmaterialsystem, das durch 3D Druck von Kunststoffen auf vorgedehntem Textil entsteht. Beim Lösen der Spannung wandelt sich der Stoff von einem flachen 2D Zustand in eine doppelt gekrümmte 3D Konfiguration.

Zu Beginn konzentrierte sich die Studie auf systematische Materialexperimente, um Fertigungsparameter wie Dehnungsmuster und die Dicke der 3D gedruckten Querschnitte auf einzelnen Flächen zu untersuchen. Eine eigens entwickelte digitale Fertigungsmethode wurde geschaffen, um Präzision und Wiederholbarkeit bei der Herstellung zu gewährleisten. Diese Experimente offenbarten zentrale Zusammenhänge zwischen Materialeigenschaften, Fertigungsmethoden und den resultierenden Geometrien der Teilflächen. Aufbauend auf den Erkenntnissen der Materialexperimente für einzelne Flächen erforscht die Arbeit den innovativen Ansatz, diese „active textile components“ zu einem Gesamt-Flächensystem zu kombinieren. Dabei werden die Wechselwirkungen zwischen den einzelnen Teilflächen und ihr kollektiver Einfluss auf die Geometrie der Gesamtfläche untersucht. Dies ermöglichte die Herstellung einer größeren, digital entworfenen Fläche und demonstrierte das Potenzial für Skalierbarkeit und verbesserte Krümmungssteuerung. Durch den Fokus auf materialgesteuerte Methoden unterstreicht diese Forschung das Potenzial von „programmable materials“ zur schnellen Herstellung komplexer doppelt gekrümmter Flächen. Trotz Einschränkungen hinsichtlich Skalierbarkeit und Materialsteifigkeit ebnen die Ergebnisse den Weg für zukünftige Fortschritte in der Fertigungstechnologie von „active textiles“ und in der Anwendung von „programmable matter“.

Die approbierte gedruckte Originalversion dieser Diplomarbeit ist an der TU Wien Bibliothek verfügbar
The approved original version of this thesis is available in print at TU Wien Bibliothek.

Acknowledgements

A sincere thank you to everyone who supported me throughout the process of this thesis. This accomplishment would not have been possible without the invaluable help and encouragement of all of you.

First, I am deeply grateful to Efilena Baseta for supervising this thesis. Her support, insightful suggestions, and guidance throughout this long journey were instrumental in keeping me on the right path whenever I needed direction.

A big special thank you also goes to Marco Palma for his enthusiasm from the very beginning, the technical expertise he generously shared, and the much-needed pep talks that helped me stay motivated.

To both of you, thank you for sparking my interest in digital fabrication and material research during the 2022 Module and for fostering that passion ever since.

Furthermore, a big thanks to the whole team of Kunst2 for their support, all the knowledge shared and their understanding when time was short. Especially thanks to the model-building workshop team for providing an exceptional workspace, welcoming me and my equipment, and accommodating my test pieces that occupied a table for so long. Your tips and tricks were immensely helpful.

Lastly, a special thank you to my wife, family, and friends for their ongoing support, encouragement, and help throughout this journey. This kept my motivation high and thanks for supporting every step and decision taken by me during all this time.

TU WIEN Bibliothek Your knowledge hub
Die approbierte gedruckte Originalversion dieser Diplomarbeit ist an der TU Wien Bibliothek verfügbar
The approved original version of this thesis is available in print at TU Wien Bibliothek.

Die approbierte gedruckte Originalversion dieser Diplomarbeit ist an der TU Wien Bibliothek verfügbar
The approved original version of this thesis is available in print at TU Wien Bibliothek.

Index

1. Introduction 9

2. Background 16
   2.1. Geometry analysis 17
   2.2. State of the art 23
      2.2.1. Fabrication of double curved surfaces 23
      2.2.2. Self-assembling systems – programmable matter 31
      2.2.3. Summary 43

3. Material system exploration 46
   3.1. Preliminary testing phase 47
   3.2. Custom-built fabrication set-up 50

4. Unit exploration 62
   4.1. Uniform fabrication parameters 67
   4.2. Non-uniform fabrication parameters 78
      4.2.1. Non-uniform stretching 78
      4.2.2. Non-uniform printing thickness 82
   4.3. Implementation of hinges 86

Die approbierte gedruckte Originalversion dieser Diplomarbeit ist an der TU Wien Bibliothek verfügbar
The approved original version of this thesis is available in print at TU Wien Bibliothek.

5. Tiling exploration 92

5.1. Single edge combination 94

5.2. Multiple edge combinations 103

5.2.1. Case study surface 3x3 106

5.2.2. Case study surface 4x4 110

5.2.3. Double layer 115

6. Design exploration 118

6.1. Digital design 119

6.2. Fabrication 125

6.2.1. Parameter assessment 125

6.2.2. Tile fabrication 130

6.3. Evaluation 137

7. Conclusion 142

Bibliography

References

Die approbierte gedruckte Originalversion dieser Diplomarbeit ist an der TU Wien Bibliothek verfügbar
The approved original version of this thesis is available in print at TU Wien Bibliothek.

1. Introduction

Across various domains, from fashion to architecture and spanning diverse scales of application, the design of double curved geometries is relevant. The fabrication of such intricate curved pieces and components often depends on complex molds and formworks, making the process expensive, time-intensive, and energy-demanding. In recent decades, researchers in a variety of fields, as well as architects and engineers have been exploring more efficient **material-centered** approaches for the design and fabrication of freeform surfaces, such as self-assembly and programmable materials. By harnessing the inherent properties of materials, these methods enable the generation of double curved geometries with greater efficiency and minimal reliance on molds and formworks. When applying this approach in a design, or when working with programmable materials in general, the progression of the design process can be shortly summarized with the following steps: starting with the material as the primary consideration, it is proceeded by investigating assembly methods, and through these two previous steps addressing the design itself with a corresponding feedback loop for adaptation at the end.[1]

Material > **Assembly** > **Design** <> **Adaptation**

> *"This alienation from materials has only been exacerbated in recent times by the rise of computing and the digital revolution. Digitalization and virtualization have tended to disconnect the average person from materiality and led us to believe that creating something "intelligent" means either a human being or a digital system with software/hardware that simulates human intelligence."*[2]

[1] (Lettner, Palma, & Baseta, 2024)
[2] (Tibbits, 2021)

Die approbierte gedruckte Originalversion dieser Diplomarbeit ist an der TU Wien Bibliothek verfügbar
The approved original version of this thesis is available in print at TU Wien Bibliothek.

The motivation for this research is based on this material-centered approach, investigating a defined material system and exploring the above mentioned "intelligence" in materials through the exploration and evaluation of active textiles, a composite material system produced through 3D printing geometries directly on a pre-stretched piece of fabric.

This method enables the self-transformation from a flat 2D state into a double curved 3D shape, activated through the released pre-stretch. Figure 1 illustrates this fabrication technique as it was first used in projects done by the Self-Assembly Lab at MIT. This method can be seen as the point of departure for the developed technique presented in this thesis.

Fabrication relies on the following three basic steps:

Stretch > **3D print** > **Release**

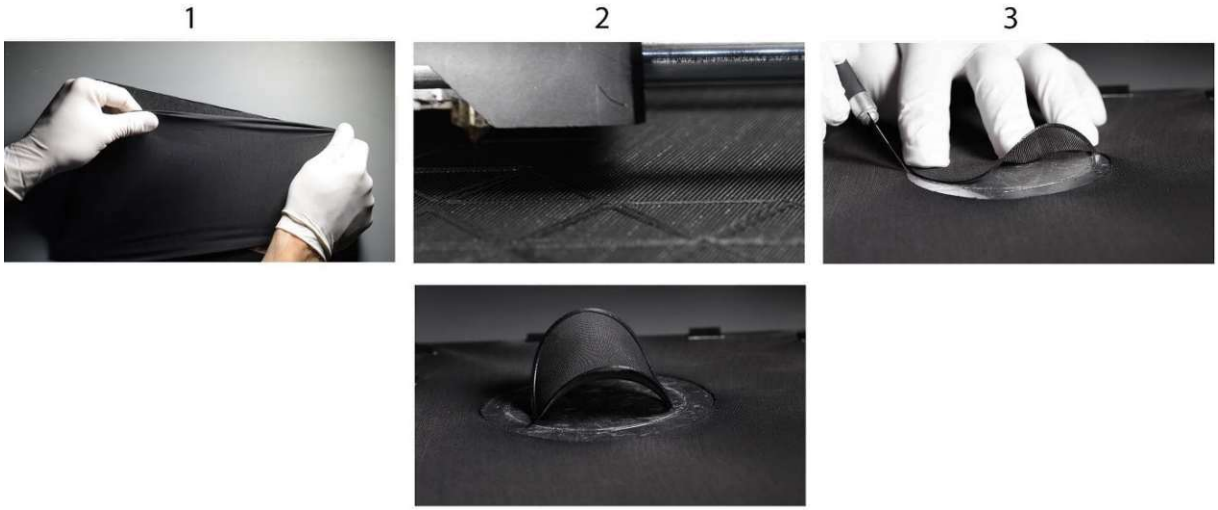

Figure 1: active textile fabrication procedure as developed by the Self-Assembly Lab at MIT (Self-Assembly Lab, n.d.)

Die approbierte gedruckte Originalversion dieser Diplomarbeit ist an der TU Wien Bibliothek verfügbar
The approved original version of this thesis is available in print at TU Wien Bibliothek.

The research discussed in this book builds upon the three fabrication steps developed by MIT and introduces a fourth operation, "Assemble." As shown in figure 2, this innovative approach leverages double curved active textile components as tiles to create surface systems. Using the chosen programmable material (active textiles), individual double curved tiles/units are fabricated and then tested in various configurations to construct larger double curved tiled surfaces. The redefined process consists of the following steps:

Stretch > **3D print** > **Release** >> **Assemble**

The underlying process of the project was a bottom-up approach focusing on a detailed investigation of individual units of the composite material system itself to generate data through various conducted experiments. Initially, this meant exploring the associated parameters, pre-stretch and 3D printed geometry, in the scale of individual tiles to establish control over the resulting curvature. The knowledge gained through this procedure was adapted in the process of fabricating case study surface systems with the produced active textile tiles. The information gathered was then reviewed by recreating an approximation of a desired, digitally designed double curved surface. The goal was not to digitally design surfaces, optimize and physically reproduce them faultlessly, but to use this design exploration to verify certain assumptions regarding scalability and curvature control made throughout the thesis.

Die approbierte gedruckte Originalversion dieser Diplomarbeit ist an der TU Wien Bibliothek verfügbar
The approved original version of this thesis is available in print at TU Wien Bibliothek.

Figure 2: diagram of the developed fabrication procedure

Die approbierte gedruckte Originalversion dieser Diplomarbeit ist an der TU Wien Bibliothek verfügbar
The approved original version of this thesis is available in print at TU Wien Bibliothek.

Why investigate "Active textile systems"?

> *"[...] designing a system so that the lowest-energy state is a very useful and interesting one."*[3]

Active textiles efficiently create intricate 3D geometries with an initial "flat" fabrication state. The chosen compound material has an easy and fast fabrication routine to rapidly produce iterations, which was crucial for the bottom-up approach taken. Additionally, the whole system aims at being lightweight and having some flexibility in it to reconfigure, adapt and find its own equilibrium.

The experiments necessary for the before mentioned approach were all achievable by developing a custom digital fabrication method, which was crucial in introducing control in the production of the desired double curved surfaces and to succeed with the intended procedure. Overall, this research tried to shift the focus from digital design tools without consideration of material properties, to physical explorations, material research and developing individual tools.

> *"We want to build active systems by embedding simple rules into materials, enabling them to transform themselves, interact with one another, and enhance their function, performance, or aesthetics."*[4]

[3] (Tibbits, 2021)
[4] (Tibbits, 2021)

Die approbierte gedruckte Originalversion dieser Diplomarbeit ist an der TU Wien Bibliothek verfügbar
The approved original version of this thesis is available in print at TU Wien Bibliothek.

The chapter **Background** gives a brief overview of common practice in fabricating double curved surfaces, introduces the concept of programmable matter and describes the specific sub-category, namely active textiles, which this research focused on.

Material system exploration illustrates initial testing done on active textiles and provides a detailed description of the material system. Additionally, the development of a custom-made fabrication set-up is highlighted in this chapter.

Under **Unit exploration** several sets of material experiments on individual tiles (units) are described. These tests isolated different fabrication parameters of active textile components and investigated their influence on the surface and edge geometry. The procedure used for evaluating the conducted experiments is detailed as well.

The chapter **Tiling exploration** shifts the focus from individual tiles to tiled surfaces and assesses methods used in creating double curved surface systems from individual active textile components through various combinations. It describes the translation of methods established for individual pieces to the global context of tiled surfaces.

Finally, **Design Exploration** examines the scalability of the proposed fabrication method and the gained curvature control over a larger area. The top-down process, aimed at reproducing a digitally designed surface through the combination of tiles, applied in the described experiment is evaluated.

Die approbierte gedruckte Originalversion dieser Diplomarbeit ist an der TU Wien Bibliothek verfügbar
The approved original version of this thesis is available in print at TU Wien Bibliothek.

Die approbierte gedruckte Originalversion dieser Diplomarbeit ist an der TU Wien Bibliothek verfügbar
The approved original version of this thesis is available in print at TU Wien Bibliothek.

2. Background

This chapter introduces some basic geometrical terms for the evaluation of the produced samples. It provides a condensed overview of different production methods used in the architectural context and other fields to create double curved surfaces. Finally, the underlying concepts of the explored material system, namely self-assembly, programmable matter and active textiles are presented.

Die approbierte gedruckte Originalversion dieser Diplomarbeit ist an der TU Wien Bibliothek verfügbar
The approved original version of this thesis is available in print at TU Wien Bibliothek.

2.1. Geometry analysis

To clarify what the fabrication of double curved surfaces is aimed at and to explain vocabulary used when evaluating the material experiments conducted in this thesis, basic geometrical terminology is introduced in this chapter. First the focus lies on curves used to later evaluate the edges of the tiles and for post-processing the point cloud meshes. Second, terminology for surface evaluation is introduced. The whole sub-chapter is built on the book "Architectural Geometry."

Curve tangents

A **tangent** to a curve is a straight line that touches the curve at a specific point, indicating its direction. To find it, a second point is chosen close to the first, forming a chord. As the second point approaches the first, the chord aligns with the tangent. Mathematically, the tangent's direction is given by the derivative c'(t)c'(t)c'(t), calculated as the limit of the difference between two points on the curve as their distance shrinks to zero.[5]

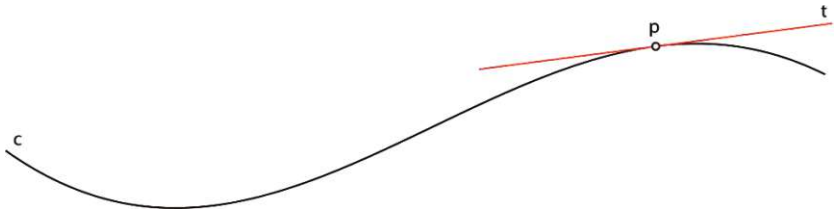

Figure 3: tangent (t) in point (p) on curve (c)

[5] (Pottmann, Asperl, Hofer, & Kilian, 2010)

Die approbierte gedruckte Originalversion dieser Diplomarbeit ist an der TU Wien Bibliothek verfügbar
The approved original version of this thesis is available in print at TU Wien Bibliothek.

Osculating plane and osculating circle

The osculating plane and osculating circle describe the geometry of curves beyond the tangent.

- **Osculating plane:** A curve can be approximated by a polygon with three points, which spans a plane. As the polygon's edges shorten, the plane aligns with the curve at a specific point, becoming the osculating plane. This plane, defined by the first and second derivatives of the curve, passes through the tangent at that point.[6]
- **Osculating circle:** The three points used to define the osculating plane also form a circle in that plane. As the points get closer together, the circle becomes the osculating circle, perfectly touching the curve at the point. The center of this circle is the curvature center, and the radius, known as the curvature radius, measures the sharpness of the curve. The curvature is the reciprocal of this radius, k=1/rk = 1/rk=1/r. [6]

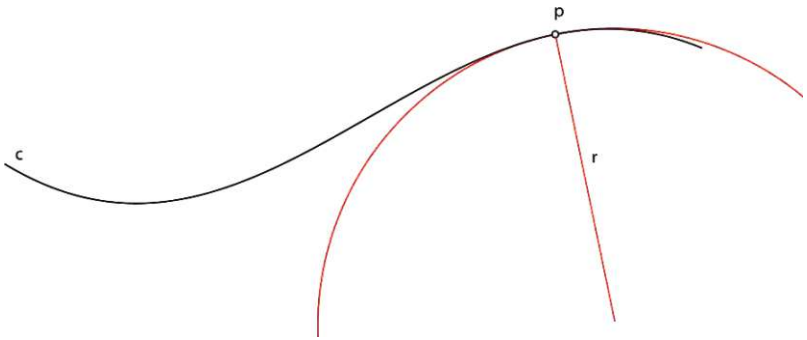

Figure 4: Osculating circle in point (p)on curve (c) with radius (r)

[6] (Pottmann, Asperl, Hofer, & Kilian, 2010)

Die approbierte gedruckte Originalversion dieser Diplomarbeit ist an der TU Wien Bibliothek verfügbar
The approved original version of this thesis is available in print at TU Wien Bibliothek.

Curvature calculation

Curvature k measures the rate of directional change of the tangent at a point. The properties of curves can be analyzed using **osculating circles** and **curvature**. Key points in curvature analysis include:

- **Vertices:** Points where the curvature reaches a local maximum or minimum. At these points, the osculating circle stays on one side of the curve, providing a precise local approximation.

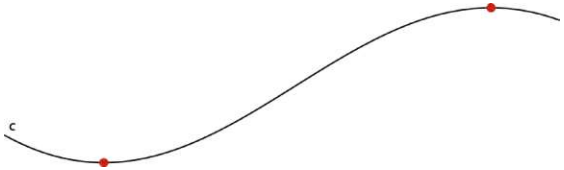

Figure 5: vertices of curve (c)

- **Inflection points:** Points where the curve changes sides relative to the tangent. Here, the osculating circle degenerates into a straight line, and the curvature is zero.

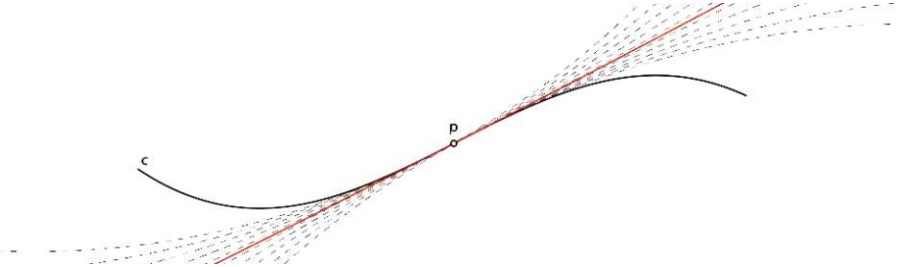

Figure 6: inflection point (p) of curve (c)

- **Flat points:** Points with zero curvature where the curve does not change sides relative to the tangent, and the tangent aligns more closely with the curve than at inflection points.[7]

[7] (Pottmann, Asperl, Hofer, & Kilian, 2010)

Die approbierte gedruckte Originalversion dieser Diplomarbeit ist an der TU Wien Bibliothek verfügbar
The approved original version of this thesis is available in print at TU Wien Bibliothek.

Nonuniform rational B-spline (NURBS)

Nonuniform rational B-spline (NURBS) curves offer even greater flexibility, with weights added to the control points, allowing for precise adjustments. NURBS curves can represent complex freeform shapes and all types of conic sections. The term "rational" in NURBS refers to their mathematical description, where weights are incorporated, expanding upon the polynomial nature of standard B-splines. A NURBS curve is essentially the central projection of a B-spline curve in a higher-dimensional space.[8]

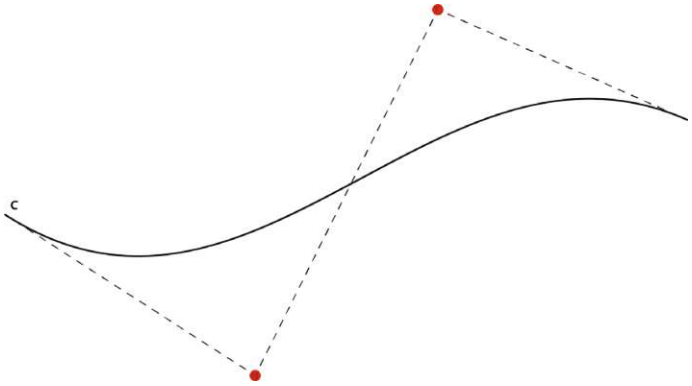

Figure 7: control points of curve (c) highlighted

NURBS surfaces

Bézier and B-spline surfaces are natural extensions of freeform curves. While Bézier surfaces inherit the same issues as Bézier curves—high degrees lead to poor shape representation and global control point changes—B-spline surfaces overcome these by offering more control over the surface through adjustable degrees for u- and v-curves. For even more control, NURBS surfaces add weights to each control point, allowing for finer adjustments, with weight changes affecting the surface similarly to NURBS curves.[8]

[8] (Pottmann, Asperl, Hofer, & Kilian, 2010)

Die approbierte gedruckte Originalversion dieser Diplomarbeit ist an der TU Wien Bibliothek verfügbar
The approved original version of this thesis is available in print at TU Wien Bibliothek.

Surface analysis

Curvature analysis starts by calculating the tangent to a curve using its first derivative, with curvature often visualized by the osculating circle. For surfaces, Gaussian curvature (the product of two principal curvatures, k1·k2) is key. Surfaces can be classified into regions based on curvature:

- **Elliptic points**: Positive Gaussian curvature (both curvatures share the same sign).
- **Hyperbolic points**: Negative Gaussian curvature (curvatures have opposite signs).
- **Parabolic/Flat points**: Zero Gaussian curvature (one curvature is zero).

Gaussian curvature ($K = k1 \cdot k2$) measures how a surface curves at a point, with examples such as the plane ($K=0$, all normals parallel) and sphere ($K=1/R^2$, positive curvature). It is defined through the Gaussian spherical mapping, which maps a surface point to a unit sphere using the outward normal vector. These curvature values reflect local area distortion and play a critical role in surface design and analysis. Typically, Gaussian curvature analysis is depicted as a color graded map ranging from red, reflecting positive curvature areas to blue, depicting negative curvature areas. [9]

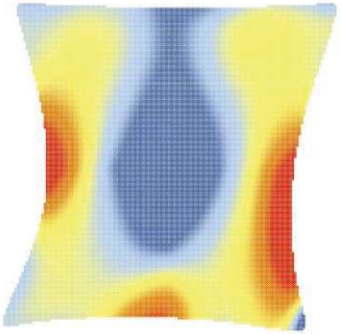

Figure 8: Gaussian curvature analysis illustrated as color graded map

[9] (Pottmann, Asperl, Hofer, & Kilian, 2010)

Die approbierte gedruckte Originalversion dieser Diplomarbeit ist an der TU Wien Bibliothek verfügbar
The approved original version of this thesis is available in print at TU Wien Bibliothek.

Developable surfaces

can be mapped onto a plane using an isometric mapping, which preserves distances, and must have zero Gaussian curvature (K=0). These single-curved surfaces, such as cylinders and cones, curve in only one direction. In contrast, double curved surfaces have non-zero Gaussian curvature and curve in two directions, making them more complex to represent and flatten. Double curved surfaces are classified as:

1. **Positive double curved surfaces**: These have positive Gaussian curvature (K>0), with curvatures having the same sign. Examples include spheres and ellipsoids, which curve outward in all directions.[10]
2. **Negative double curved surfaces**: These have negative Gaussian curvature (K<0), with curvatures having opposite signs, creating a saddle shape. Examples include the hyperboloid of one sheet and paraboloids.[10]

Meshes

Meshes are collections of points (vertices) arranged into basic elements known as faces. These faces are typically bounded by polygons, with common shapes like triangles, quadrilaterals, or hexagons, which fit together along shared edges to approximate the shape of a smooth surface. While meshes can represent smooth surfaces, they may also include non-smooth features such as sharp edges or corners. Meshes are a discrete way of representing surfaces, much like how polygons are used to represent smooth curves. However, transitioning from curves to surfaces is a more complex task, and essential surface details like curvature are not easily extracted from meshes.[10]

[10] (Pottmann, Asperl, Hofer, & Kilian, 2010)

Die approbierte gedruckte Originalversion dieser Diplomarbeit ist an der TU Wien Bibliothek verfügbar
The approved original version of this thesis is available in print at TU Wien Bibliothek.

2.2. State of the art

This subchapter explores current methods for fabricating double curved surfaces across various applications, highlighting the material properties and limitations of these systems. Before discussing the emergence and prior research regarding programmable matter and active textiles, three innovative research projects are discussed bridging the gap between industry standards and research in material systems and fabrication techniques. The examples portrayed in this subchapter range from rigid parts and materials to flexible structures, setting up the framework for active textile systems.

2.2.1. Fabrication of double curved surfaces

Following an enumeration of several widely used materials to create double curved surfaces and their associated fabrication techniques, three research projects are presented challenging these industry standards.

Industry standards

Depending on the material used several fabrication techniques can be applied to create double curved surfaces. All these processes rely on some sort of sub-structure. Either in terms of molds during production or as an integral part of the finished structure. The enumeration below links fabrication and molding techniques to give an overview of current standards.

Die approbierte gedruckte Originalversion dieser Diplomarbeit ist an der TU Wien Bibliothek verfügbar
The approved original version of this thesis is available in print at TU Wien Bibliothek.

Cast materials

In the construction industry, cast materials like concrete are of paramount importance, serving as structural elements or, in the case of materials like GRG (Glass Reinforced Gypsum), as components for interior design. While there are various methods for creating double curved surfaces with such materials, this paragraph focuses on the expansion of "traditional" formworks through 2D milling/cutting and cladding techniques. Single-curved surfaces can be constructed easily by wooden boards. However, the use of waffle structures fabricated with 2D milled plates (figure 9, left) has facilitated the creation of double curved surfaces. These structures are clad with wooden boards or metal sheets to achieve the desired geometry (figure 9, right), requiring less material than fully 3D milled molds. Such prefabricated formwork components can be used to cast double curved concrete structures on-site. For surfaces with low repetition or highly intricate designs, timber molds are widely employed in modern precast projects.[11,12]

Figure 9: Peri – double curved formwork system for concrete structures (PERI, n.d.)

[11] (Schipper & Janssen, 2011)

[12] (Pastor, Lauret, Vergara, & Aguirregabiria, 2012)

Die approbierte gedruckte Originalversion dieser Diplomarbeit ist an der TU Wien Bibliothek verfügbar
The approved original version of this thesis is available in print at TU Wien Bibliothek.

Composite materials (**e.g.: Fiber-reinforced plastics**)

This group of materials finds extensive applications not only in architecture, such as façade panels, but also in the automotive, aerospace, and marine industries. The production of composites typically requires a 3D milled mold, often created from materials like expanded polystyrene (EPS) (figure 10). The milled geometry is coated with a harder polymer or synthetic resin, resulting in a high-quality surface finish and allowing for multiple reuses of the mold. While this fabrication process enables the creation of highly customized components, it becomes costly when producing a large number of unique elements. The technique is most efficient for repetitive surfaces. However, the significant waste generated by these subtractive methods raises ongoing concerns about material efficiency and sustainability.[13,14]

Figure 10: 3D milling process for a mold made from a block of foam (nedcam : shaping technology, n.d.), (Scott System, n.d.)

[13] (Kima, Sonb, Kimb, & Kima, 2015)
[14] (Casta˜neda, Lauret, Lirola, & Ovando, 2015)

Die approbierte gedruckte Originalversion dieser Diplomarbeit ist an der TU Wien Bibliothek verfügbar
The approved original version of this thesis is available in print at TU Wien Bibliothek.

Sheet materials

Sheet metal forming methods rely on mechanical forces, constraining tools, heat, or steam to induce plastic deformation. Techniques such as CNC punching, folding, and bending, along with a wide variety of other methods like multi-point forming, are extensively used in industries like automotive, aerospace, and shipbuilding (figure 11, left). However, these technologies are often impractical for architectural use due to the low repetition of parts and the high cost of mold fabrication.[15] Other sheet materials, such as plywood, pre-cured composite panels, or cellulose-based sheets, can be shaped using processes like thermoforming (figure 11, middle). This process also requires prefabricated molds, which can be constructed from 2D cut elements or 3D milled solids, depending on whether one or both sides of the surface need to be smooth.[16] For surfaces that allow openings, 2D milling can be used for example with plywood sheets. These sheets are cut with numerous lattice hinges to create a flexible material that can form double curved surfaces, as illustrated in figure 11, right.

Figure 11: left: digital sheet forming (Olbrechts, 2023), middle: corian forming process (Pastor, Lauret, Vergara, & Aguirregabiria, 2012), right: 2D milled plywood sheets (Mamou-Mani, 2021)

[15] (Casta˜neda, Lauret, Lirola, & Ovando, 2015)

[16] (Pastor, Lauret, Vergara, & Aguirregabiria, 2012)

Die approbierte gedruckte Originalversion dieser Diplomarbeit ist an der TU Wien Bibliothek verfügbar
The approved original version of this thesis is available in print at TU Wien Bibliothek.

Membranes

Membranes, in general, are thin, flexible materials classified as form-active tension systems. This distinguishes them from the previously discussed systems, as membranes exclusively transfer tensile forces, naturally forming double curved anticlastic surfaces in response to applied loads. To maintain their desired shape, they rely on supporting elements such as cable or skeleton frames, which curve in alignment with the force flow within the membrane. These inherent properties make membrane structures an effective choice for double curved surfaces. However, they are not suitable for all architectural applications, particularly when only a single layer is used.[17,18]

Figure 12: left: membrane and sub-structure (Fu, 2019), middle: interior ceiling design (Interdesign, n.d.), Right: Membranes used as building facade (Fassade aus Sonnensegeln mit integrierter Illumination, 2014)

[17] (AMA: architectural membraneassociation, 2024)
[18] (Fu, 2019)

Die approbierte gedruckte Originalversion dieser Diplomarbeit ist an der TU Wien Bibliothek verfügbar
The approved original version of this thesis is available in print at TU Wien Bibliothek.

Research and innovation

The examples presented should give a condensed view of different research strategies and innovations in the industry regarding the fabrication of double curved surfaces. They range from literally re-designing the art of molding, to the use of flexible, lightweight material systems for structures without the need for formworks.

ADAPA

In the architectural field, the adaptive mold developed by ADAPA is already in use. This system consists of a rigid membrane mounted on individually controlled, numerically actuated pistons, as shown in figure 13. The membrane adjusts to the activated points, creating smooth curves. The precision as well as the achievable complexity of the resulting surface depend on the number of control points and the stiffness of the membrane. By enabling reconfiguration and reuse, it eliminates the need for time- and material-intensive 3D milled molds. However, the system is limited by the achievable range of curvature, making it best suited for large, double curved surfaces with relatively small curvature variations across individual elements.[19]

Figure 13: fabrication principle of ADAPA mold (Raun & Kirkegaard, 2015)

[19] (Raun & Kirkegaard, 2015)

Die approbierte gedruckte Originalversion dieser Diplomarbeit ist an der TU Wien Bibliothek verfügbar
The approved original version of this thesis is available in print at TU Wien Bibliothek.

CASTonCAST

This system enables the design and production of double curved structures using precast, stackable components. It employs a distinctive manufacturing technique for complex geometries, where each component serves as a mold for casting the next one (figure 14, left). This approach eliminates the need for separate molds to create double curved structures. However, the geometry of each individual component is constrained by the requirement to be stackable. Consequently, the resulting surface geometry is influenced by the fabrication parameters of the individual pieces (figure 14, right).[20]

Figure 14: left: stacks created with the CASTonCAST method, right: fabricated surface (Enriquea, Cepaitisb, Ordóñezc, & Pilesd, 2016)

[20] (Enriquea, Cepaitisb, Ordóñezc, & Pilesd, 2016)

Die approbierte gedruckte Originalversion dieser Diplomarbeit ist an der TU Wien Bibliothek verfügbar
The approved original version of this thesis is available in print at TU Wien Bibliothek.

Isoropia

The "Isoropia" project belongs to the field of hybrid-textile structures, focusing on "active bent" systems. This term describes a construction approach for creating membrane-like structures, as outlined before in this section, with the key distinction of leveraging an equilibrium state between flexible rods and a stretchable textile. Specifically, the project employs a textile membrane in structural balance with bent glass fiber rods of varying thickness and stiffness. In this setup, the bending-active rods pre-stress the tensile fabric, which in turn locks the rods into their bent positions. This interdependence results in a highly adaptable system where the overall shape is influenced by the degree of pre-stress and the cutting pattern of the knitted fabric. Furthermore, the Isoropia system adapts to its external boundary conditions. The fabric gains a three-dimensional form through a tensegrity-like arrangement of internal compression rods.[21]

Figure 15: project Isoropia using flexible textiles to generate a double curved structure (Tamke, et al., 2020)

[21] (Tamke, et al., 2020)

Die approbierte gedruckte Originalversion dieser Diplomarbeit ist an der TU Wien Bibliothek verfügbar
The approved original version of this thesis is available in print at TU Wien Bibliothek.

2.2.2. *Self-assembling systems – programmable matter*

Since the advent of the digital revolution, particularly in architecture and design, the emphasis on form has grown to the extent that its materialization has become largely standardized, rendering material secondary to form. While new digital design tools have provided unprecedented freedom for formal expression, they have also deepened the distinction between matter and form. This shift has further accentuated the separation between modeling, analysis, and fabrication processes, with material often being treated as inherently passive and static.[22]

However, the discovery of new materials has consistently driven significant social and technological progress. In recent years, notable advancements across various fields, including materials science, computer-aided design, and digital fabrication, have led to the emergence of programmable matter and self-assembling systems, redefining the possibilities in design and engineering.[23]

The following paragraphs present the definition and development of these material systems, with a focus on the specific sub-groups of programmable matter relevant for understanding the inherent concepts of active textiles. Additionally, the fabrication method of 4D printing is briefly addressed, highlighting its principles and direct connection to active textiles, which are explored further in the concluding paragraphs.

[22] (Andreoletti & Rzezonka, 2016)
[23] (Scalet, 2024)

Die approbierte gedruckte Originalversion dieser Diplomarbeit ist an der TU Wien Bibliothek verfügbar
The approved original version of this thesis is available in print at TU Wien Bibliothek.

What are programmable materials?

> *"To create self-assembling systems, we first need to understand why self-assembly works and how things move toward equilibrium. Then, we need to find ways to take advantage of this equilibrium seeking to promote order from chaos. ...we define self-assembly through its three core ingredients – energy, geometry and interactions"24*

An abstract definition of programming is understood as the creation of a set of instructions that can be processed or performed by a specific medium. When applied to materials, this involves the embedding of such instructions into the material itself, allowing it to sense and respond. Thus, programmable materials are defined as physical structures, embedded with information and the capabilities to for example actuate, or sense. Active matter, a field related to this concept, is used to describe the broader field of research focused on the development of dynamic structures that can self-assemble or undergo physical transformations. At their core, these material systems build on the activation of individual material components through energy, enabling them to assemble, transform, and exhibit new physical behaviors as illustrated by figure 16.[25]

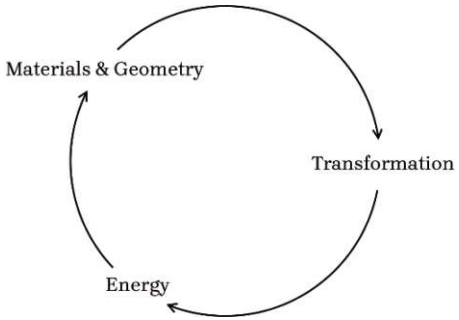

Figure 16: illustration of basic principle behind programmable materials.

[24] (Tibbits, 2021)
[25] (Tibbits, 2021)

Die approbierte gedruckte Originalversion dieser Diplomarbeit ist an der TU Wien Bibliothek verfügbar
The approved original version of this thesis is available in print at TU Wien Bibliothek.

The concept of programmable matter is not new, but advancements in computing, digital fabrication, and material science have shaped its current definition. The term, as used in this research, was first introduced in 2010, defined as a material whose properties can be programmed to undergo specific changes in shape or stiffness upon command. In the same year, the term was further influenced by the rise of new manufacturing technologies, such as 4D printing. This emerging trend in stimuli-responsive materials uses additive manufacturing to create structures with complex geometries that can evolve in shape and function over time, the "fourth dimension", in response to external stimuli after production. Skylar Tibbits introduced the term "4D printing" 2013, applying the technology to the development of programmable machines. This fabrication method is discussed in more detail later in this chapter.[26]

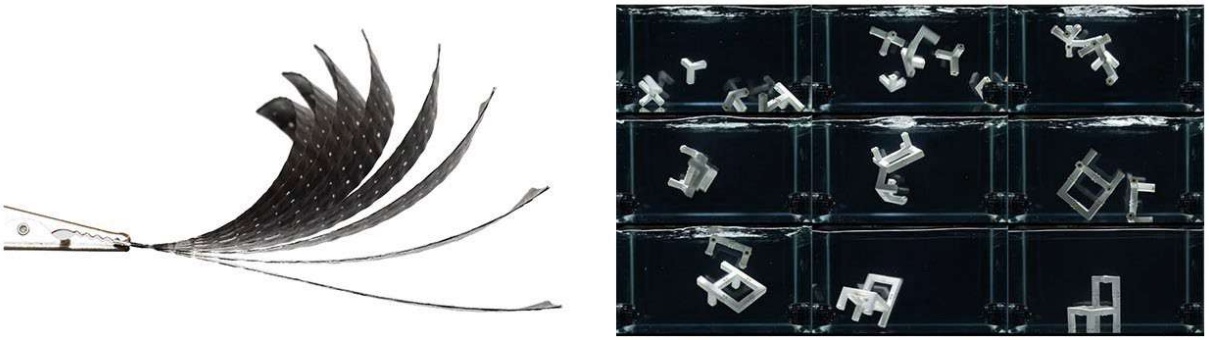

Figure 17: types of programmable materials, left: self-transformation, right: self-assembly (Self-Assembly Lab, n.d.)

[26] (Scalet, 2024)

Die approbierte gedruckte Originalversion dieser Diplomarbeit ist an der TU Wien Bibliothek verfügbar
The approved original version of this thesis is available in print at TU Wien Bibliothek.

The concept of programmable materials involves a self-assembly process that allows structures to autonomously change their shape and/or functional properties, without the need for human intervention or robotic mechanisms such as motors, wires, or electronics. Based on this definition, two types of programmable matter are identified:

- Self-transforming structures made from pre-connected elements. (figure 17, left)
- Unconnected voxels that can autonomously assemble or disassemble to form structures. (figure 17, right)

The material system investigated in this thesis belongs to the first mentioned category, which encompasses various classifications of programmable properties. Programming a material's behavior refers to the potential for the material to feature one or more properties that can be adjusted to different situations, needs, or environmental changes, or to achieve functions that would be impossible with fixed properties. Particularly, programmable behavior involves changes in shape and/or physical or functional properties. The focus of this project lies on "shape-changing" properties, with shape programming being the main area of interest in prior research as well.[27],[28]

From a practical standpoint, shape changes from 2D to 3D space are of great interest. When an initially flat structure is programmed to undergo three-dimensional shape transformations upon the application of a stimulus, several benefits are provided, including the simple and cost-effective fabrication of components, as well as efficient stacking for storage, transport, and deployment. [29],[30]

[27] (Modes & Warner, 2016)
[28] (Scalet, 2024)
[29] (Liu, Genzer, & Dickey, 2016)
[30] (Janbaz, Hedayati, & Zadpoor, 2016)

Die approbierte gedruckte Originalversion dieser Diplomarbeit ist an der TU Wien Bibliothek verfügbar
The approved original version of this thesis is available in print at TU Wien Bibliothek.

The "shape-changing" category is further divided into sub-categories of different types (figure 18) and various programming strategies. Programmable materials can consist of two or more constituent materials, each with distinct properties. These varying properties allow the materials to respond differently to external stimuli, providing the ability to program the behavior of the final material. This strategy is also known as "patterning"[31] or "material tessellation"[32]. It is particularly effective for programming the transformation from a 2D to a 3D shape[33]. In this context, bilayer approaches represent the simplest method for inducing the folding of a 2D material structure[34], due to the distinct properties of the two material layers.[35] These principles serve as the foundation of this thesis. By embedding instructions and utilizing the inherent properties of materials, it becomes possible to achieve complex double curved geometries with greater efficiency.

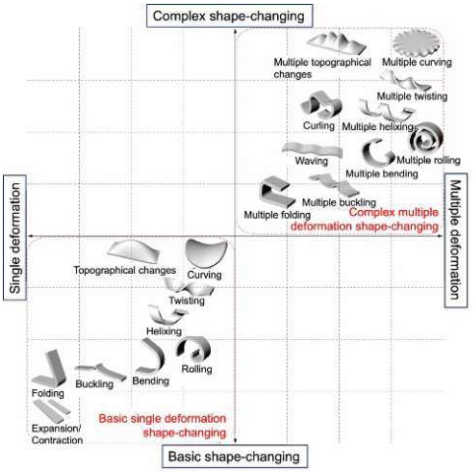

Figure 18: matrix of deformation types in shape changing materials. (Scalet, 2024)

[31] (Puza & Lienkamp, 2022)
[32] (Manen, Janbaz, & Zadpoor, 2018)
[33] (Liu, Genzer, & Dickey, 2016)
[34] (Janbaz, Hedayati, & Zadpoor, 2016)
[35] (Scalet, 2024)

Die approbierte gedruckte Originalversion dieser Diplomarbeit ist an der TU Wien Bibliothek verfügbar
The approved original version of this thesis is available in print at TU Wien Bibliothek.

4D Printing

Additive manufacturing, or 3D printing, is a technique that can build complex structures, offering high flexibility in design, significant material savings, and the ability for customization and individuality. 4D printing involves creating material structures capable of intentionally changing their properties over time. In this context, the fourth dimension represents the temporal aspect, during which these property changes occur following the 3D printing process. This is illustrated by the corresponding image in the middle depicted in figure 19, showing experiments done at the Self-assembly Lab.[36],[37]

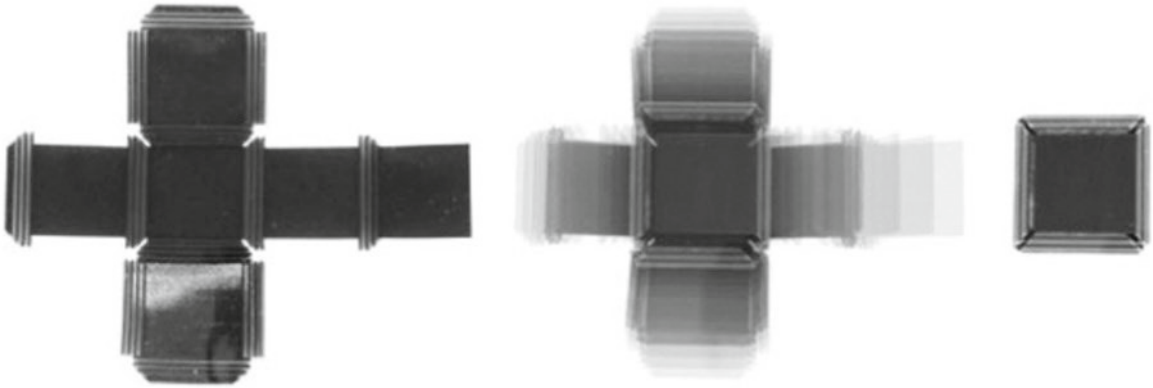

Figure 19: shape-changing system created with a 4D printing process at MIT. (Self-Assembly Lab, n.d.)

[36] (Mitchell, Lafont, Hołyńska, & Semprimoschnig, 2018)
[37] (Aldawood, 2023)

Die approbierte gedruckte Originalversion dieser Diplomarbeit ist an der TU Wien Bibliothek verfügbar
The approved original version of this thesis is available in print at TU Wien Bibliothek.

In 4D printing, the change in material properties is activated by an external stimulus, with the energy required for the transformation either stored within the material or provided by the stimulus. The fundamental building blocks of 4D printing are:

- **3D Printing facility**: Within a single 3D printing process, a 4D printed structure is produced by strategically combining multiple materials according to their properties. Differences in material properties drive the intended shape-shifting behavior.
- **Stimulus**: Activating changes in the shape, properties, or functionality of a 4D printed structure requires a stimulus. The choice of stimulus is dictated by the specific application, which also influences the selection of smart materials incorporated into the structure.
- **Smart or stimulus-responsive material**: Stimulus-responsive materials are crucial components of 4D printing. Characteristics such as self-sensing, responsiveness, shape memory, self-adaptability and self-repair define these materials.
- **Interaction mechanism**: In some cases, the stimulus must be applied in a specific sequence and over a certain duration.[38]

A further distinction is made in 4D printing between active and passive materials. Active materials can undergo property changes when stimulated by external factors, such as heat, light, or electric fields. These materials are often combined with passive or basic materials, which do not change over time. Passive materials are typically used for functions like forming connections between components or limiting certain sections within a structure. The changes that active materials undergo can either be reversible or irreversible, depending on the specific material and the type of stimulus applied.[39],[40]

[38] (Momeni, Hassani.N, Liu, & Ni, 2017)
[39] (Koch, Schmelzeisen, & Gries, 2021)
[40] (Pei & Loh, 2018)

Die approbierte gedruckte Originalversion dieser Diplomarbeit ist an der TU Wien Bibliothek verfügbar
The approved original version of this thesis is available in print at TU Wien Bibliothek.

Active textiles

The concept of 4D printing, when applied to textiles, evolves into a hybrid material structure that can change shape over time, enabled by additive manufacturing techniques. This advanced approach is often referred to using various terms, such as programmable textiles, postforming composites, self-shaping textiles, and active textiles. These materials integrate time-varying properties, allowing them to adapt and respond to external stimuli, leading to dynamic, functional textile structures.[41]

Active Textiles, or Programmable Textiles are members of the before established categories of programmable materials and refer to a technique for transforming flat sheets into three-dimensional shapes, as illustrated in figure 20. This area of research explores the development of bending-active systems by employing the "4D printing" concept to fabricate composite material structures.[42]

Figure 20: illustration of shape change in active textiles (Vivanco, Valencia, & Yuan, 2020)

[41] (Koch, Schmelzeisen, & Gries, 2021)
[42] (Lettner, Palma, & Baseta, 2024)

Die approbierte gedruckte Originalversion dieser Diplomarbeit ist an der TU Wien Bibliothek verfügbar
The approved original version of this thesis is available in print at TU Wien Bibliothek.

The functional principle of active textiles is based on the interaction between the properties of an elastically pre-stretched textile and beam-shaped 3D printed reinforcements (figure 20). Through the process of pre-stretching, the textile is enabled to store potential energy as an anisotropic spring. Next, a specific geometry is 3D printed on the textile. By releasing the pre-tension, the textile generates a restoring force, which is resisted by the elastic stiffness of the reinforcements in the printed areas. The system transforms from a flat shape into a three-dimensional form until it reaches an equilibrium state, causing the printed structure to bend.[43] This process results in double curved surfaces, representing the lowest energy state of the system. The resulting shape, either synclastic (dome-shaped) or anticlastic (saddle-shaped), depends on whether the perimeter of the surface is free to contract during pre-stress release or is constrained by the reinforcements. The deformation of the 3D printed parts is determined through their stiffness.[44] Additionally, the tension within the material allows 4D textiles to possess multiple equilibrium states, enabling the shape to change.[45]

To sum up the underlying principle, an exemplary fabrication process is described, with corresponding parts highlighted in figure 21:

To start, a piece of elastic textile is pre-stretched (figure 21: Prestressed textile), wrapped around a plate and fixed in place (figure 21: Build Surface). The later material transformation can be influenced by the specific pattern of pre-stretching. In the next step rigid or flexible material layers are applied on top (figure 21: Using a 3D printing extruder head). The transformation of the overall shape is guided by the geometrical pattern. The behavior during transformation is influenced by factors such as type of material used, thickness of the layer, and 3D printed geometry applied to the textile.[46]

[43] (Gengnagel, 2005)
[44] (Aldinger, Margariti, Körner, Suzuki, & Knippers, 2018)
[45] (Koch, Schmelzeisen, & Gries, 2021)
[46] (Tibbits, 2021)

Die approbierte gedruckte Originalversion dieser Diplomarbeit ist an der TU Wien Bibliothek verfügbar
The approved original version of this thesis is available in print at TU Wien Bibliothek.

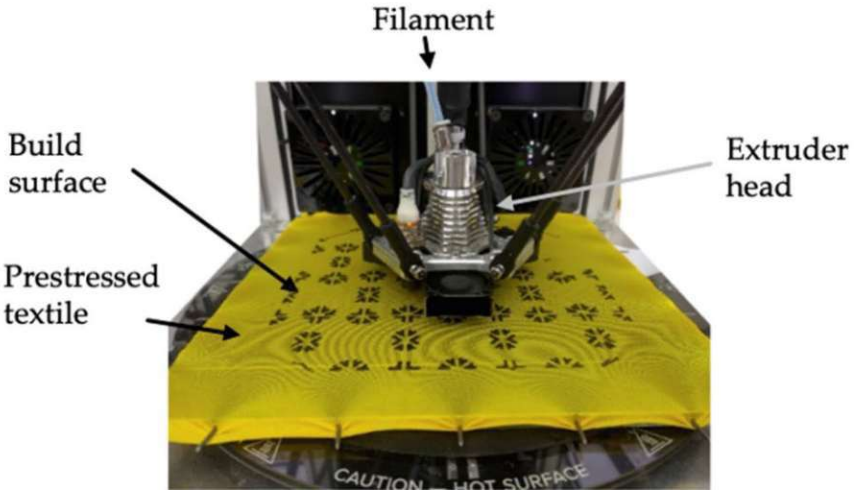

Figure 21: fabrication process of active textiles in prior research (Koch, Schmelzeisen, & Gries, 2021)

Several methods for producing active textiles utilize standard FDM 3D printers (figure 21), where the textile is fixed to the build plate, which then serves as the new build surface. To store energy in the fabric, it must be pre-stretched, requiring the addition of a clamping mechanism to the build plate. Various approaches have been implemented to achieve this: for example, using double sided adhesive tape to fix the textile to the print bed, though this approach lacks consistent repeatability. Alternatively, a tension board with nails can be used to stretch the textile, although causing damage to the fabric. This issue can be mitigated by using clamps to apply tension, but this still suffers from reduced accuracy. Depending on the specific application, the textile can be pre-stressed in a biaxial, uniaxial, or radial manner.[47],[48]

[47] (Koch, Schmelzeisen, & Gries, 2021)
[48] (Lettner, Palma, & Baseta, 2024)

Die approbierte gedruckte Originalversion dieser Diplomarbeit ist an der TU Wien Bibliothek verfügbar
The approved original version of this thesis is available in print at TU Wien Bibliothek.

Previous research has concentrated on the challenging task of developing precise digital tools for simulating and predicting the behaviors of these complex composite materials. The developed tools have been particularly effective in addressing applications in small scale, for example as a modelbuilding technique for shell structures, as described by (Jourdan, Skouras, Vouga, & Bousseau, 2020) and portrayed in figure 22. Through the parametric manipulation of a digital input-grid (figure 22, left) a corresponding shell structure is generated digitally (figure 22, middle) and can be reproduced physically (figure 22, right).[49]

As researchers began addressing larger scales, their focus shifted toward alternative fabrication methods. Fiber placement technologies have been explored for creating large-span shell structures by integrating carbon fiber rods into a pre-stretched piece of textile (figure 23), as well as manual lamination techniques utilizing readily available materials to enable surface activation.[50]

However, the upscaling of active textile systems still needs further investigations into the fabrication parameters involved, along with the establishment of standardized testing protocols and advancements in production technology.[51] Reproducing a simulated geometry with reliable control over curvature has not yet been fully explored. Recent advancements have introduced the use of hinges, achieved through abrupt changes in the cross-section of 3D printed elements, as an innovative technique for generating shape variations in active textiles. This method allows for more dynamic and adaptable structural behaviors, though the precise control of curvature remains a challenge.[52],[53]

[49] (Lettner, Palma, & Baseta, 2024)
[50] (Aldinger, Margariti, Körner, Suzuki, & Knippers, 2018)
[51] (Koch, Schmelzeisen, & Gries, 2021)
[52] (Vivanco, Valencia, & Yuan, 2020)
[53] (Lettner, Palma, & Baseta, 2024)

Die approbierte gedruckte Originalversion dieser Diplomarbeit ist an der TU Wien Bibliothek verfügbar
The approved original version of this thesis is available in print at TU Wien Bibliothek.

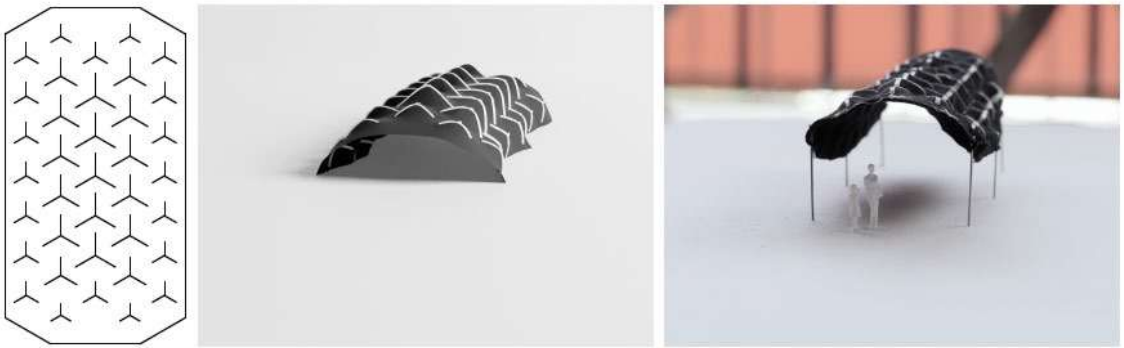

Figure 22: rapid prototyping of shell structures with active textiles (Jourdan, Skouras, Vouga, & Bousseau, 2020)

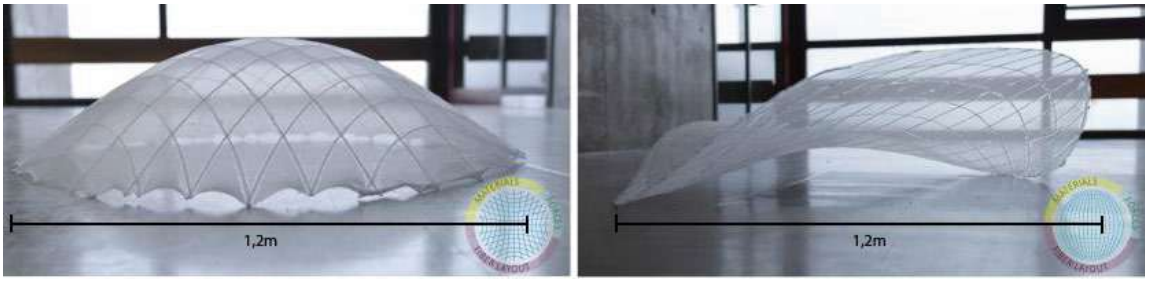

Figure 23: shift in material system for large scale tests (Aldinger, Margariti, Körner, Suzuki, & Knippers, 2018)

Die approbierte gedruckte Originalversion dieser Diplomarbeit ist an der TU Wien Bibliothek verfügbar
The approved original version of this thesis is available in print at TU Wien Bibliothek.

2.2.3. Summary

To sum up, one of the major disadvantages of active textile systems is the lack in applicability, especially because of limited scalability and geometry control. The method of sub-dividing a single piece of fabric through a print-pattern used in small- and large-scale experiments shows a cap for achievable geometries and size. When comparing prior research, the lack of a precise and repeatable fabrication method, especially for textile pre-stretching is evident.

The chapters presenting the material experiments conducted in the framework of this thesis are dedicated to the performed investigations in fabrication parameters of individually produced active textile units (figure 24, top) and the explored possibility to combine these tiles to form larger double curved surfaces: tiled surfaces (figure 24, bottom).

To achieve this, a deep understanding of the material system of active textiles was required, as well as custom-made digital fabrication tools for introducing control in the production of the active textile components. The journey from initial tests done with the proposed material system to the development of a custom-made digital fabrication setup are discussed in detail in the following chapter.

Die approbierte gedruckte Originalversion dieser Diplomarbeit ist an der TU Wien Bibliothek verfügbar
The approved original version of this thesis is available in print at TU Wien Bibliothek.

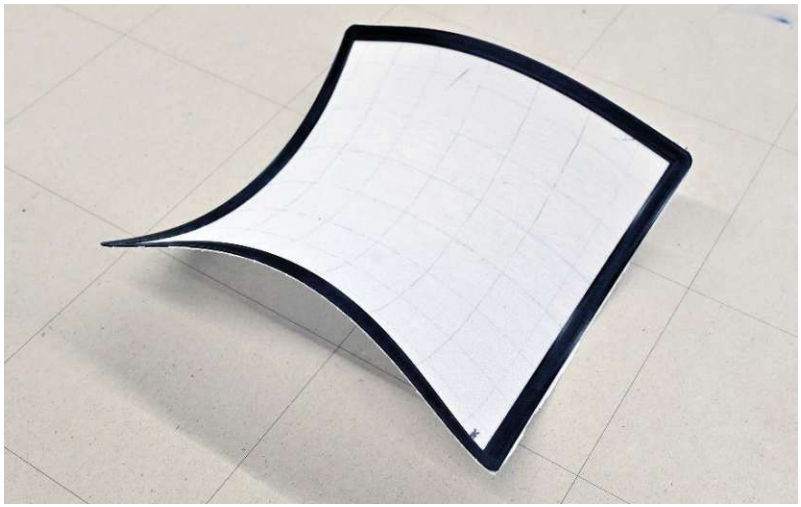

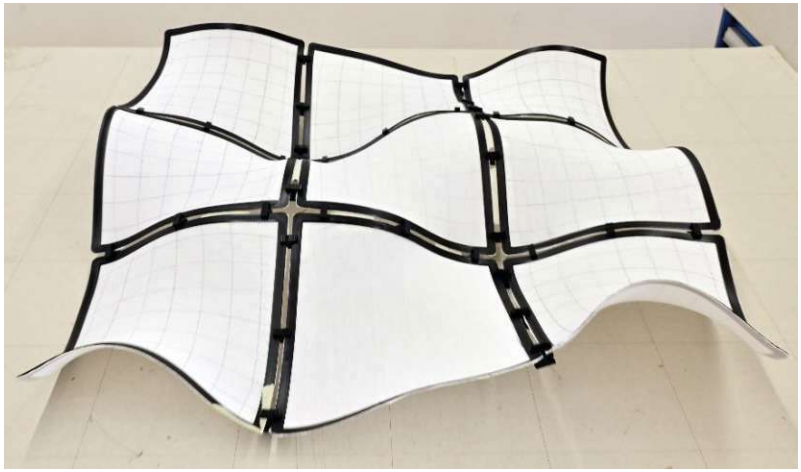

Figure 24: top: individual tile, bottom: tiled surface exploration

Die approbierte gedruckte Originalversion dieser Diplomarbeit ist an der TU Wien Bibliothek verfügbar
The approved original version of this thesis is available in print at TU Wien Bibliothek.

Die approbierte gedruckte Originalversion dieser Diplomarbeit ist an der TU Wien Bibliothek verfügbar
The approved original version of this thesis is available in print at TU Wien Bibliothek.

3. Material system exploration

The journey from initial experiments conducted on active textile components to the development of a custom-built fabrication set-up is outlined in this chapter. The progression made from manually pre-stretching and laminating 3D printed frames onto textiles to utilizing computer-controlled pre-stretching and directly 3D printing onto the fabric is highlighted. Additionally, insights into the components used to construct the custom fabrication setup employed during the material experimentation phase are offered.

Die approbierte gedruckte Originalversion dieser Diplomarbeit ist an der TU Wien Bibliothek verfügbar
The approved original version of this thesis is available in print at TU Wien Bibliothek.

3.1. Preliminary testing phase

The exploration of the active textile material system in this research began with a manual approach, involving the lamination of a 3D printed boundary onto a pre-stretched textile. Initial testing was carried out in three distinct phases. First, the fabric and PLA frame were prepared as highlighted in figure 25, left. As the next step the 3D printed boundary was glued to the pre-stretched textile (figure 25, middle). Finally, the tension was released and the active textile piece formed into a three-dimensional shape as illustrated by figure 25, right. The 3D printing was performed using an Anycubic i3 Mega S desktop FDM 3D printer with PLA filament.

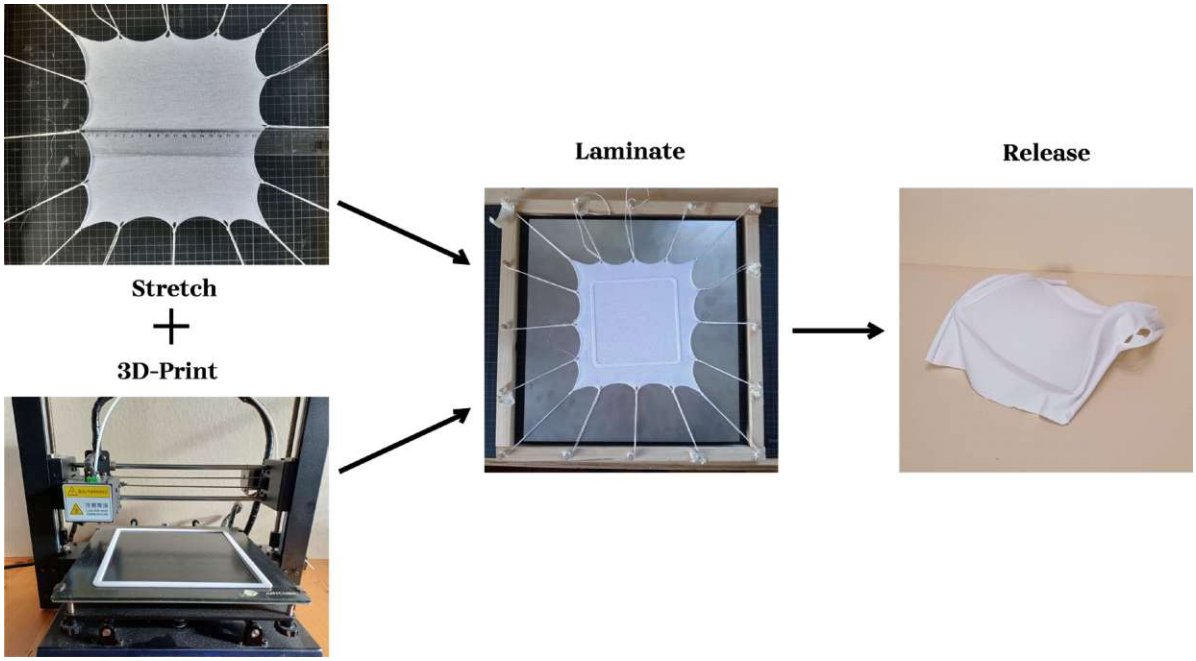

Figure 25: diagram of initial fabrication technique used to produce active textile tiles

Die approbierte gedruckte Originalversion dieser Diplomarbeit ist an der TU Wien Bibliothek verfügbar
The approved original version of this thesis is available in print at TU Wien Bibliothek.

Several methods for pre-stretching the fabric were tested. Initially, the textile was stretched and secured to a surface with tape (figure 26), ensuring that either the entire edge length, or certain parts were clamped. Additionally, inspiration from the ancient craft of parchment-making (figure 27, left) was drawn to construct a wooden frame, allowing manual control of pre-stretching at specific points (figure 27, right).

Figure 26: manual pre-stretching with tape used for clamping

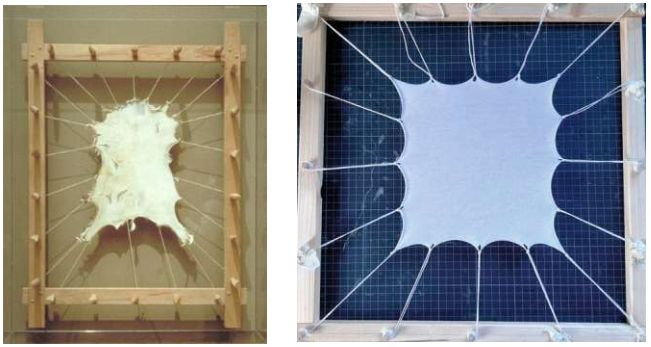

Figure 27: left: parchment making technique (flickr, n.d.) right: inspired wooden frame for textile pre-stretching

Die approbierte gedruckte Originalversion dieser Diplomarbeit ist an der TU Wien Bibliothek verfügbar
The approved original version of this thesis is available in print at TU Wien Bibliothek.

The next set of experiments involved similar active textile fabrication methods as described in section 2.2.2, focusing on a combined process of pre-stretching the textile and directly 3D printing on it to eliminate the need for manual lamination. The Anycubic i3 Mega S desktop FDM 3D printer was used again, with the textile directly taped onto the print bed as shown in figure 28. This setup allowed testing of printing parameters and adhesion of filament to various fabrics with results portrayed in figure 29. This process proved to be labor-intensive and imprecise. It became evident that a more precise method for pre-stretching the textile in combination with 3D printing was necessary.

Figure 28: using a FDM 3D printer with a pre-stretched piece of fabric fixed to the print bed

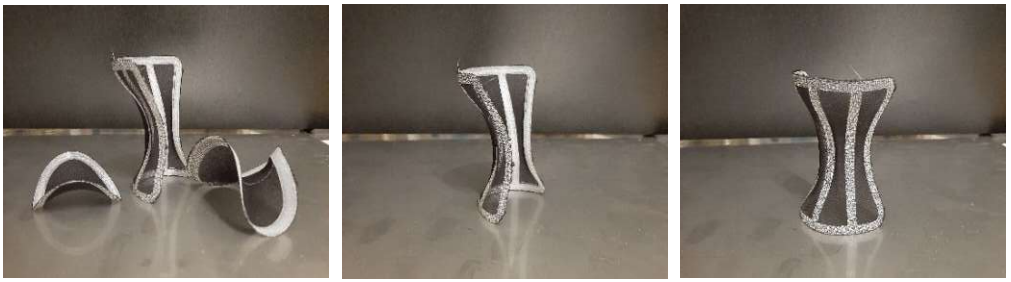

Figure 29: resulting pieces from the initial fabrication process

Die approbierte gedruckte Originalversion dieser Diplomarbeit ist an der TU Wien Bibliothek verfügbar
The approved original version of this thesis is available in print at TU Wien Bibliothek.

3.2. Custom-built fabrication set-up

The development of a custom digital fabrication setup was essential to gain control over the production of active textile components. Specifically, improvements were needed in the clamping and pre-stretching methods to accurately control the amount of force stored in the textile. This precision was necessary to ensure consistent and reliable results in the fabrication process.

Therefore, a numerically controlled base plate for pre-stretching was designed paired with a 3D printing unit specifically tailored to this fabrication method. The overall design of the custom-built hardware is illustrated in figure 30.

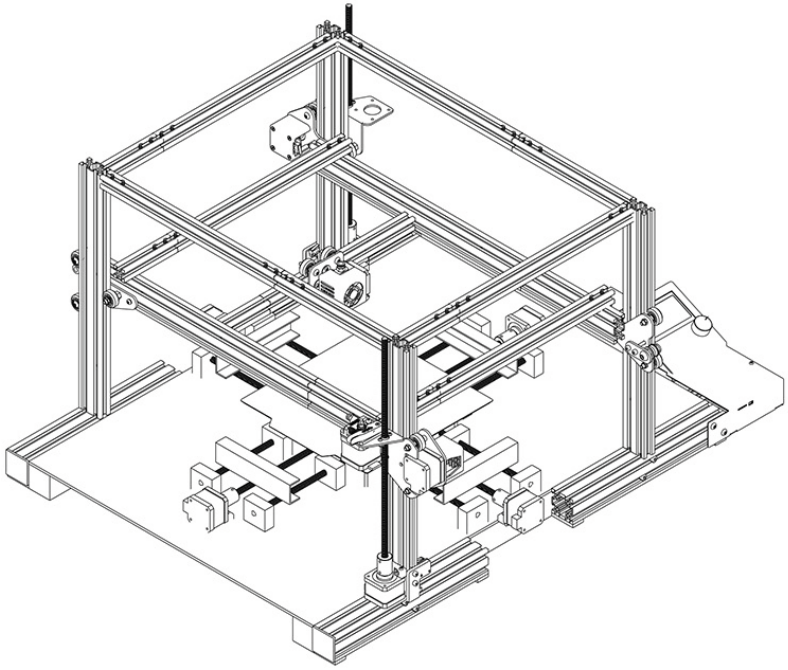

Figure 30: digital model of custom printing rig

Die approbierte gedruckte Originalversion dieser Diplomarbeit ist an der TU Wien Bibliothek verfügbar
The approved original version of this thesis is available in print at TU Wien Bibliothek.

Pre-stretching

Initially, a baseplate for numerically controlling the amount of pre-stretching was developed using wood for rapid prototyping. It was designed to accommodate the mechanics necessary for stretching a piece of textile along the two perpendicular axes X and Y (figure 31, left). To ensure uniform activation, the textile needed to be stretched with identical but opposing forces along axis X and Y. Nema 17 stepper motors were positioned at the ends of these axes, each connected to a threaded spindle (8 mm diameter, 2 mm pitch). Aluminum brackets were mounted on these spindles to either hold a tool or directly clamp the textile, allowing precise control over the pre-stretch applied to the textile in X and Y direction. This initial design was run by an Arduino UNO equipped with a TB6600 stepper motor controller for each Nema 17 connected to a CNC shield. In figure 31, right a layout of these components is depicted. This fast proof of concept later evolved into the custom-built ground plate of the fabrication set-up. As shown in figure 32, the final digital design of the set-up consists of a revised version of this ground plate and an independent part hosting the functions for 3D printing.[54]

3D printing

Not only the specific build volume and accessibility of the base plate made it crucial to design a custom-made 3D printing unit (figure 32, right), but as well the specific movement system needed. Most standard desktop FDM 3D printers, known as rectilinear or Cartesian printers, operate along straight X, Y, and Z axes, typically with the print head moving along two axes and the print bed moving along one. However, to accommodate textile clamping and pre-stretching, the print bed had to remain static. As a result, the movement along all three axes had to be incorporated into the print head, which made a custom-designed solution the most efficient choice. To avoid starting from scratch, the design was based on a standard desktop FDM 3D printer, Model: Creality Ender 3.[55]

[54] (Lettner, Palma, & Baseta, 2024)
[55] (Lettner, Palma, & Baseta, 2024)

Die approbierte gedruckte Originalversion dieser Diplomarbeit ist an der TU Wien Bibliothek verfügbar
The approved original version of this thesis is available in print at TU Wien Bibliothek.

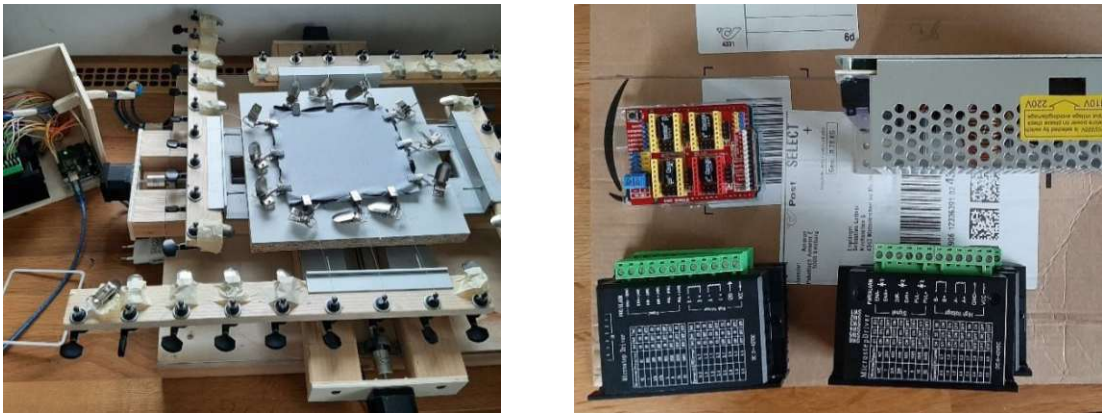

Figure 31: left: first iteration of a baseplate for numerically controlled textile pre-stretching, right: layout of electronics used to control the amount of pre-stretching

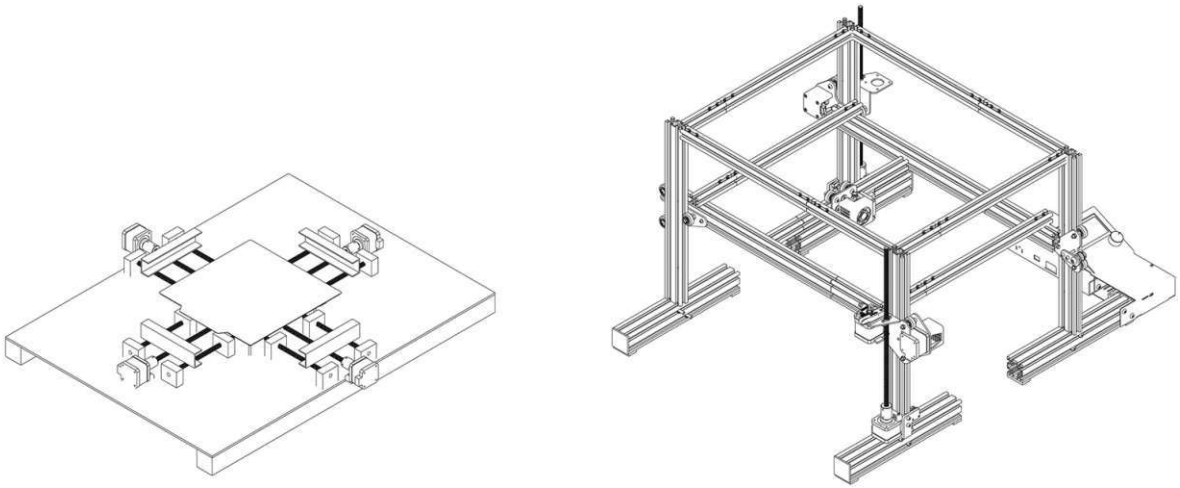

Figure 32: digital model, left: custom-built base plate, right: 3D printing set-up

Die approbierte gedruckte Originalversion dieser Diplomarbeit ist an der TU Wien Bibliothek verfügbar
The approved original version of this thesis is available in print at TU Wien Bibliothek.

For better understanding, the individual components of the custom 3D printing setup are depicted in figure 33, with the numbers in the following description corresponding to those in the diagram. The main frame of the setup is composed of two A-frames (1), each supporting a movable truss that functions as the Y-axis (3). This setup mirrors the Ender 3 design but features a wider span between the vertical aluminum profiles that form the Z-axis. To improve stability, the A-frames are connected at the top (2), resulting in a box-like structure commonly seen in commercial printers. Additionally, the two movable Y-axis trusses are linked together (4), creating a square frame that features the X-axis of the printer (5). These are the structural parts of the printing system (6).

The movement of the individual axes is facilitated by a combination of stepper motors, threaded spindles, linear guide rails, and belts. The Z-axis is driven by two stepper motors positioned at diagonally opposite corners of the frame (7), each connected to an 8 mm diameter, 2 mm pitch threaded spindle. The two non-powered corners of the Y-axis frame are guided along the Z-axis using V-slot wheels. For movement along the Y axes, the entire X-axis moves along the Y-frame. This is accomplished with one stepper motor at each Y-truss (8), which pulls the X-axis using a belt drive system along linear guide rail. Similarly, the print head moves along the X-axis on a guide rail, driven by a belt and a stepper motor system. (9)[56]

All movements, heating, extrusion, and other operations are controlled by a GT2560 printer mainboard, to which A4988 stepper motor controllers are connected. In addition to the standard features of the Ender 3, a BL-Touch probe was installed for automatic bed leveling, and two end switches were added for X and Y homing. Modifications and updates to the printer's firmware were done using Visual Studio Code with the extensions "Auto Build Marlin" and "PlatformIO." (figure 34).[57]

[56] (Lettner, Palma, & Baseta, 2024)
[57] (Lettner, Palma, & Baseta, 2024)

Die approbierte gedruckte Originalversion dieser Diplomarbeit ist an der TU Wien Bibliothek verfügbar
The approved original version of this thesis is available in print at TU Wien Bibliothek.

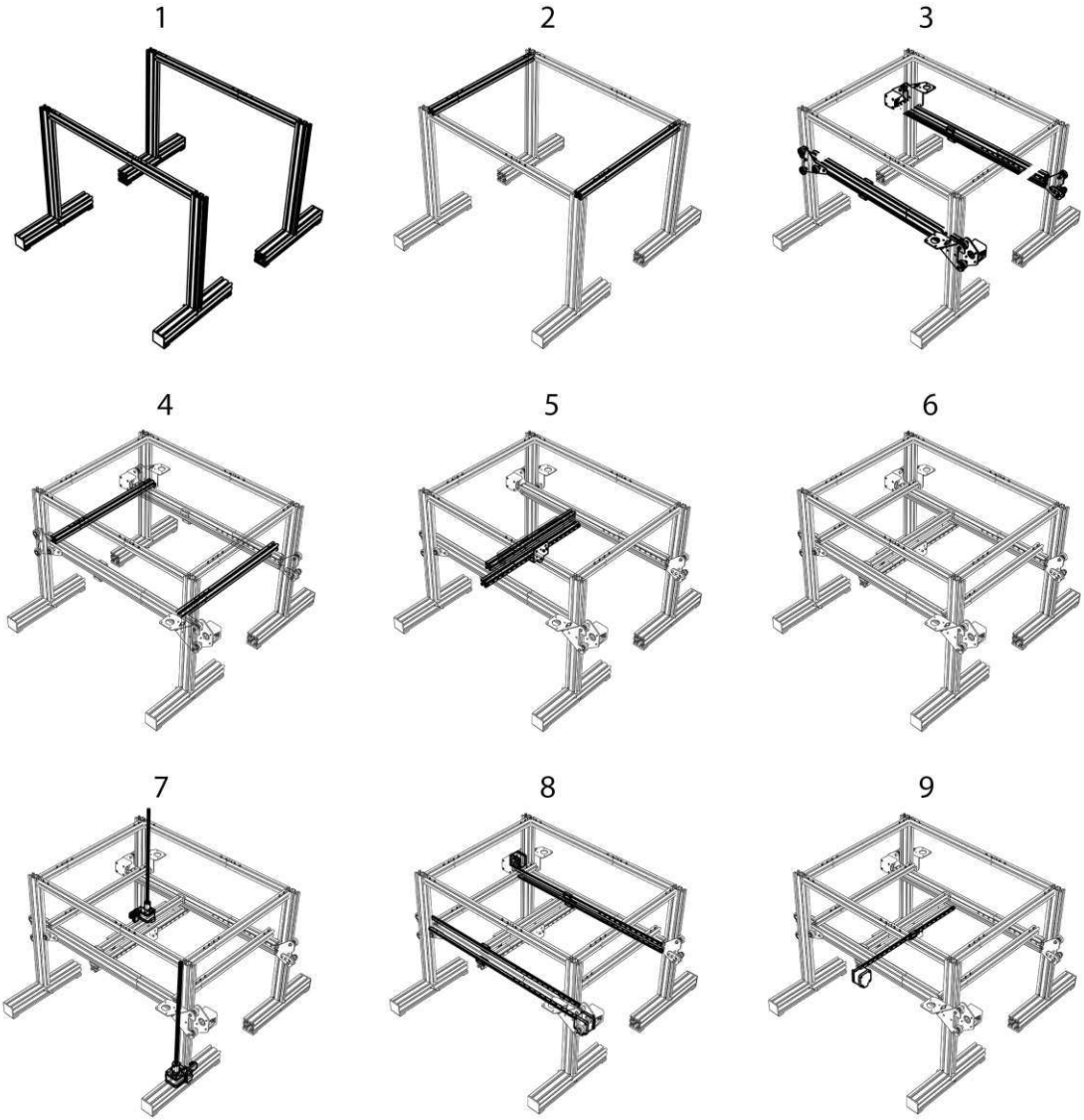

Figure 33: illustration of the individual parts of the printing system

Die approbierte gedruckte Originalversion dieser Diplomarbeit ist an der TU Wien Bibliothek verfügbar
The approved original version of this thesis is available in print at TU Wien Bibliothek.

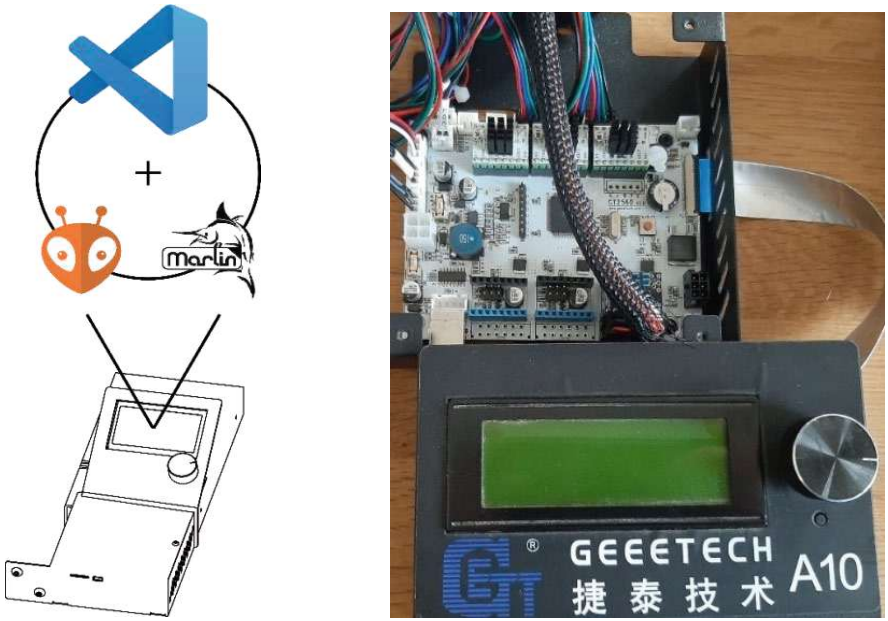

Figure 34: left: programs used to modify the printer firmware, right: actual electronic components

Die approbierte gedruckte Originalversion dieser Diplomarbeit ist an der TU Wien Bibliothek verfügbar
The approved original version of this thesis is available in print at TU Wien Bibliothek.

Initially, the printing unit was integrated with the first iteration of a custom-built wooden base plate, as shown in figure 31. However, this design proved inadequate for prolonged use. Consequently, the wooden base was replaced with an aluminum construction, and the wooden rails guiding the clamping mechanism connected to the threaded spindle, were removed. Instead, two linear guide rails were installed alongside each threaded spindle to ensure precise, parallel movement along each axis.

The final version of the fabrication setup includes a steel plate measuring 235x235x2 mm, fixed to the heated bed of the 3D printer, as shown in figure 35, left. This configuration features two orthogonal clamping and pulling mechanisms aligned with the X and Y axes of the 3D printer. Textile clamping is achieved mechanically, while the pulling mechanism operates through numerical control.[58]

Linear as well as pointwise clamping along all four edges of the textile is enabled by the designed mechanism as shown in figure 36. In the linear clamping configuration, the entire length of each edge is secured. In the pointwise configuration, each edge is clamped at seven evenly spaced points using independent pins. Despite these adjustments, the stretching mechanism continues to be powered by four Nema 17 stepper motors, two for the X and Y axes respectively and aligned with them. The control of the setup remained unchanged and is managed by an Arduino UNO equipped with a CNC shield and connected to a TB6600 stepper controller for each Nema 17 motor. 150 mm maximum pulling distance per edge for pointwise, and 160 mm for linear clamping are achievable.[59]

The completed custom-built set-up integrated with the before mentioned revised version of the custom-built ground plate is portrayed in figure 37.

[58] (Lettner, Palma, & Baseta, 2024)
[59] (Lettner, Palma, & Baseta, 2024)

Die approbierte gedruckte Originalversion dieser Diplomarbeit ist an der TU Wien Bibliothek verfügbar
The approved original version of this thesis is available in print at TU Wien Bibliothek.

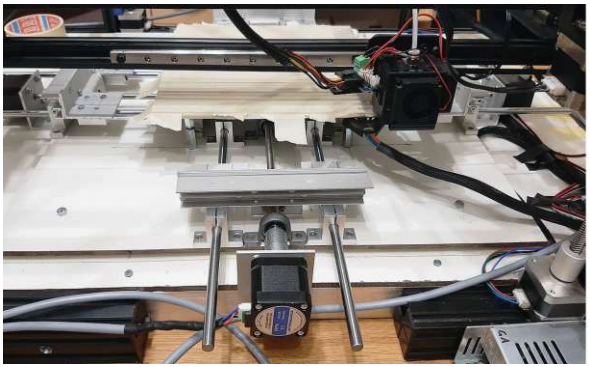

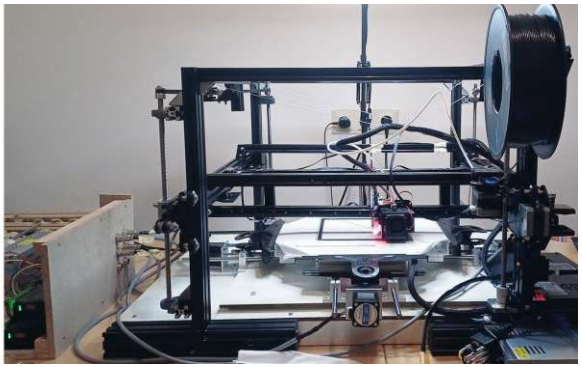

Figure 35: left: revised version of ground plate added to the fabrication set-up, right: full view of custom hardware

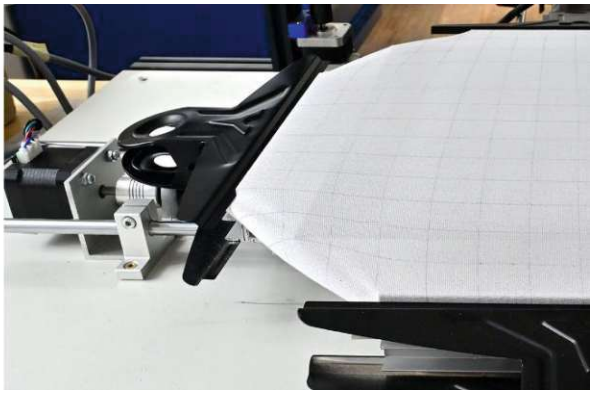

Figure 36: left: pointwise clamping mechanism with individual pins, right: linear clamping mechanism

Die approbierte gedruckte Originalversion dieser Diplomarbeit ist an der TU Wien Bibliothek verfügbar
The approved original version of this thesis is available in print at TU Wien Bibliothek.

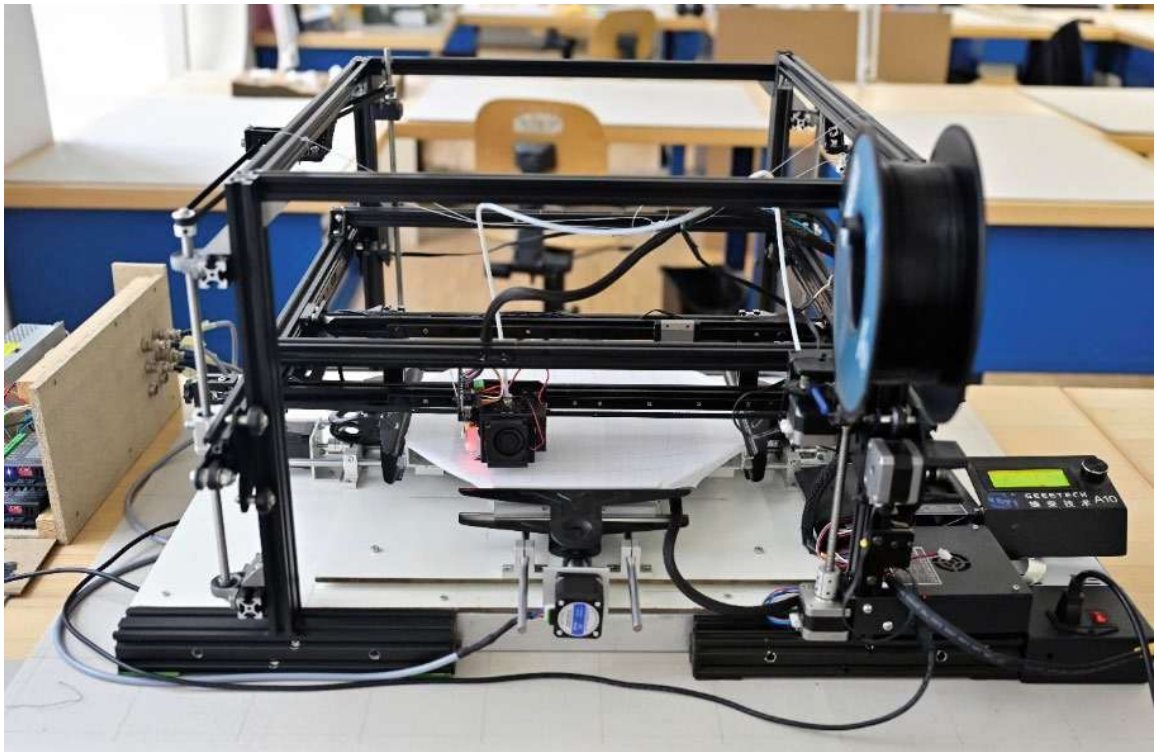

Figure 37: completed custom-built fabrication set-up at the modelbuilding workshop

Die approbierte gedruckte Originalversion dieser Diplomarbeit ist an der TU Wien Bibliothek verfügbar
The approved original version of this thesis is available in print at TU Wien Bibliothek.

Workflow

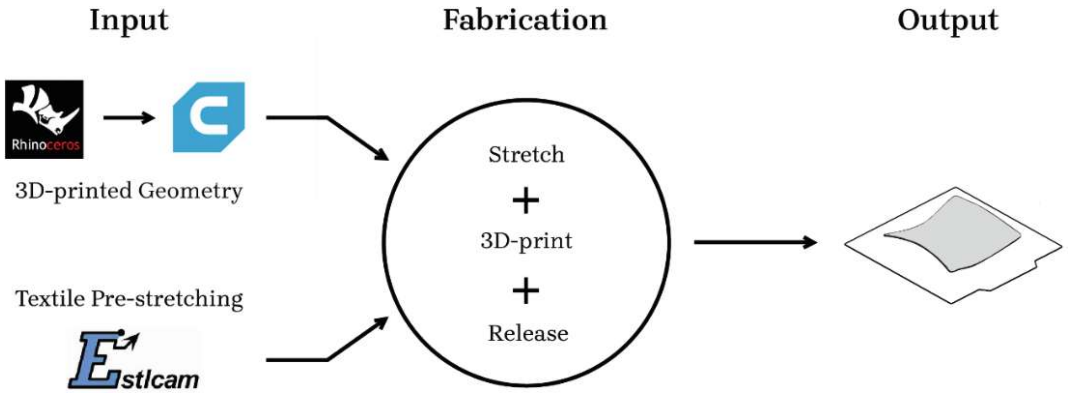

Figure 38: diagram of fabrication workflow from digital input to physical output

As illustrated in figure 38, the tile fabrication process starts with preparing the digital input parameters for the custom-built setup. This involves creating a 3D model of the boundary geometry in the Rhinoceros software environment. The model is then exported as an .stl file and imported into Ultimaker Cura, where it is "sliced," the 3D printing settings adjusted, and the data sent to the machine. Before printing, a piece of fabric is placed on the print bed, clamped, and the controller of the ground plate connected to the Estlecam Controller software, where the desired amount of pre-stretch is set. This input is automatically translated into corresponding movements by the stepper motors (figure 39, step 1). Once the pre-stretch is configured, the 3D printing process begins (step 2).

After printing, a specific post-production procedure was followed for all experiments conducted to avoid any unwanted alterations to the tile until full activation. The fabricated components were held in their stretched state for 10 minutes (Step 3). Next, the pre-stretch was released, the fabric unclamped (Step 4), and the tiles were left on a table for 30 minutes with the excess fabric still surrounding the 3D-printed frame (Step 5). Finally, the fabric was carefully trimmed (step 6).[60]

[60] (Lettner, Palma, & Baseta, 2024)

Die approbierte gedruckte Originalversion dieser Diplomarbeit ist an der TU Wien Bibliothek verfügbar
The approved original version of this thesis is available in print at TU Wien Bibliothek.

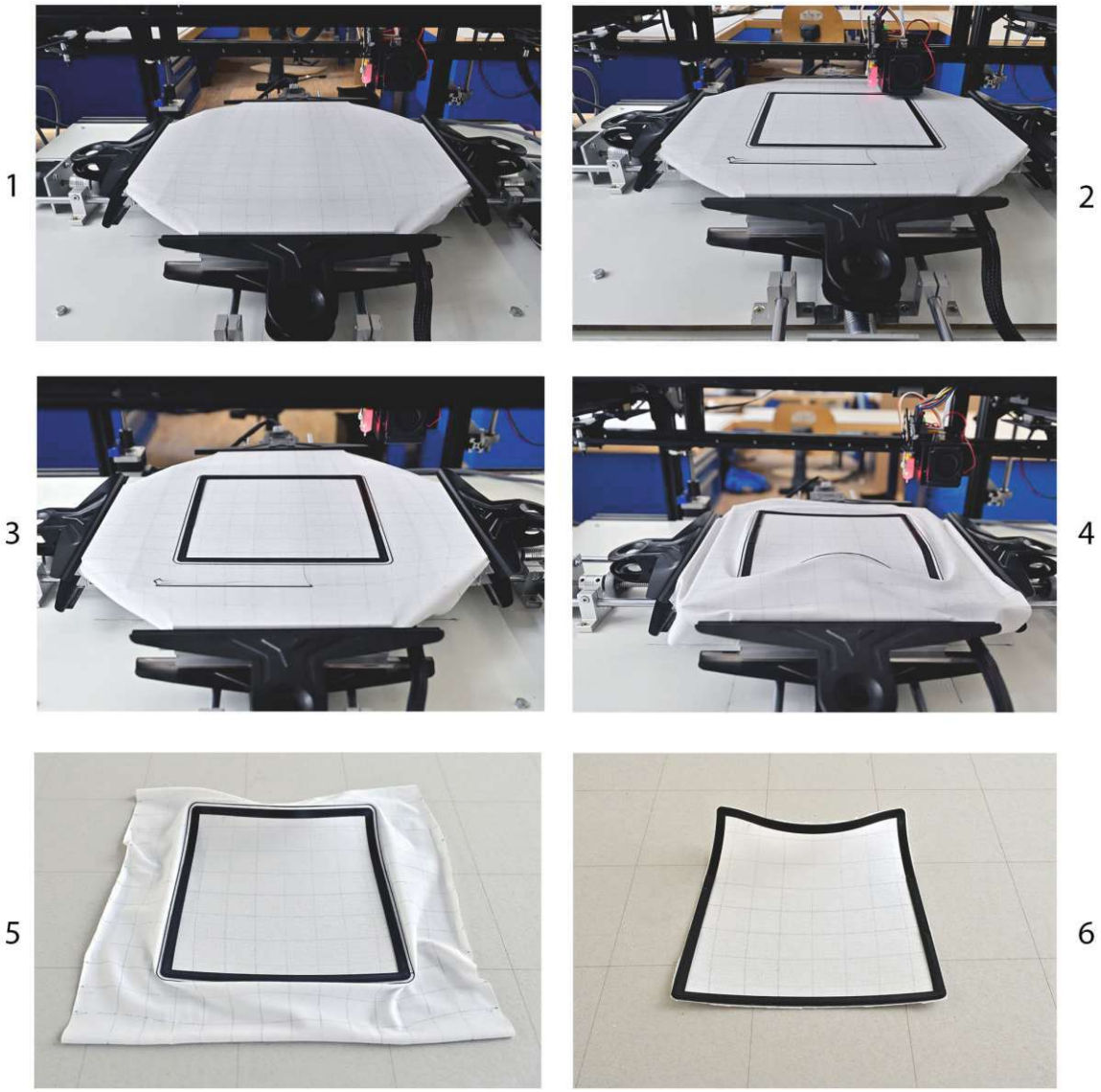

Figure 39: fabrication workflow: stretch – 3D print – release and post-printing procedure

Die approbierte gedruckte Originalversion dieser Diplomarbeit ist an der TU Wien Bibliothek verfügbar
The approved original version of this thesis is available in print at TU Wien Bibliothek.

Die approbierte gedruckte Originalversion dieser Diplomarbeit ist an der TU Wien Bibliothek verfügbar
The approved original version of this thesis is available in print at TU Wien Bibliothek.

4. Unit exploration

This chapter presents a series of material experiments aimed at understanding the inherent properties of individual active textile tiles (units) and examining how various fabrication parameters, such as the amount and pattern of pre-stretching or the 3D printed cross-section, affect the curvature. This was achieved through the custom-built fabrication setup (chapter 3.2.) enabling a series of systematic material experiments. The primary focus was on understanding how different fabrication techniques and parameters influence the resulting surface curvature, particularly along the edges of individual tiles. This exploration sought to enhance knowledge of the material system, enabling greater control over resulting curvature. The achievable range of double curvature within single tiles was examined and the relationships between these geometries were explored. The aim was to build upon these findings regarding active textile units when transitioning to fabricating tiled surfaces.

Before delving into these experiments, the chapter outlines the general framework, materials, and fabrication parameters used. Additionally, the evaluation process used for obtaining digital data from the physical tiles produced in the experiments is explained.

Die approbierte gedruckte Originalversion dieser Diplomarbeit ist an der TU Wien Bibliothek verfügbar
The approved original version of this thesis is available in print at TU Wien Bibliothek.

Material experiments

Following the initial testing phase outlined in chapter 3.1, viscose jersey fabric (figure 40) and PLA filament for 3D printing (figure 41) were selected as the materials for all subsequent experiments in this research. The material properties are provided in table 1. To achieve optimal print quality and ensure adequate adhesion between the textile and the PLA, 3D printing settings investigated in previous research and described in table 2 were used.[61],[62]

Table 1: material parameters used in all experiments.

	Material	Weight	Thickness	Geometry
Fabric	92% viscose, 8% elastane	220g/m²	0.3mm	280mm x 280mm
PLA	Geeetech Pure PLA		1.75mm	180mm x 180mm, 7.5mm wide, 0.7mm high

Table 2: print settings of 3D printer for every experiment.

			Layer Hight			
Hot End	Flow	Speed	Initial	Rest	Infill	z-Probe Offset
210°C	105%	25mm/s	0.15mm	0.2mm	100%	1.625mm

Computational design methods were employed to efficiently create digital input geometries (chapter 3.2, workflow) and obtain data on the curvature from the scanned physical samples. The 3D printed boundary geometry was standardized to square frames measuring 180x180 mm, as outlined in table 1. Throughout the experiments, the 3D printing settings and overall boundary geometry (except height) remained unchanged. Additionally, the weave pattern of the textile was meticulously aligned along the X and Y axes, ensuring consistency, and enabling a focused assessment of the effects of 3D printed boundary cross-section and textile pre-stretching variations on the activated tiles. No surface subdivisions of the textile through additional printed elements other than a boundary geometry were applied to individual tiles during these tests, differing from research done before as described under 2.2.2. [63]

[61] (Lettner, Palma, & Baseta, 2024)
[62] (Sitotaw, Ahrendt, Kyosev, & Kabish, 2020)
[63] (Lettner, Palma, & Baseta, 2024)

Die approbierte gedruckte Originalversion dieser Diplomarbeit ist an der TU Wien Bibliothek verfügbar
The approved original version of this thesis is available in print at TU Wien Bibliothek.

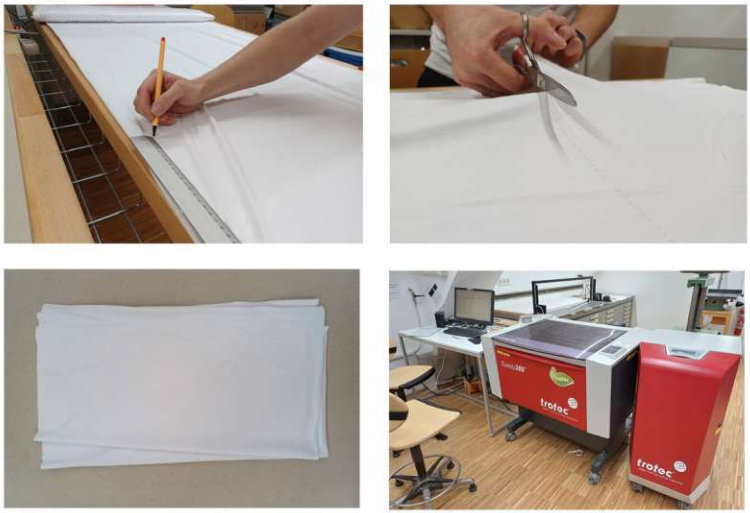

Figure 40: preparation of fabric pieces for printing

Figure 41: 3D printing filament used for all experiments

Die approbierte gedruckte Originalversion dieser Diplomarbeit ist an der TU Wien Bibliothek verfügbar
The approved original version of this thesis is available in print at TU Wien Bibliothek.

Evaluation process

To assess the geometries generated by the described methods, the fabricated sample tiles were measured using 3D scanning techniques. An Intel RealSense L515 LiDAR camera, with a 1024x768 pixel depth sensor resolution, was fixed in place relative to the samples (figure 42, left). Data capture as well as post-processing were automated within the McNeel Rhinoceros/Grasshopper environment, as shown in figure 43. Real-time depth data was streamed into Grasshopper (figure 42, right) using the "RS_GH" plugin[64]. With the "Get Frame" component, multiple point clouds of a single tile could be generated by saving individual frames. Post-processing involved clipping excess points and averaging the point clouds to minimize noise. The "Pico Grid" component was used to restructure the point cloud, which was then convoluted into a mesh and converted to an untrimmed N.U.R.B.S. surface. For each tile, two evaluations were conducted: a) z-displacement, visualized as a greyscale image and b) gaussian curvature analysis, rendered as a color gradient map.

Additionally, the surface edges of the fabricated tiles were extracted as curves from the digital data generated through the previously described process and analyzed for comparison. Evaluating the edges of the fabricated tiles was crucial for achieving the goal of tiling larger surfaces, particularly for the design exploration detailed in chapter 6, since precise control over the resulting edge curvature was essential. From the digitally extracted edges of each tile, one significant edge curve was identified as the *evaluation edge*. This edge was analyzed for its curvature and the z-displacement at the high point / low point of the curve, as well as its symmetry and consistency across curves produced with identical fabrication parameters (referred to as repeatability tests).[65]

The same labeling structure is applied to all test surfaces across the experiments discussed in this and the following two chapters. Individual tiles are labeled with capital letters (A, B, C, ...). The edges of these tiles or tiled surfaces, as described in chapters 5 and 6, are labeled with lowercase letters (a, b, c, ...). Numbers (B-1, B-2, ...) are used to distinguish between different versions of the same surface or multiple trials. The direction of textile pre-stretching is represented by the X and Y axes

[64] (Palma, 2024)

[65] (Lettner, Palma, & Baseta, 2024)

Die approbierte gedruckte Originalversion dieser Diplomarbeit ist an der TU Wien Bibliothek verfügbar
The approved original version of this thesis is available in print at TU Wien Bibliothek.

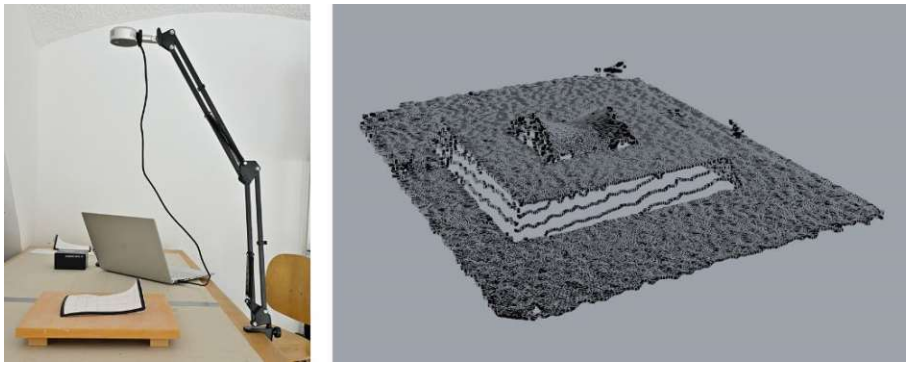

Figure 42: left: static scanning procedure with Intel RealSense L515 LiDAR camera, right: point cloud generated in the Grasshopper environment

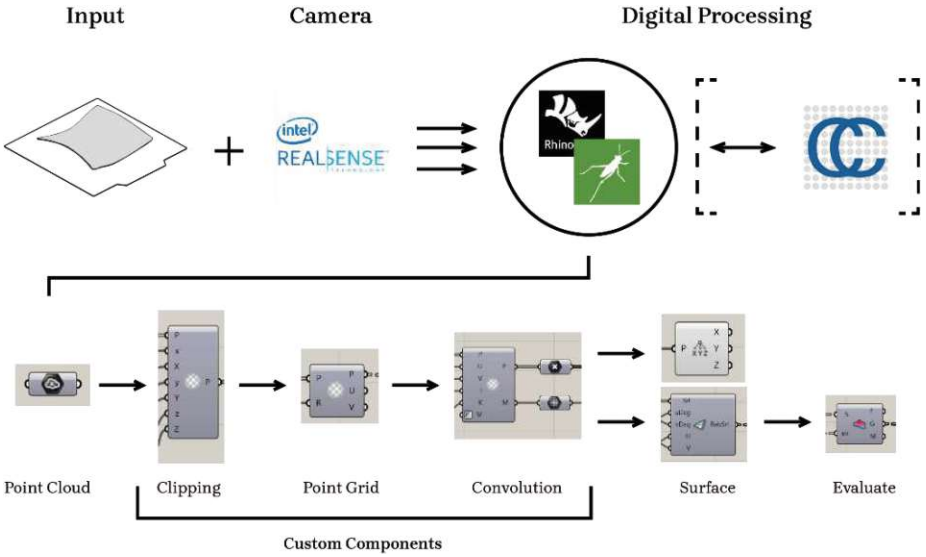

Figure 43: evaluation routine, focused on the aspect of digital point cloud processing

Die approbierte gedruckte Originalversion dieser Diplomarbeit ist an der TU Wien Bibliothek verfügbar
The approved original version of this thesis is available in print at TU Wien Bibliothek.

4.1. Uniform fabrication parameters

This series of experiments investigated how uniform pre-stretching, where the textile is stretched equally in both the X and Y directions, and the height of a uniformly 3D printed boundary, characterized by a constant printing thickness, affect the overall double curved geometry of an active textile tile. The goal was to establish a relationship between these parameters and the amount of curvature observed in the resulting test pieces, particularly at the edges of the tiles. It was assumed that the amount of pre-stretching applied to the textile inversely affects the curvature change in active textiles, in relation to the height of the 3D printed boundary geometry. The fabrication of all sample tiles was done using the linear clamping method described in chapter 3.2 and depicted in figure 44.

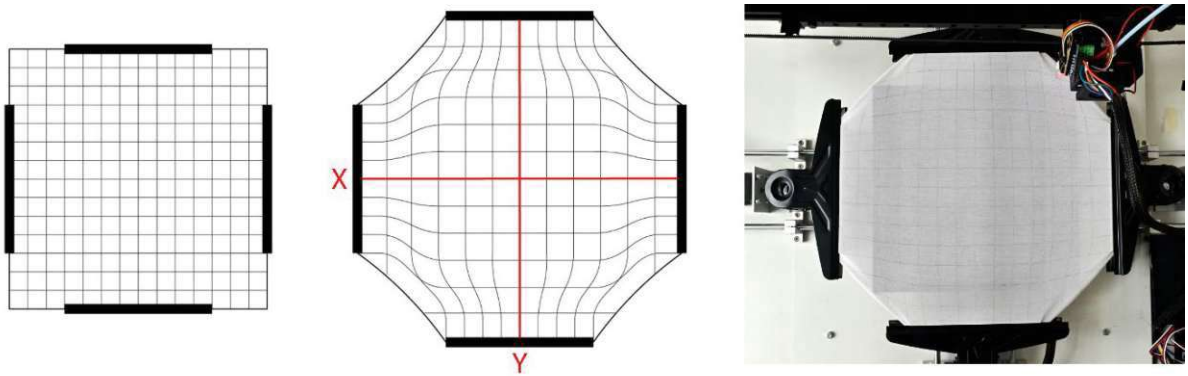

Figure 44: visualization of uniform pre-stretching and linear clamping.

Die approbierte gedruckte Originalversion dieser Diplomarbeit ist an der TU Wien Bibliothek verfügbar
The approved original version of this thesis is available in print at TU Wien Bibliothek.

Variation in uniform pre-stretching

The first subset of tiles was fabricated by varying the amount of uniform textile pre-stretching applied to each tile while maintaining a constant thickness for the 3D printed boundary geometry. This test provided insights into the range of achievable amount curvature at a constant 3D printed boundary geometry and changing intensity in pre-stretching. A total of four tiles were produced, with the pre-stretch in the X and Y directions of the textile linearly increasing from 56 mm (corresponding to 20% stretch of the initial textile size – figure 45, A) to 98 mm (35% stretch of the initial textile size – figure 45, D), as detailed in table 3 and illustrated by the resulting tiles in figure 45. This test revealed limitations in the custom fabrication setup and the textile used, with 98 mm representing the maximum achievable pre-stretch.

Table 3: increasing amount of pre-stretching used and constant parameters of 3D printed boundary geometry.

Fabric	A)	stretch X = Y = 56mm, 20%
	B)	stretch X = Y = 72mm, 25%
	C)	stretch X = Y = 84mm, 30%
	D)	stretch X = Y = 98mm, 35%
Border		180mm x 180mm, 7.5mm wide, 0.75mm high

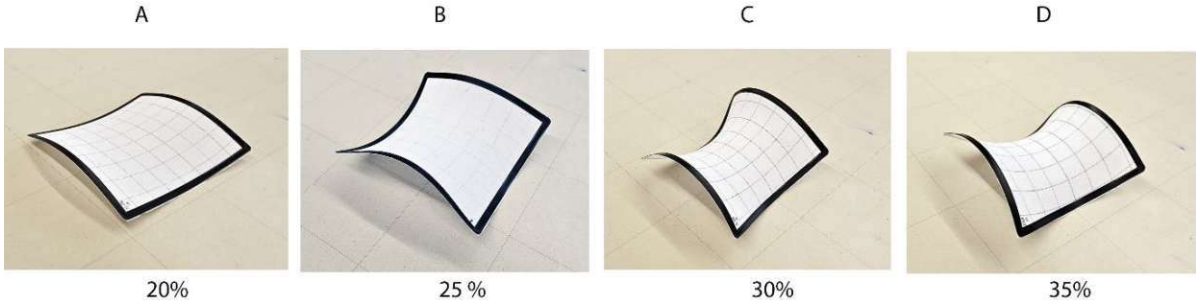

Figure 45: resulting tiles with increasing amounts of stretching.

Die approbierte gedruckte Originalversion dieser Diplomarbeit ist an der TU Wien Bibliothek verfügbar
The approved original version of this thesis is available in print at TU Wien Bibliothek.

Variation in uniform 3D printed boundary height

The second subset of tiles was fabricated by varying the height of the uniformly 3D printed boundary for each tile while keeping the amount of pre-stretching and other boundary geometry parameters (see table 4) constant throughout the tests. This experiment gave insights into the range of achievable curvature by changing the thickness of the 3D printed geometry at a constant 25% pre-stretching. Five tiles were produced with a linear increase in the thickness of the 3D printed boundary, as detailed in table 4. The tile with intermediate settings, 0.75 mm boundary height and 25% pre-stretching, tile G in figure 46, was carried over from the previous tile set. Tiles with a boundary height of 0.25 mm (figure 46, E) exhibited insufficient resistance for uniform activation, while those with a height of 1.25 mm (figure 46, I) demonstrated excessive resistance, hindering proper tile activation and were therefore excluded from evaluation later.

Table 4: increasing height of the 3D printed boundary geometry and constant pre-stretching used

Border	E)	Height: 0.25mm
	F)	Height: 0.5mm
	G)	Height: 0.75mm
	H)	Height: 1.0mm
	I)	Height: 1.25mm
Fabric		stretch X = Y = 72mm, 25%

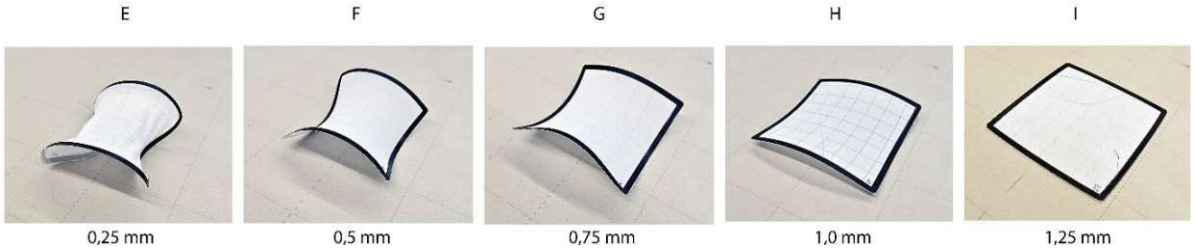

Figure 46: resulting tiles with increasing 3D printed boundary height and 25% pre-stretching.

Die approbierte gedruckte Originalversion dieser Diplomarbeit ist an der TU Wien Bibliothek verfügbar
The approved original version of this thesis is available in print at TU Wien Bibliothek.

The matrix presented in figure 47 integrates the results of the two test runs, offering a clear visual representation of the correlation between pre-stretching amount and 3D printed boundary height. The images of the tiles reveal a noticeable relationship in curvature: tiles with increased pre-stretch show similarities to those with reduced printing thickness. To further analyze this correlation, the tiles were evaluated as described in the beginning of chapter 4.

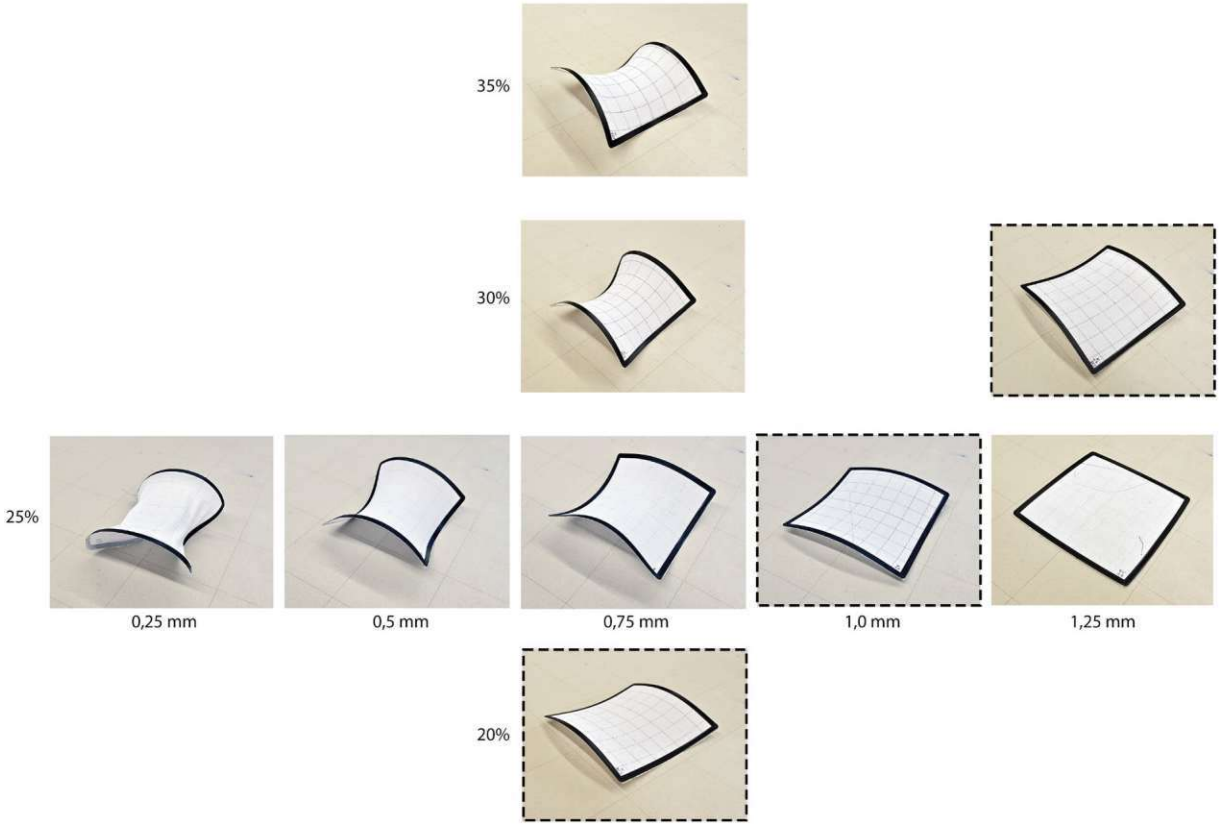

Figure 47: matrix of all fabricated tiles with parameters tested in sub-chapter 4.1.

Die approbierte gedruckte Originalversion dieser Diplomarbeit ist an der TU Wien Bibliothek verfügbar
The approved original version of this thesis is available in print at TU Wien Bibliothek.

Surface evaluation

The surface geometry evaluation highlights the correspondence between pre-stretching and boundary thickness as well. No comparable data could be gained from tile E = 25% / 0,25 mm (see figure 46) due to the strong wrinkling of the textile and from tile I = 25% / 1,25 mm (see figure 46) due to the tile being completely flat. Therefore, only three tiles are depicted in figure 49 representing the evaluation of the subset of tiles fabricated with varying 3D printed thickness and constant pre-stretch.

The greyscale images depicting z-displacement show an increase at higher amounts of pre-stretching (figure 48, top) and at reduced printing thickness (figure 49, top). Surface D = 35% in figure 48 shows only a slight variation to surface C = 30%, but a clearly noticeable difference in curvature (figure 48, bottom). This could hint at a possible cap of achievable z-displacement with the chosen 3D printed geometry. Nonetheless the greyscale images and the gaussian curvature analysis reflect a similar behavior of the tiles in the two sub-sets depicted in their corresponding figures 48 and 49. The main difference lies in the activation of the textile. A decrease in printing thickness quickly leads to wrinkling and loss of structural integrity as described before (figure 46).

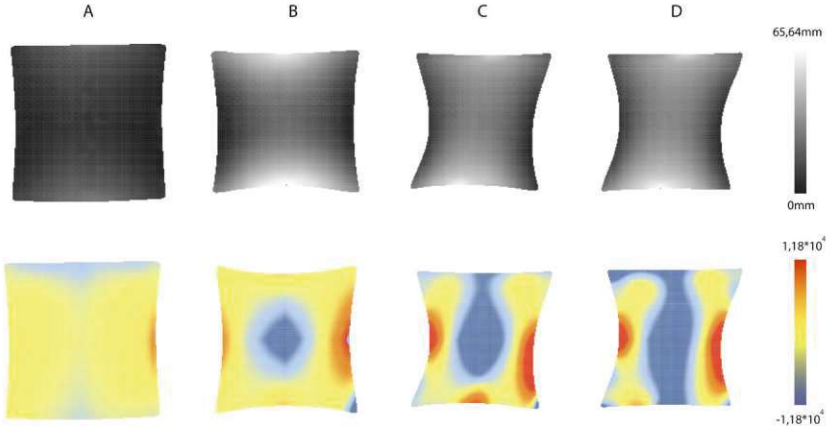

Figure 48: variable parameters of pre-stretching - top: z-displacement evaluation of point cloud, bottom: Gaussian curvature analysis of N.U.R.B.S. surface

Die approbierte gedruckte Originalversion dieser Diplomarbeit ist an der TU Wien Bibliothek verfügbar
The approved original version of this thesis is available in print at TU Wien Bibliothek.

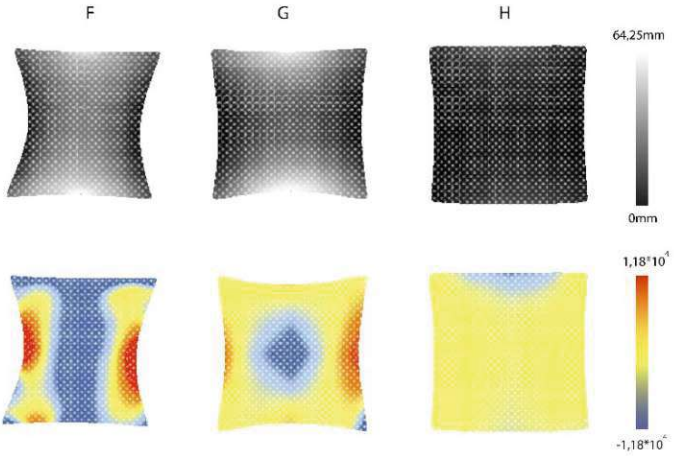

Figure 49: variable parameters of 3D printed boundary height - top: z-displacement evaluation of point cloud, bottom: Gaussian curvature analysis of N.U.R.B.S. surface

Edge evaluation

As noted in the beginning of the chapter, the curvature and z-displacement of the fabricated tile edges are key parameters for tiling applications. To analyze the behavior of tile edges in relation to specific fabrication parameters, the corresponding edge curves from the experiments are overlaid and color-coded. Figure 50, top illustrates the results for the series of tests with increasing pre-stretch, while figure 50, bottom shows the results for the series with increasing 3D printed boundary height.

The color-coded curves demonstrate a high degree of symmetry and clearly distinguish between the respective fabrication parameters. They further emphasize the inverse relationship between 3D printing height (e.g., figure 50, top: red curve) and the amount of pre-stretch (e.g., figure 50, bottom: red curve) in the resulting curvature.

Die approbierte gedruckte Originalversion dieser Diplomarbeit ist an der TU Wien Bibliothek verfügbar
The approved original version of this thesis is available in print at TU Wien Bibliothek.

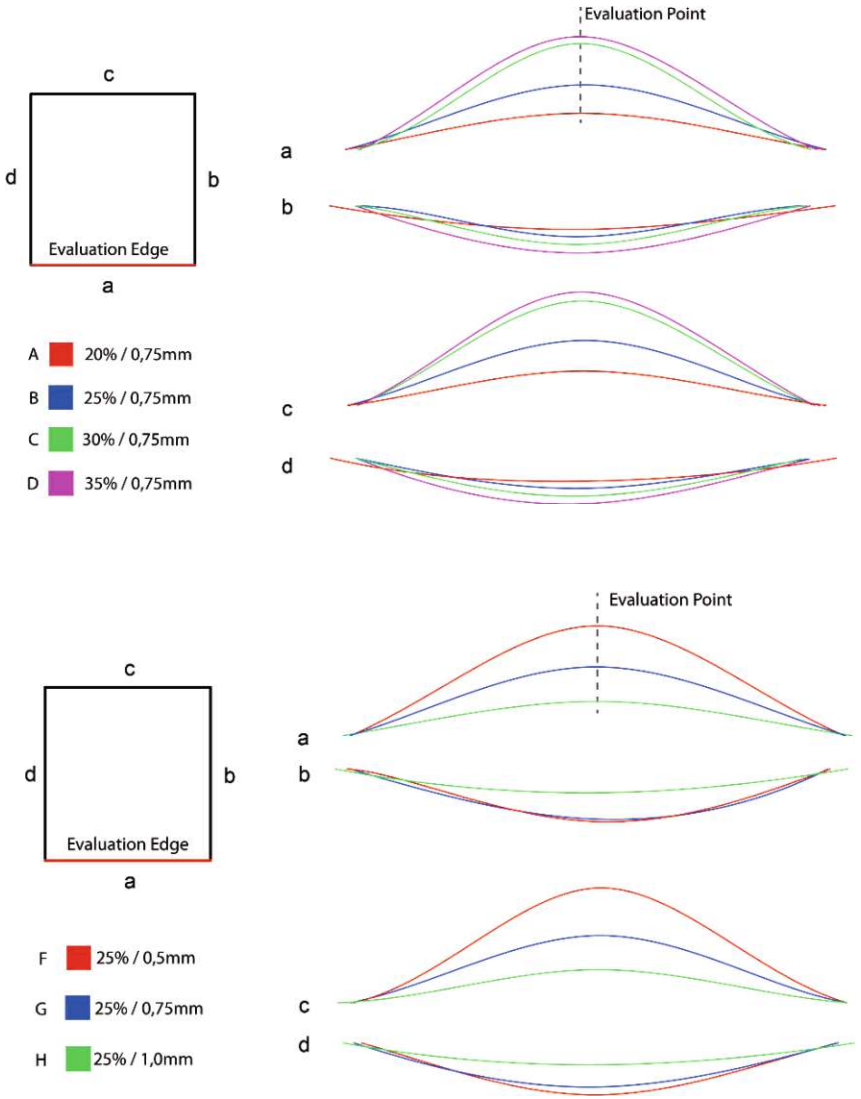

Figure 50: edge evaluation - top: tiles with changing amount of pre-stretching, bottom: tiles with increase in 3D printed boundary thickness

Die approbierte gedruckte Originalversion dieser Diplomarbeit ist an der TU Wien Bibliothek verfügbar
The approved original version of this thesis is available in print at TU Wien Bibliothek.

In the following graphs the resulting curvature (figure 51) and z-displacement (figure 52) at the evaluation points highlighted in figure 50 of the associated edge-curves are mapped to the fabrication parameters. Both datasets match somewhat the linear change in parameters used for the experiments described in table 3 and 4.

To investigate deeper the linear behavior of resulting curvature through linear variation of the corresponding parameters the sub-set highlighted in the matrix (figure 47) is compared. The tiles A, H and J show again strong similarities in z-displacement and gaussian curvature analysis with some deviation, especially at tile J.

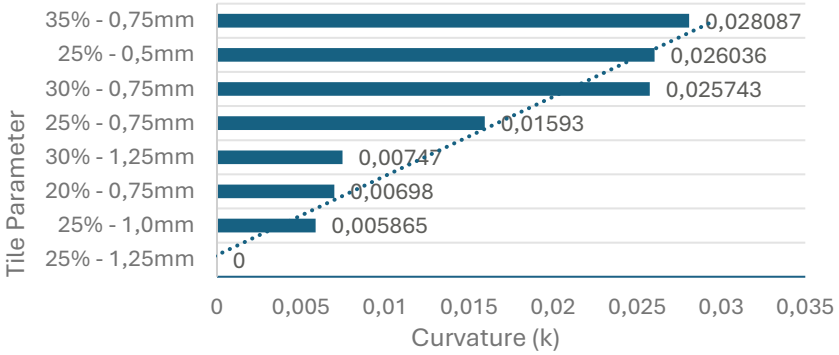

Figure 51: graph mapping curvature of the evaluated tile edge to the fabrication parameters

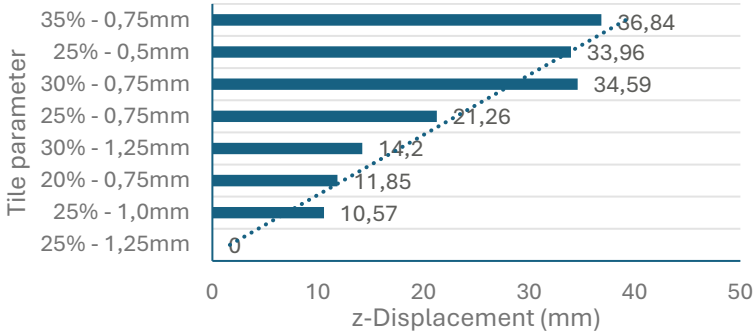

Figure 52: graph mapping z-displacement of the evaluated tile edge to the fabrication parameters

Die approbierte gedruckte Originalversion dieser Diplomarbeit ist an der TU Wien Bibliothek verfügbar
The approved original version of this thesis is available in print at TU Wien Bibliothek.

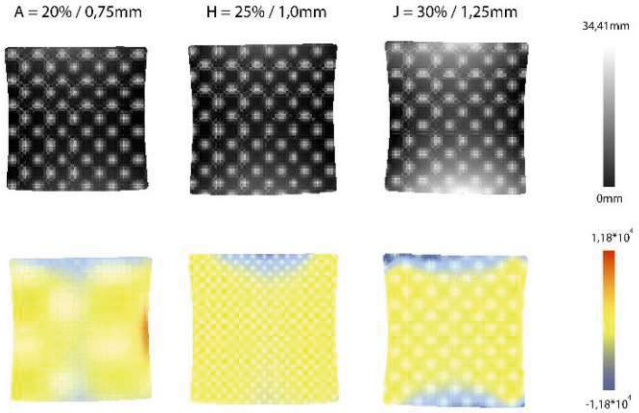

Figure 53: three corresponding tiles marked in figure 47 - top: z-displacement evaluation of point cloud, bottom: Gaussian curvature analysis of N.U.R.B.S. surface

Respectively, the comparison of the edge-curves as illustrated in figure 54 reveals high degrees with a maximum deviation of 2,25 mm observed at curve d. The maximum deviation at curves a and c is located close to the high point in contrast to curve b and d where it is close to the end of the curves. The greatest deviation from this linear behavior appears in figure 52, at the tile with 30% pre-stretch and a 1.25 mm boundary height.

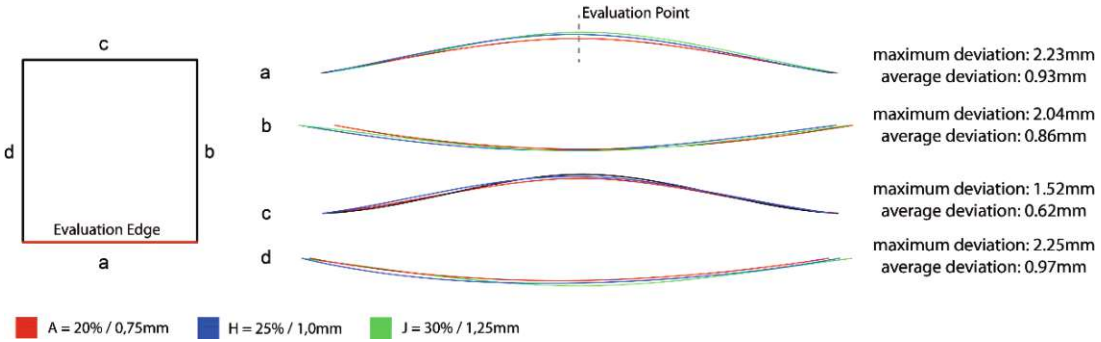

Figure 54: edge evaluation of the three corresponding tiles marked in figure 47

Die approbierte gedruckte Originalversion dieser Diplomarbeit ist an der TU Wien Bibliothek verfügbar
The approved original version of this thesis is available in print at TU Wien Bibliothek.

Repeatability

A third subset of three tiles (figure 55) was produced, all featuring identical design and fabrication parameters, including clamping type, textile pre-stretch, 3D printing settings, and boundary geometry to evaluate the repeatability of the proposed fabrication setup. The pre-stretch applied was 75 mm in both the X and Y directions (equating to a 25% stretch of initial textile size), and the same 3D printed uniform boundary cross-section as used in subset one, tile B, was applied, as detailed in table 3.[66]

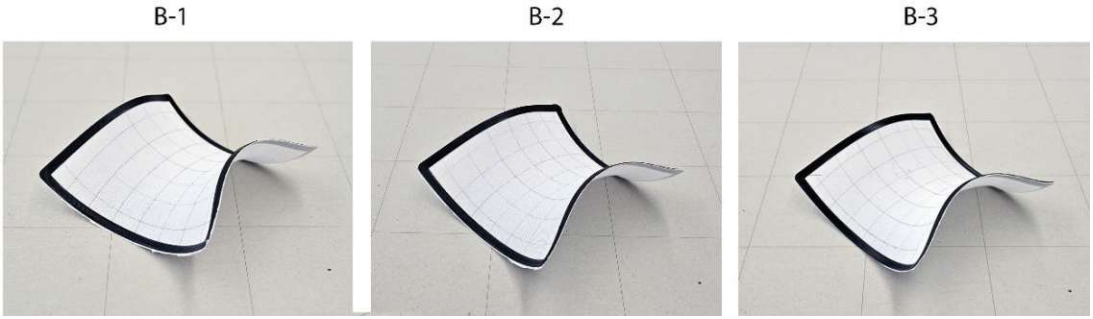

Figure 55: resulting tiles - uniform pre-stretching (25%) and uniform boundary cross sections

A distinct visual correlation is evident across the sample tiles in both z-displacement (figure 56, top) and Gaussian curvature (figure 56, bottom). The results generally demonstrate consistent activation across the entire tile surface. The Gaussian curvature analysis highlights the greatest deviations at the centers of the test pieces. The most pronounced anomaly occurs on surface B-3, where the region of highest positive curvature along the top edge is displaced 12.2 mm to the right of the tile.[67]

[66] (Lettner, Palma, & Baseta, 2024)
[67] (Lettner, Palma, & Baseta, 2024)

Die approbierte gedruckte Originalversion dieser Diplomarbeit ist an der TU Wien Bibliothek verfügbar
The approved original version of this thesis is available in print at TU Wien Bibliothek.

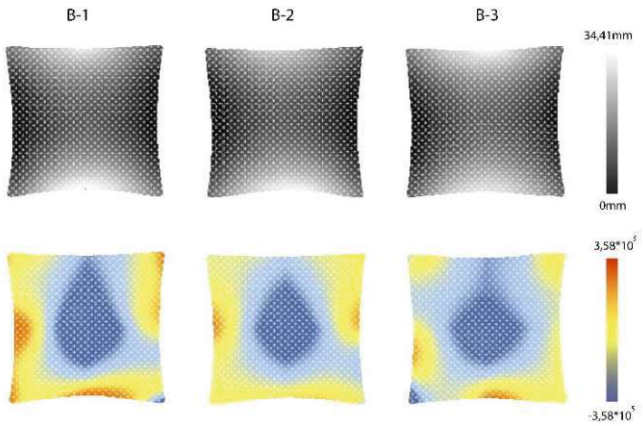

Figure 56: repeatability test - uniform stretching and uniform printing thickness – top: z-displacement evaluation of point cloud, bottom: Gaussian curvature analysis of N.U.R.B.S. surface

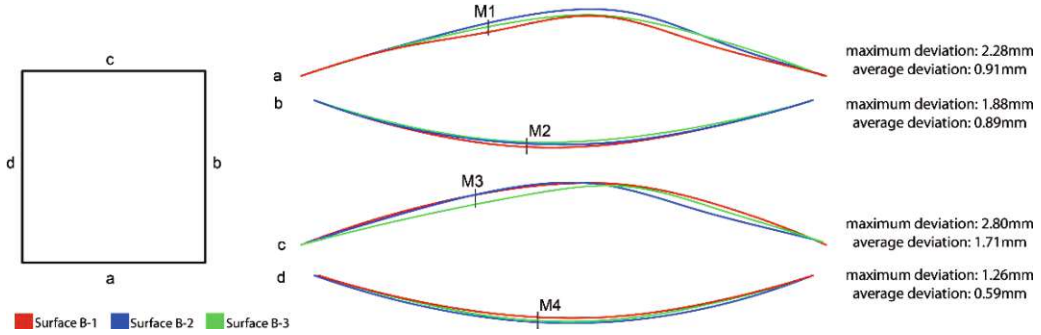

Figure 57: repeatability test - analysis of edges

Aligned with the curvature analysis, the edge comparison (figure 57) further emphasizes the noted shift on edge C of surface B-3. The peak of the curve on edge a is consistently offset by 8.5 mm from the center across all surfaces. The maximum deviation occurs at one-third of the curve for edge a (point M1) and edge c (point M3), while for edge b (point M2) and edge d (point M4), it is situated near the center. These offsets seem to correspond with opposing edges.

Die approbierte gedruckte Originalversion dieser Diplomarbeit ist an der TU Wien Bibliothek verfügbar
The approved original version of this thesis is available in print at TU Wien Bibliothek.

4.2. Non-uniform fabrication parameters

This sub-chapter presents two alterations to the previously described fabrication process, aimed at exploring the geometric possibilities of individual tiles within the proposed system. Specifically, it examines the effects of non-uniform pre-stretching and non-uniform printing thickness on the resulting surface geometries by manipulating individual tile edges. For both methods, as in the previous sub-chapter, repeatability is assessed, and parameter variations are tested to evaluate the range of achievable curvatures.

4.2.1. Non-uniform stretching

A modification to the fabrication method introduced in this thesis explored the effect of non-uniform pre-stretching along the textile boundary on the curvature of the resulting sample tiles. This approach aimed at demonstrating the feasibility of controlling the overall surface curvature by selectively manipulating a specific edge of the tile. In these experiments, the fabric was pre-stretched following a trapezoidal pattern using the point-wise clamping mechanism (see figure 58). Similar to the experiments described in section 4.1, the 3D printed boundary geometry, detailed in table 3, had a uniform cross-section. Two subsets of tiles were fabricated, focusing on activating the same edge: one to test repeatability and the other to test variability. For repeatability testing, three tiles were produced applying 90 mm of pre-stretch (30% of initial edge length) along axis X-1 (see figure 59, top). For variability testing, three additional samples were fabricated with varying pre-stretch levels of 20%, 40%, and 50% applied again to axis X-1 (see figure 59, bottom). Detailed parameters for these tests are provided in table 5.[68]

[68] (Lettner, Palma, & Baseta, 2024)

Die approbierte gedruckte Originalversion dieser Diplomarbeit ist an der TU Wien Bibliothek verfügbar
The approved original version of this thesis is available in print at TU Wien Bibliothek.

Table 5: variable fabrication parameters of non-uniform pre-stretching tiles

Fabric	A)	20% stretch: X-1 = 60mm, X-2 = 10mm, Y = 12mm
	B)	30% stretch: X-1 = 90mm, X-2 = 10mm, Y =12mm
	C)	40% stretch: X-1 = 120mm, X-2= 10mm, Y =12mm
	D)	50% stretch: X-1 = 150mm, X-2 = 10mm, Y =12mm
Border		180mm x 180mm, 7.5mm wide, 0.75mm high

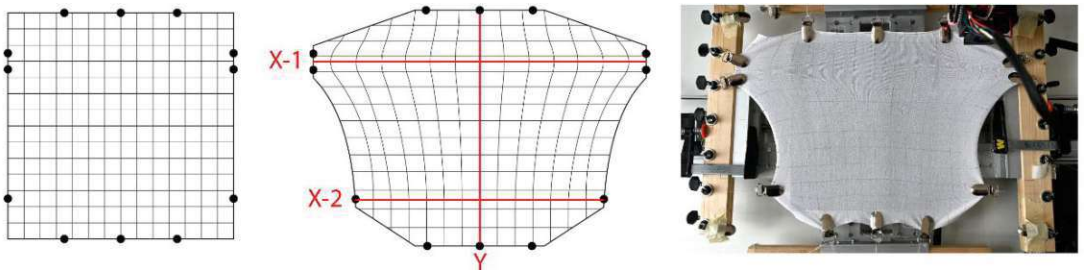

Figure 58: visualization of non-uniform pre-stretching and pointwise clamping

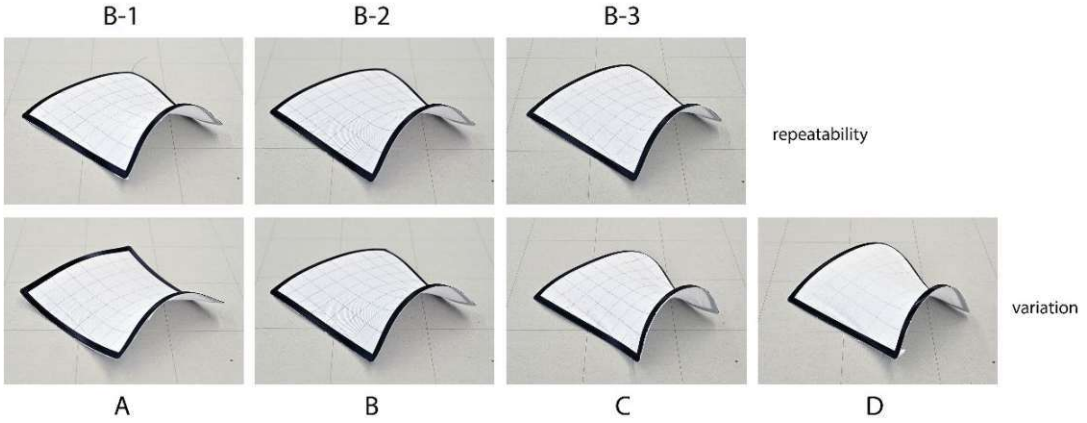

Figure 59: produced tiles – non-uniform pre-stretching top: repeatability test, bottom: test with variable pre-stretching parameter and resulting curvature

Die approbierte gedruckte Originalversion dieser Diplomarbeit ist an der TU Wien Bibliothek verfügbar
The approved original version of this thesis is available in print at TU Wien Bibliothek.

For the repeatability test tiles shown in figure 59, top, the grayscale images depicting z-displacement (figure 60, top) again highlight overall similarities between the samples. Both the z-displacement and the Gaussian curvature analysis (figure 60, bottom) point to the largest deviations occurring at the middle of the top edge. The most significant anomaly is observed on surface B-3, where the region of highest positive curvature appears along the top edge, accompanied by minor deviations in the tile outlines.

The grayscale images and Gaussian curvature analysis in figure 61 correspond to the variability test (figure 59, bottom). Surfaces A to D exhibit distinct visual differences, with the Gaussian curvature analysis confirming these variations but showing some deviations for the tile with 20% pre-stretching (Surface A). This surface geometry (figure 59) resembles those with uniform pre-stretching, as seen in the experiments discussed in section 4.1. It is inferred that a tile with non-uniform pre-stretching must exceed a specific threshold to induce a significant curvature change. This relationship is further illustrated by the graph in figure 62, which plots curvature as a function of pre-stretch percentage. The Gaussian curvature analysis of Surface D reveals numerous imperfections attributed to textile wrinkling under 50% pre-stretching, highlighting the material limitations of the textile used in these experiments.

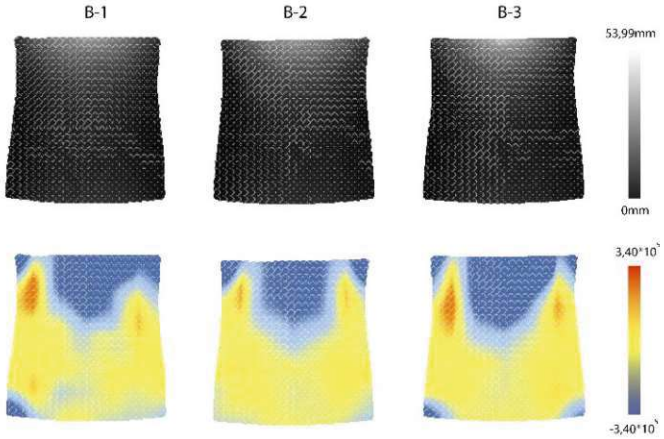

Figure 60: repeatability test – non-uniform pre-stretching– top: z-displacement evaluation of point cloud, bottom: Gaussian curvature analysis of N.U.R.B.S. surface

Die approbierte gedruckte Originalversion dieser Diplomarbeit ist an der TU Wien Bibliothek verfügbar
The approved original version of this thesis is available in print at TU Wien Bibliothek.

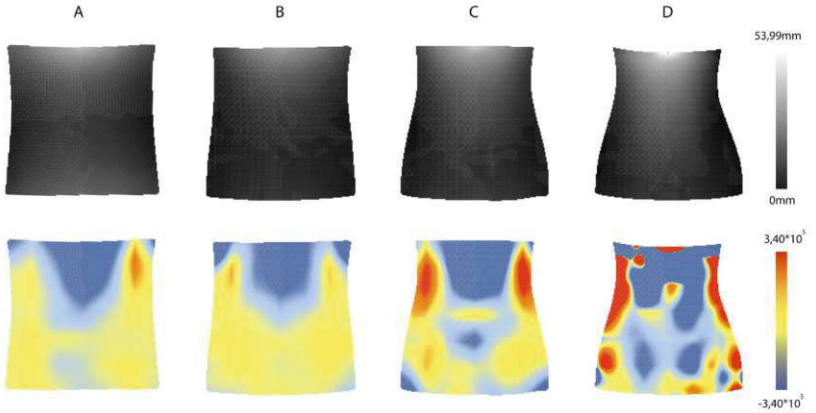

Figure 61: variable parameter of pre-stretching – non-uniform pre-stretching– top: z-displacement evaluation of point cloud, bottom: Gaussian curvature analysis of N.U.R.B.S. surface

Comparing the edge, highlighted in figure 62, left and correlating to X-1 (figure 58), of the active textile units tested for repeatability reveals a maximum deviation of 2.27 mm. The relationship between curvature and the amount of pre-stretch is illustrated in a graph (figure 62, right), which demonstrates exponential growth and highlights the previously mentioned threshold. Overall, the curves of the relevant edges exhibit some asymmetry and minor imperfections (figure 62, left).

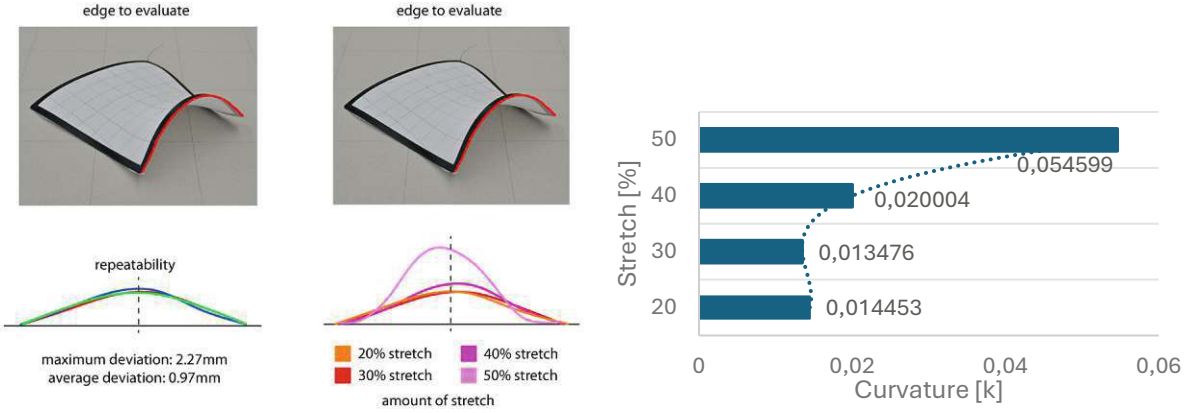

Figure 62: non-uniform pre-stretching - left: edge analysis, right: graph mapping curvature to amount of pre-stretch

Die approbierte gedruckte Originalversion dieser Diplomarbeit ist an der TU Wien Bibliothek verfügbar
The approved original version of this thesis is available in print at TU Wien Bibliothek.

4.2.2. Non-uniform printing thickness

Building on the modification of the fabrication method described in chapter 4.2.1, the fabrication procedure discussed in this sub-chapter explored how maintaining a constant textile pre-stretch along all four edges, while locally adjusting the geometry of the 3D printed boundary, could influence the bending resistance at the tile edges and, consequently, the overall surface curvature. As in section 4.2.1, three samples were produced to test repeatability (see figure 64, top), and three additional samples were created to test variability (figure 64, bottom). All tests applied a uniform pre-stretching of 75 mm (25% of the initial length) along both axes, as in the repeatability tests from section 4.1. The variability of the cross-section of the 3D printed boundary was defined by a parametric model, dividing the edges into segments of different heights, as shown in figure 63. This approach provided control in specific areas and at particular edges of the tile. The geometric parameters for the three different boundary designs are detailed in table 6.[69]

Table 6: variable fabrication parameters of non-uniform boundary cross section

Border	A)	Height: a = 0.5mm, b = 0.9mm, c = 1.3mm
	B)	Height: a = 0.8mm, b = 1.2mm, c = 1.6mm
	C)	Height: a = 1.1mm, b = 1.5mm, c = 1.9mm
Fabric		stretch X = Y = 72mm, 25%

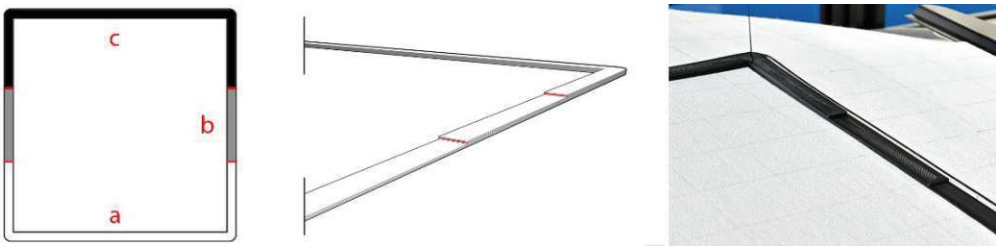

Figure 63: visualization of non-uniform boundary cross section

[69] (Lettner, Palma, & Baseta, 2024)

Die approbierte gedruckte Originalversion dieser Diplomarbeit ist an der TU Wien Bibliothek verfügbar
The approved original version of this thesis is available in print at TU Wien Bibliothek.

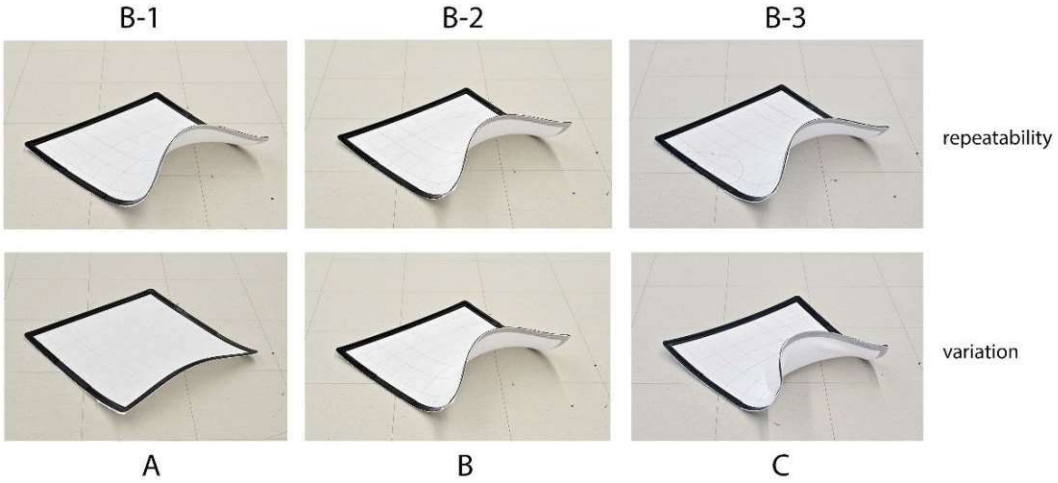

Figure 64: produced tiles – non-uniform boundary cross section, top: repeatability test, bottom: test with variable boundary cross section parameter and resulting curvature

A sharp incline on one side of an otherwise flat tile, as depicted in Figure 64, creates a noticeable gradient in the grayscale image. The lower edges of the tiles illustrated white in figure 65, top, display this bend in the geometry as z-displacement, with some variation between the surfaces. Since two-thirds of the tiles are flat, the Gaussian curvature analysis shown in figure 65, bottom provides limited data.

Examining the relationship between the resulting curvature and the 3D printed cross-section reveals a clear influence on the boundary of the tiles (figure 66), corresponding with figure 64, bottom. The maximum z-displacement (figure 66, top) occurs at Surface B, associated with the settings listed in table 4. The sharp incline at Surface C, which has the minimum cross-section, forms an overhang, accounting for the reduced z-displacement with simultaneously higher curvature (figure 66, bottom)

Die approbierte gedruckte Originalversion dieser Diplomarbeit ist an der TU Wien Bibliothek verfügbar
The approved original version of this thesis is available in print at TU Wien Bibliothek.

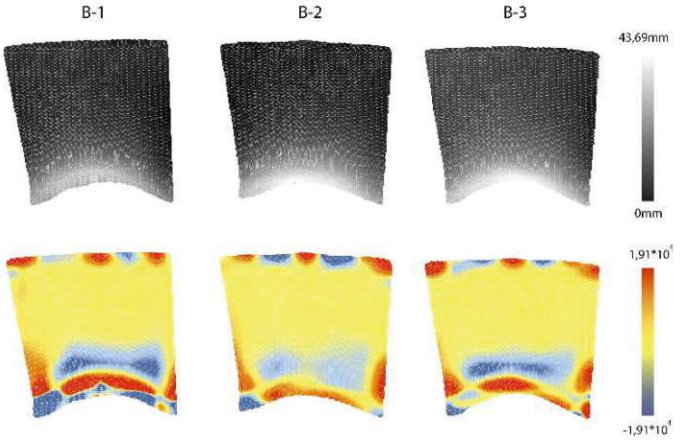

Figure 65: repeatability test – non-uniform boundary cross section – top: z-displacement evaluation of point cloud, bottom: Gaussian curvature analysis of N.U.R.B.S. surface

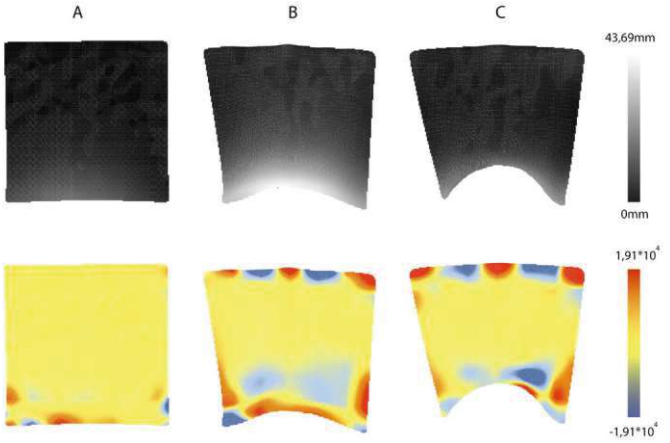

Figure 66: variable parameter of boundary cross section – non-uniform boundary cross section– top: z-displacement evaluation of point cloud, bottom: Gaussian curvature analysis of N.U.R.B.S. surface

Die approbierte gedruckte Originalversion dieser Diplomarbeit ist an der TU Wien Bibliothek verfügbar
The approved original version of this thesis is available in print at TU Wien Bibliothek.

The curves extracted from the relevant edge (figure 67, top) again provide data on the maximum and average deviations, which align with previously measured values. The graph mapping the resulting curvature to the boundary height (figure 67, bottom) exhibits an almost linear relationship. In these experiments, the curves display fewer imperfections and demonstrate a high degree of symmetry.

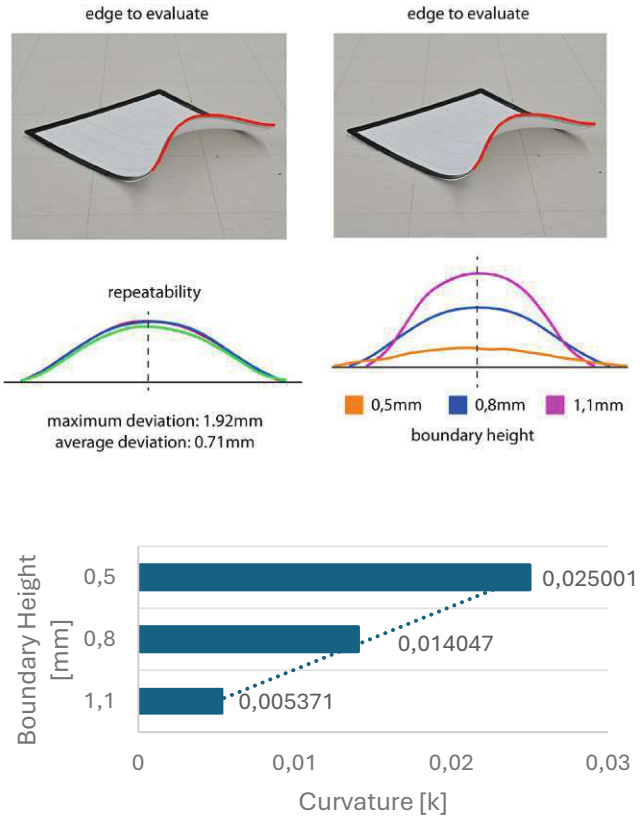

Figure 67: non-uniform boundary cross section - top: analysis of edges, bottom: graph mapping curvature to cross section thickness

Die approbierte gedruckte Originalversion dieser Diplomarbeit ist an der TU Wien Bibliothek verfügbar
The approved original version of this thesis is available in print at TU Wien Bibliothek.

4.3. Implementation of hinges

In addition to the modifications in the fabrication processes described in sections 4.2.1 and 4.2.2, a third method to control the curvature of the tile edges was explored. This sub-chapter focuses on the idea that by maintaining constant textile pre-stretching along all four edges and locally altering the geometry of the 3D printed boundary at the corners, the direction of the edge curvature in relation to one another can be controlled. To move beyond the regular geometry of the tiles produced in section 4.1, where opposing edges curve in the same direction, these experiments explored the ability to individually control the curvature direction of each edge. This approach was aimed at enabling edge-matching between tiles. The effect of fixed and bendable corners on the edges of the active textile tiles were examined, as described by (Vivanco, Valencia, & Yuan, 2020). Initially, four sample tiles were produced to test different hinge variations, followed by five additional tiles using one selected hinge type to explore different combinations. All tests again used a uniform pre-stretching of 75 mm (25% of the initial length) along both axes (as in section 4.2.2) and the same overall boundary geometry, except for the corners, as in chapter 4.1. The parameters for these tests are outlined in table 7.

Table 7: fabrication parameters of hinge tests

Fabric	stretch X = Y = 72mm, 25%
Border	180mm x 180mm, 7.5mm wide, 0.75mm high

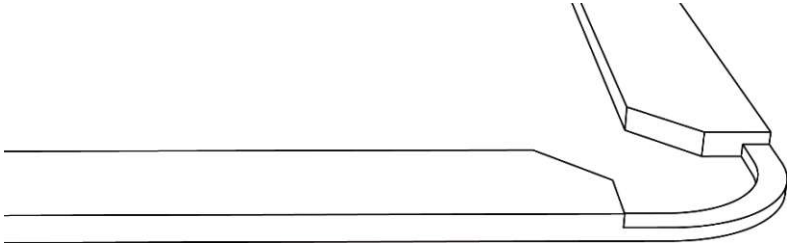

Figure 68: hinge design in Rhinoceros 3D

Die approbierte gedruckte Originalversion dieser Diplomarbeit ist an der TU Wien Bibliothek verfügbar
The approved original version of this thesis is available in print at TU Wien Bibliothek.

Table 8 provides a detailed description of the different hinge types tested as illustrated in figure 69. Tests V-1 to V-4 involved slits placed either diagonally in the corner (V-1, V-3) or perpendicular to each other (V-2). However, these slits proved inadequate for inducing significant changes in the overall geometry of the tile. As a result, the amount of PLA printed in the corners was further reduced to increase their flexibility. Hinge-type V-4 is a direct outcome of this adjustment, where two adjacent edges are connected only at the outline of the tile. This modification yielded the best results, offering improved flexibility at the corner.

With hinge-type V-4 identified as suitable for this fabrication method, five additional tiles were produced to explore various hinge placements.

Table 8: geometrical properties of the designed hinges

Hinge V-1	diagonal slit, cross section: 3.0mm long, 1.0mm wide, 0.25mm high
Hinge V-2	two perpendicular slits, cross section: 7.0mm long, 1.0mm wide, 0.5mm high
Hinge V-3	diagonal slit, cross section: 3.0mm long, 1.0mm wide, 0.5mm high
Hinge V-4	curve, cross section: 1.0mm wide, 0.5mm high

Figure 70 illustrates the tested configurations, ranging from a single hinge added to the 3D printed geometry in tile A to the maximum of four hinges in tile E. Tiles A, C, and D exhibit similar behaviors in geometric transformation with the addition of hinges. Along the diagonal where hinges are placed, the tile tends to fold, creating a noticeable "crease line" that significantly influences the overall geometry. Tile C, in particular, represents a unique case, as its specific diagonal not only forms a "crease line" but also serves as the axis of symmetry for the tile. In tiles B and E, the placement of hinges at consecutive corners clearly isolates the enclosed edge. This isolation allows all edges in tile E to curve in the same direction while leaving the remaining fabric in an otherwise completely flat state for both tiles.

Die approbierte gedruckte Originalversion dieser Diplomarbeit ist an der TU Wien Bibliothek verfügbar
The approved original version of this thesis is available in print at TU Wien Bibliothek.

Figure 69: different hinge-designs tested for function

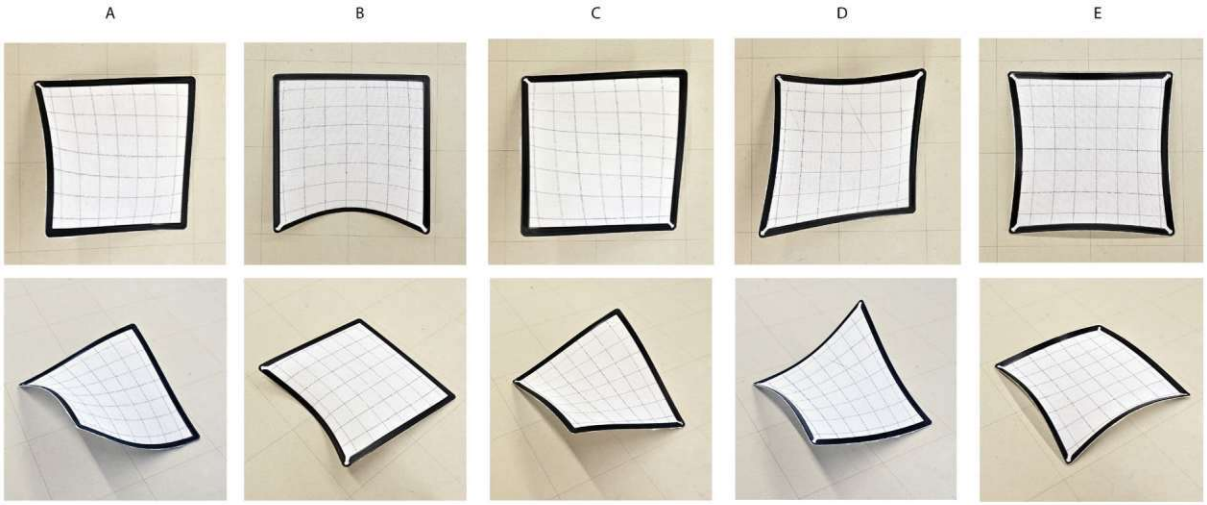

Figure 70: resulting tiles - different hinge placements - adding 1 – 4 hinges

Die approbierte gedruckte Originalversion dieser Diplomarbeit ist an der TU Wien Bibliothek verfügbar
The approved original version of this thesis is available in print at TU Wien Bibliothek.

The gaussian curvature analysis (figure 71, bottom) confirms this observation of a flat tile with curvature only at the edges enclosed by hinges for tile B and E with the latter still showing overall double curvature of the tile. Similarities of tiles A, C and D can be found in the color graded map when compared and especially in the greyscale images depicting z-displacement (figure 71, top) the strong influence of the diagonal where the hinges were placed on the overall tile geometry is evident.

The diagram in figure 72 presents a lineup of the corresponding edge curves for the individual tiles depicted in figure 70, with symbols indicating their behavior. Similar to the surface analysis (figure 71), tiles A, C, and D exhibit comparable characteristics, though this curve comparison highlights distinct differences. Tile D distinctly demonstrates a pattern of three edges curving downward and one curving upward, whereas the curvature directions in tiles A and C are less clearly defined. As previously noted, tile C represents a unique case, with all edge curves displaying nearly identical curvature and strong symmetry along the diagonal. Tile E exhibits consistent curvature direction across all edges, a result of edge isolation caused by the hinge placement, as also observed in tile B in figure 70.

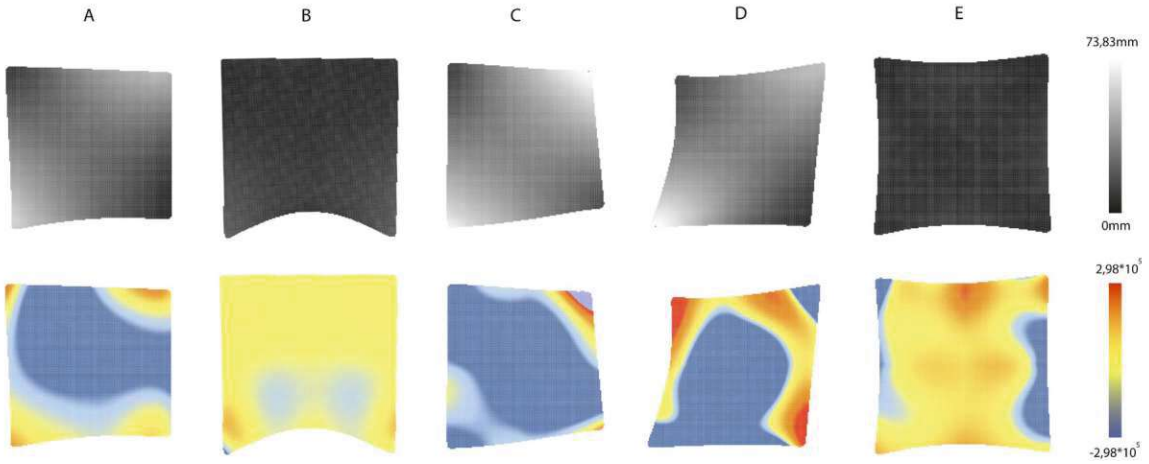

Figure 71: different hinge placements– top: z-displacement evaluation of point cloud, bottom: Gaussian curvature analysis of N.U.R.B.S. surface

Die approbierte gedruckte Originalversion dieser Diplomarbeit ist an der TU Wien Bibliothek verfügbar
The approved original version of this thesis is available in print at TU Wien Bibliothek.

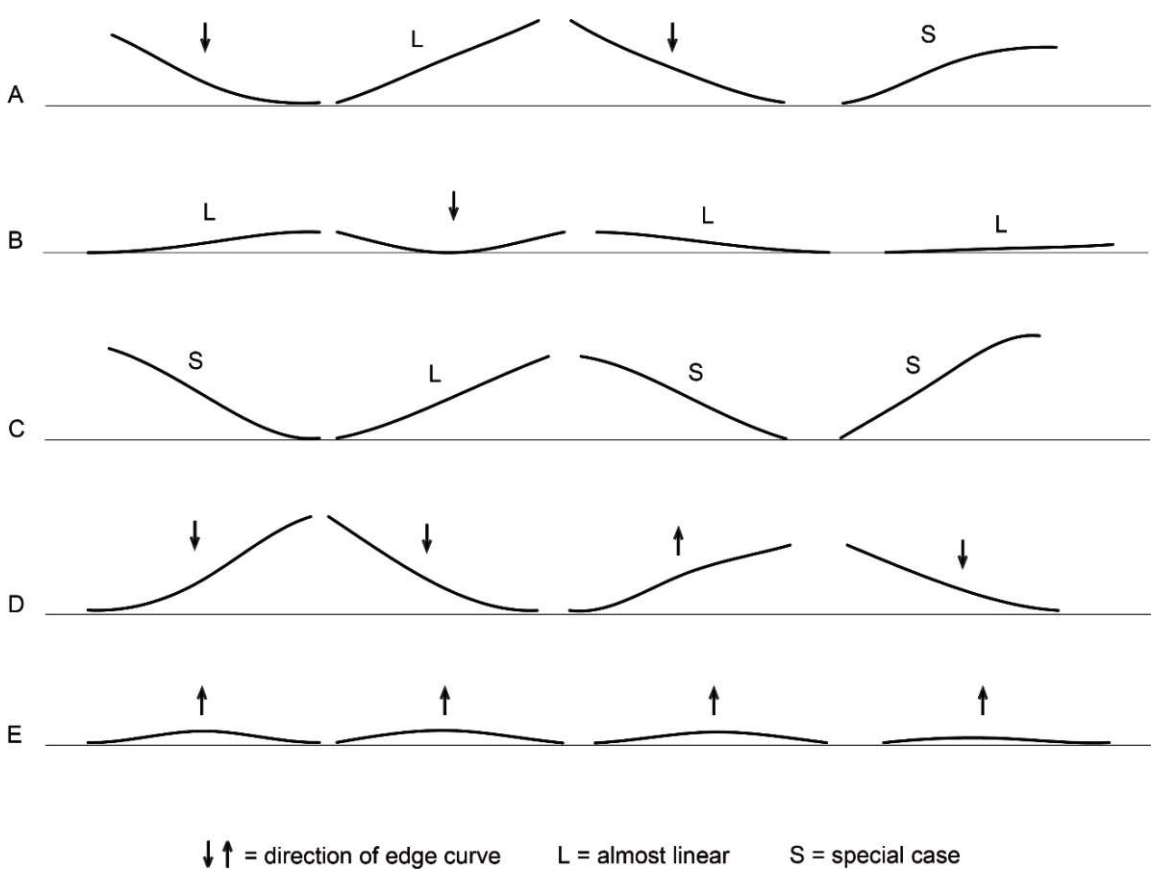

Figure 72: different hinge placements - diagram of direction of edge curvature in relation to one another

Die approbierte gedruckte Originalversion dieser Diplomarbeit ist an der TU Wien Bibliothek verfügbar
The approved original version of this thesis is available in print at TU Wien Bibliothek.

Die approbierte gedruckte Originalversion dieser Diplomarbeit ist an der TU Wien Bibliothek verfügbar
The approved original version of this thesis is available in print at TU Wien Bibliothek.

5. Tiling exploration

After various fabrication methods and parameters examined in previously conducted experiments to understand the material system and achieve control over the double curved geometry of individual active textile tiles, particularly at the edges, this chapter shifts focus to the explored potential of tiling surfaces, referred to as systems of tiles, adapting the knowledge gathered in chapter 4 to a larger scale. The following experiments investigated the interaction between individual tiles and a global surface system, as well as the influence they exerted on one another and possible resulting geometries of tiled surfaces. Additionally, the flexibility of the composite material and the adaptability of the entire system were analyzed to identify potential advantages. Insights gained from these experiments aim to enhance the ability to predict and control the outcomes of a tiled surface.

All experiments in this chapter were based on the fabrication parameters outlined in previous sections: uniform tiles from chapter 4.1 (tables 3 and 4) and hinged tiles from chapter 4.3 (tables 7 and 8, using hinge-type V-4). The overall geometry of the 3D printed boundary remained consistent throughout this chapter, with variations limited to printed height and the amount of textile pre-stretching.

Die approbierte gedruckte Originalversion dieser Diplomarbeit ist an der TU Wien Bibliothek verfügbar
The approved original version of this thesis is available in print at TU Wien Bibliothek.

Evaluation process

The evaluation process for individual pieces (see chapter 4) was adapted for larger tiled surfaces, with multiple edge combinations, that exceeded the camera's frame. A 6-axis collaborative robot was employed (figure 73) which facilitated capturing multiple frames of the entire surface by ensuring camera movement aligned in one plane with the model. The post-processing of the data gained required some additional steps for aligning and merging the various point clouds captured from one surface (figure 43). Initial alignment of individual sections was performed in Grasshopper, followed by precise alignment and merging using the 3D processing software CloudCompare. After cleaning and combining the data, a sub-sampled version of the point cloud was re-imported into the Grasshopper environment to complete the same processing routine applied to smaller samples described in chapter 3.

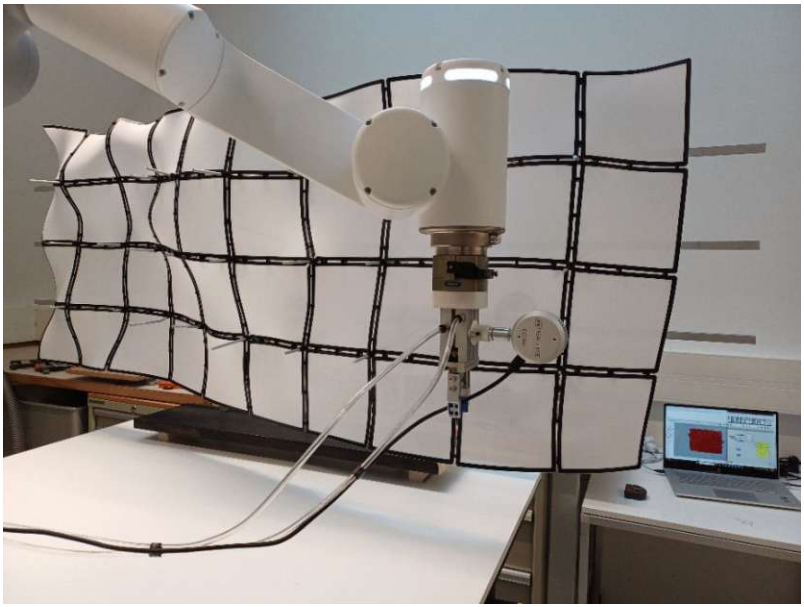

Figure 73: scanning procedure with Intel RealSense L515 LiDAR camera and the aid of a 6-axis collaborative robot

Die approbierte gedruckte Originalversion dieser Diplomarbeit ist an der TU Wien Bibliothek verfügbar
The approved original version of this thesis is available in print at TU Wien Bibliothek.

5.1. Single edge combination

For the first subset of experiments a basic combination method was applied, focusing on two-tile systems made exclusively from uniform tiles (fabricated in section 4.1) joined along one edge. To ensure comparable data was gathered, one uniform tile remained constant across all experiments (tile A in table 9), while it was paired with four other uniform tiles featuring varying parameters (tile B to D in table 9). This setup explored two distinct combination methods and their effects on the resulting system. The first method assumed when tiles with different fabrication parameters, and therefore different curvatures, are combined, they achieve a new equilibrium state, with both tiles adapting. In this approach, only edges curved in the same direction, referred to as **"matching edges,"** were joined (figure 74, middle row). The second method explored the deliberate pairing of edges that curved in opposite directions (figure 74, bottom row). This approach assumed that the tiles would adapt to a new equilibrium state with more pronounced differences in geometry and edge curvature, thereby broadening the design possibilities. This method is referred to as **"opposing edges."** Table 9 outlines the key parameters, printed height and pre-stretch amount, of the uniform tiles used, with detailed fabrication parameters provided in section 4.1 (table 4). The matrix in figure 74 summarizes the tested combinations, highlighting the test involving two tiles with identical parameters.

Table 9: fabrication parameters of changing combinations 1 to 4

1)	A = 0.75mm / 25% + B = 1.25mm / 25%
2)	A = 0.75mm / 25% + C = 1.0mm / 25%
3)	A = 0.75mm / 25% + A = 0.75mm / 25%
4)	A = 0.75mm / 25% + D = 0.5mm / 25%

Die approbierte gedruckte Originalversion dieser Diplomarbeit ist an der TU Wien Bibliothek verfügbar
The approved original version of this thesis is available in print at TU Wien Bibliothek.

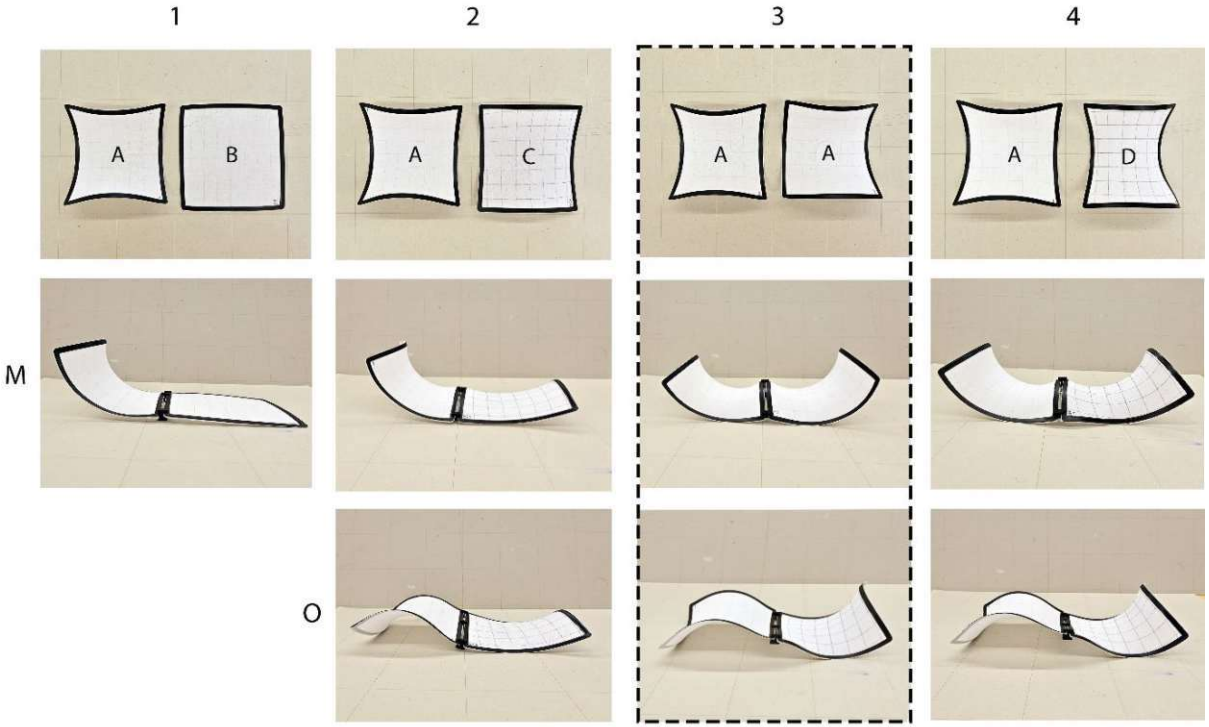

Figure 74: matrix of combination tests done on one edge

Die approbierte gedruckte Originalversion dieser Diplomarbeit ist an der TU Wien Bibliothek verfügbar
The approved original version of this thesis is available in print at TU Wien Bibliothek.

Matching edges

Figure 75 illustrates the subset of combinations where the "matching edges" method was applied. The differences in tile parameters are particularly evident in columns 1-M and 2-M, where the curvature of tile B and C significantly contrasts with that of tile A when observed individually. Upon combination, the curvature of tile A appears to adapt to that of the other tiles. In column 4-M, a slight variation can be observed compared to column 3-M when the tiles are combined. This suggests that the 3D printed boundary height plays a critical role in the interaction between active textile tiles. The side with the lower boundary height tends to adjust to the side with the greater height. As a result, in combinations 1-M and 2-M, tile A adapts to the other tiles, while in combination 4-M, tile D adjusts to tile A.

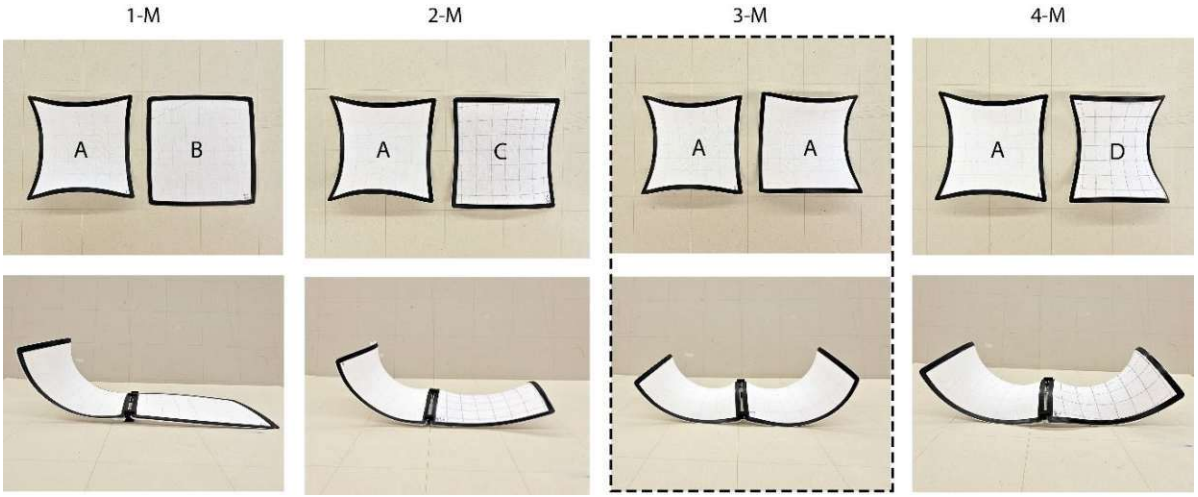

Figure 75: matrix of subset of combination test: matching edges

Die approbierte gedruckte Originalversion dieser Diplomarbeit ist an der TU Wien Bibliothek verfügbar
The approved original version of this thesis is available in print at TU Wien Bibliothek.

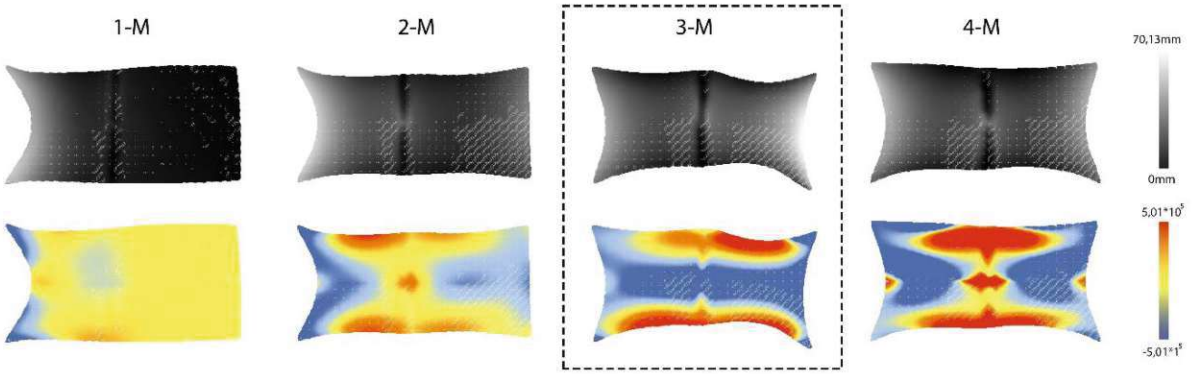

Figure 76: matching edges – combinations - top: z-displacement evaluation of point cloud, bottom: Gaussian curvature analysis of N.U.R.B.S. surface

This assumption is supported by the Gaussian curvature analysis of the combined surfaces shown in figure 76, bottom. The color-graded map for 1-M highlights a significant decrease in curvature across the 2-tile system. Combinations 2-M through 4-M exhibit greater similarity, with a noticeable increase in curvature from 2-M to 3-M and a slight further increase in 4-M. When combining similar tiles with corresponding edges, the individual tiles appear to remain largely independent of each other. This is indicated by the prominent connection line, which acts as an axis of symmetry in the Gaussian curvature analysis. The analysis of the shared edge, illustrated in figure 77, section, where the tiles are connected, shows notable variations in curvature, particularly when compared to the dashed red curve representing the original edge curve of tile A. This finding further supports the assumption that the tiles adjust to establish a new equilibrium state. The graph in figure 78 presents the resulting curvature values at the high points of the section curves.

Die approbierte gedruckte Originalversion dieser Diplomarbeit ist an der TU Wien Bibliothek verfügbar
The approved original version of this thesis is available in print at TU Wien Bibliothek.

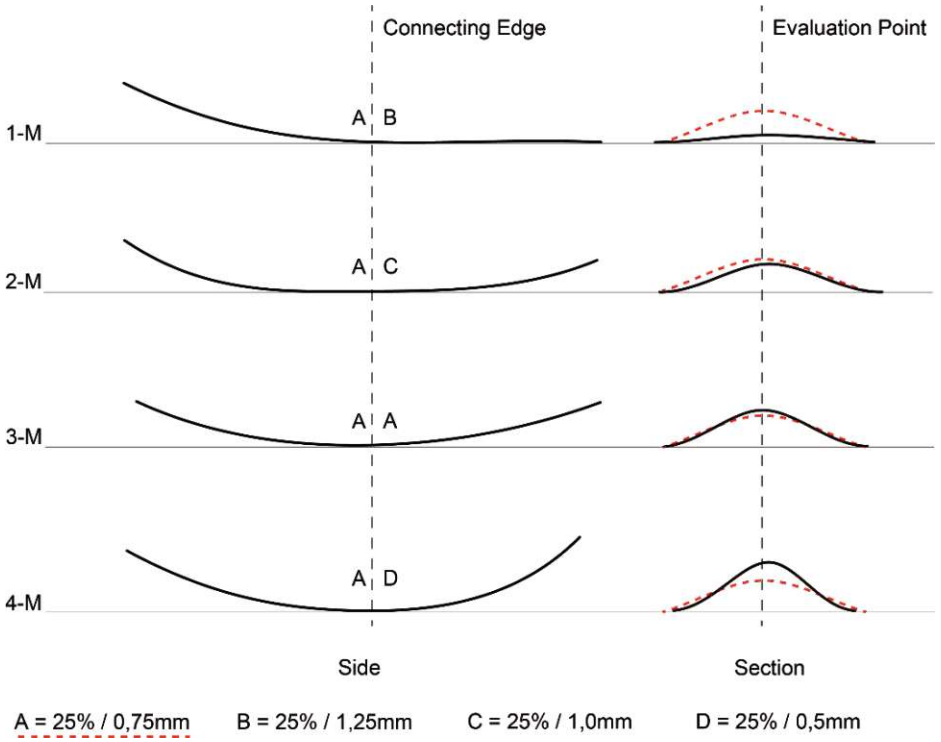

Figure 77: matching edges combinations – diagram of adjacent curves and shared edge curves

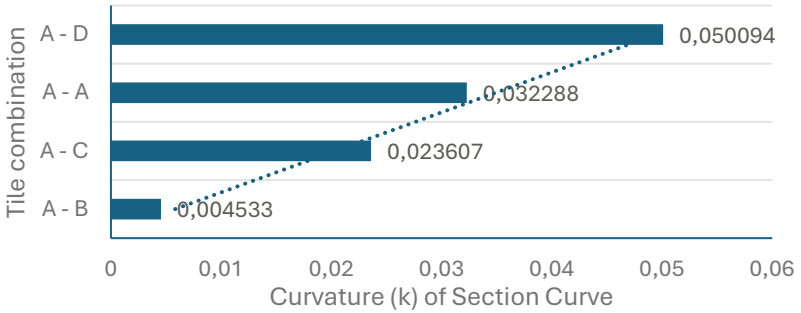

Figure 78: matching edges combinations – graph of curvature at high point of section curves

Die approbierte gedruckte Originalversion dieser Diplomarbeit ist an der TU Wien Bibliothek verfügbar
The approved original version of this thesis is available in print at TU Wien Bibliothek.

Opposing edges

As the next step, the combination of uniform tiles at edges that curve in opposite directions was tested, as shown in figure 79. This sub-set took advantage of the material system's flexibility, allowing manipulation of the curvature of the edges. For columns 2-O to 4-O an overall similar behavior can be observed with the "opposing edge" method, where a significant change in edge geometry occurs. The curvatures of the joined edges appear to cancel each other out, following a similar pattern as the previous "matching edges" approach, where the edge with the smaller 3D printed cross-section aligns with the edge having the larger printed cross-section. Of particular interest are the two long adjacent edges of the 2-tile system, which form an inflection point near the junction where the tiles meet.

Still some similarities can be found between the different combinations when comparing the greyscale image (figure 80, top) and the color graded map (figure 80, bottom), but in general not a lot can be said just by looking at the gaussian curvature analysis or the z-displacement. The most prominent difference to the approach of combining “matching edges” (figure 76) is the missing symmetry and blending of the curvature of the two tiles, highlighting a global activation of the combined system of tiles.

Die approbierte gedruckte Originalversion dieser Diplomarbeit ist an der TU Wien Bibliothek verfügbar
The approved original version of this thesis is available in print at TU Wien Bibliothek.

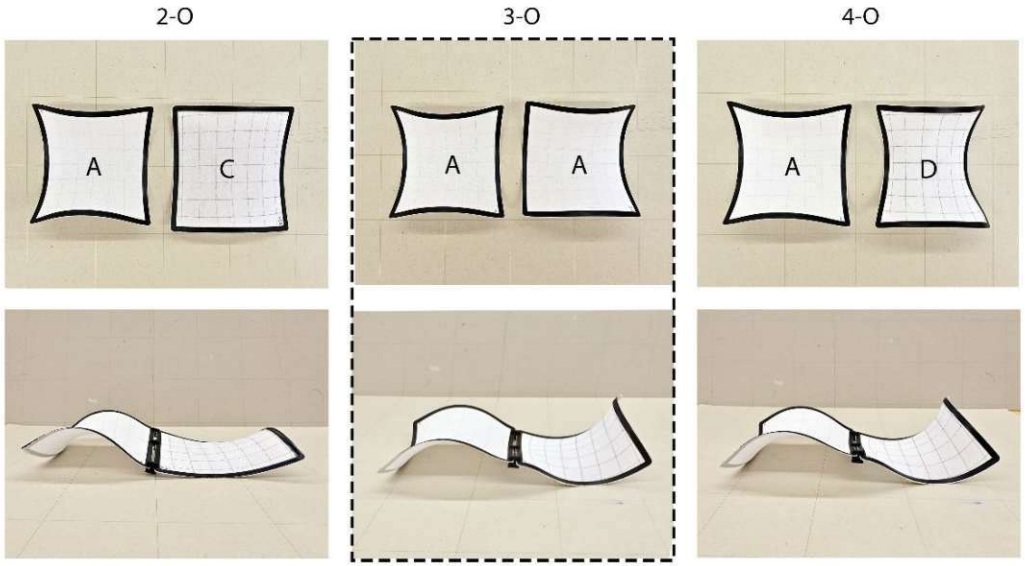

Figure 79: matrix of subset of combination test: opposing edges

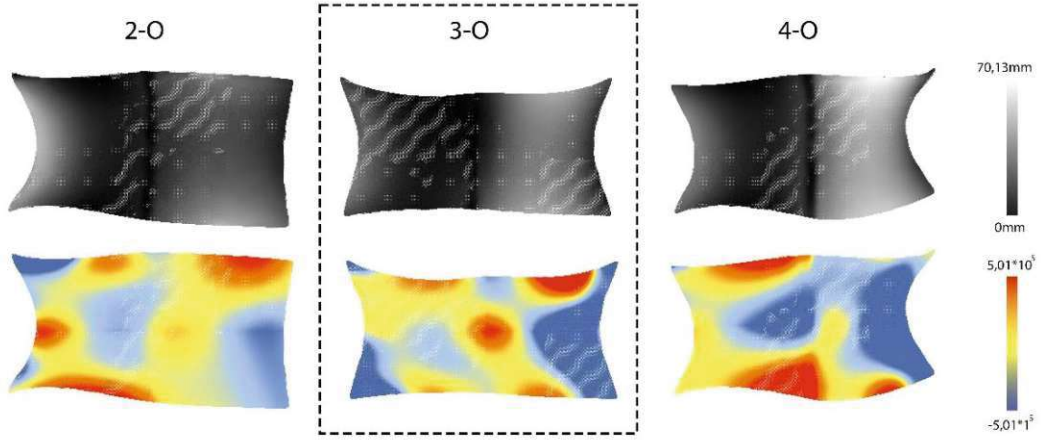

Figure 80: opposing edges – combinations - top: z-displacement evaluation of point cloud, bottom: Gaussian curvature analysis of N.U.R.B.S. surface

Die approbierte gedruckte Originalversion dieser Diplomarbeit ist an der TU Wien Bibliothek verfügbar
The approved original version of this thesis is available in print at TU Wien Bibliothek.

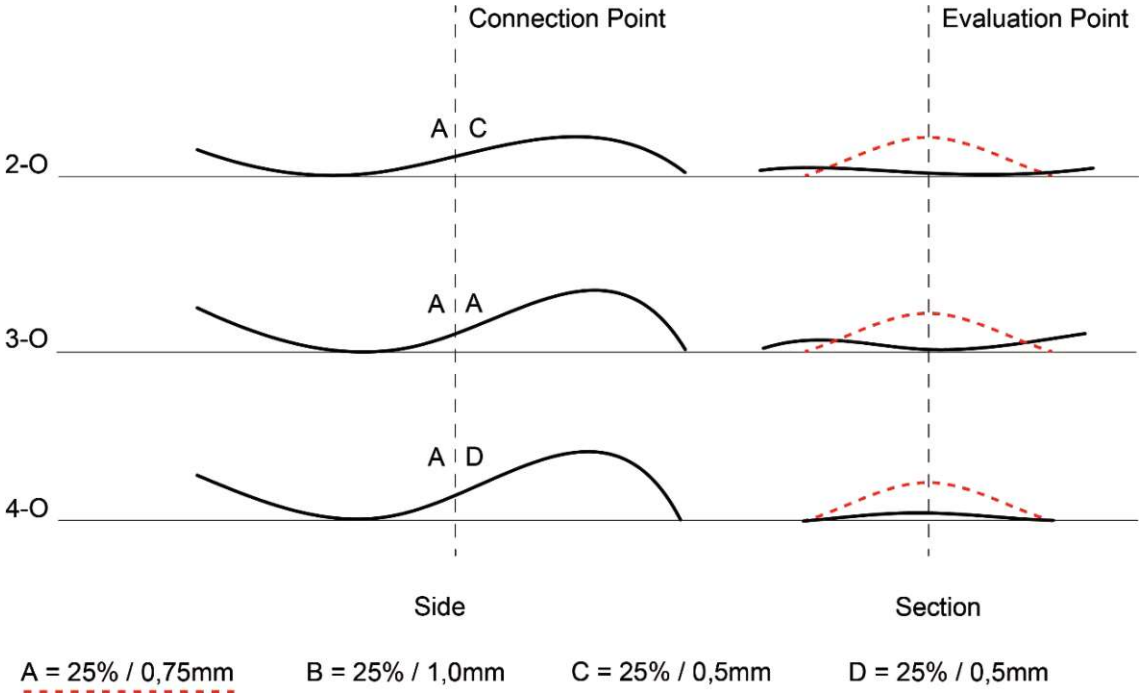

Figure 81: opposing edges combinations – diagram of adjacent curves and shared edge curves

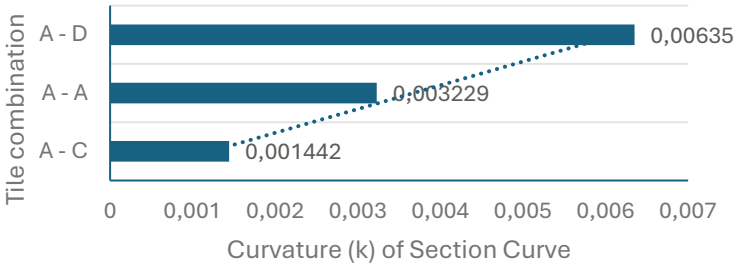

Figure 82: opposing edges combinations – graph of curvature at high point of section curves

Die approbierte gedruckte Originalversion dieser Diplomarbeit ist an der TU Wien Bibliothek verfügbar
The approved original version of this thesis is available in print at TU Wien Bibliothek.

The edge evaluation of this method confirms the observations made earlier (figure 81). First, examining the adjacent side edges, columns 2-O to 3-O show similar overall geometries, with varying amounts of curvature aligning with the individual curvature of each tile. An inflection point can be found on the curve near the connection point of the two tiles. When considering the shared edge, the curvatures of the individual tile edges nearly cancel each other out. In figure 82, the graph presents the resulting curvature values at the high points of the section curves, with all three curvature values being significantly lower compared to the graph in figure 78.

With the “opposing edges” method, the curvature of the connected edges is nearly canceled out, causing the 2-tile system to remain in one plane when combined. This contrasts with the “matching edges” approach, where the tiles tend to “curl up”. If more tiles were added using the same method, the “opposing edges” technique would result in a tiled double curved surface that stays in one plane (figure 83, left). In contrast, connecting additional tiles with the matching edge method would create the inside of a torus (figure 83, right) with strong limitations in possible designs.

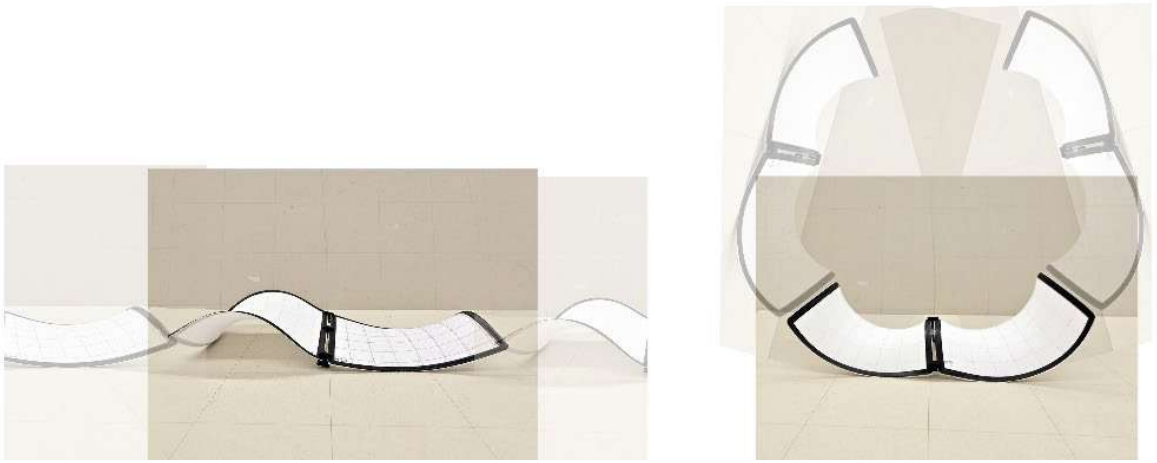

Figure 83: collage of further connected tiles – left: opposing edges, right: matching edges

Die approbierte gedruckte Originalversion dieser Diplomarbeit ist an der TU Wien Bibliothek verfügbar
The approved original version of this thesis is available in print at TU Wien Bibliothek.

5.2. Multiple edge combinations

The next logical step was to explore not only the influence of a 2-tile combination on the overall geometry and edge curvature, but also the combination of multiple tiles. In this initial test, a central uniform tile with a 25% uniform pre-stretch and a 0.75 mm uniform 3D printed boundary height, parameters consistent with the tile used in the experiments from chapter 5.1 (tile A in table 9), was used. Additional uniform tiles with varying parameters were connected to each edge of the central tile. As surrounding tiles, the same tiles as in the previous sub-chapter 5.1. (detailed in table 10, tiles B to E) were used for these connections with both combination methods, "matching edges" and "opposing edges," applied. It was assumed that after attaching a uniform tile to each edge of the central tile (tile A), the geometry of the central tile, particularly the curvature of the connected edges, would adjust according to the previously established principle regarding the influence of the 3D printed boundary cross sections. The evaluation focuses on the central uniform tile, observing changes in surface geometry and edge curvature as it reacts to the addition of other tiles on all four edges. Table 10 outlines the basic parameters, 3D printed boundary height and pre-stretching amount, for the tiles used in the experiment. Figure 84 provides an overview of the combined surface and illustrates the combination method employed.

Table 10: fabrication parameters of tiles according to the combination sequence

A	0.75mm / 25%
B	0.75mm / 25%
C	0.5mm / 25%
D	1.0mm / 25%
E	1.25mm / 25%

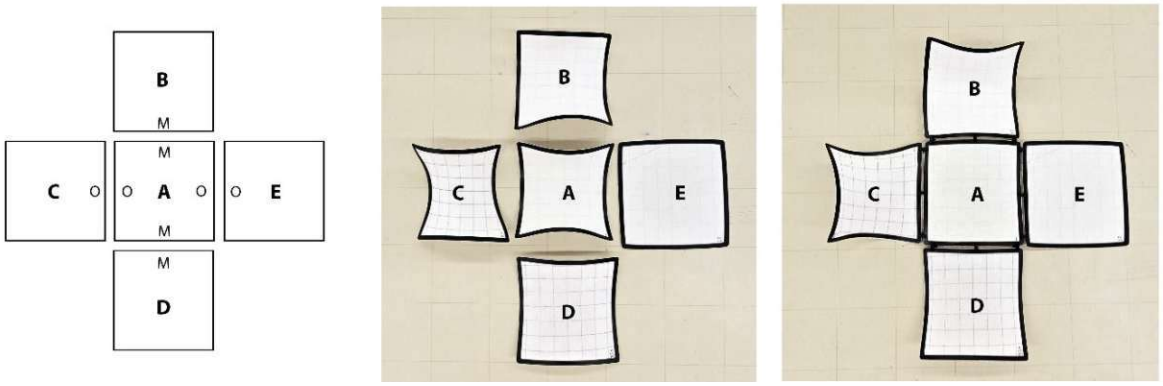

Figure 84: matrix of combination test done on multiple edges

During the process of attachment depicted in figure 85 (tiles A to E) no complications like wrinkling, damage to the 3D printed boundary, or tiling issues while the tile was forced into the new activation-state could be observed. Central tile A could accommodate the transition between the surrounding tiles and a new equilibrium state was established.

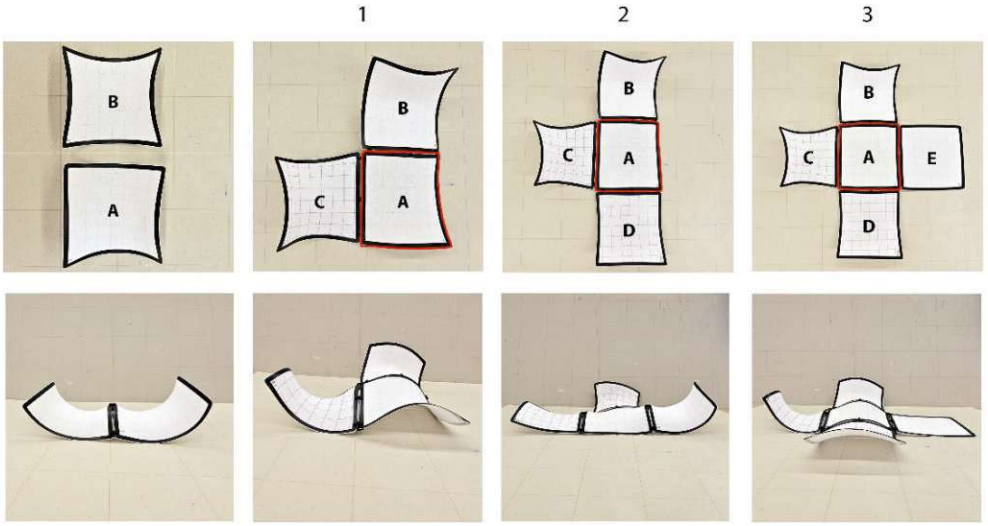

Figure 85: order of attachment – multiple edge test

Die approbierte gedruckte Originalversion dieser Diplomarbeit ist an der TU Wien Bibliothek verfügbar
The approved original version of this thesis is available in print at TU Wien Bibliothek.

Die approbierte gedruckte Originalversion dieser Diplomarbeit ist an der TU Wien Bibliothek verfügbar
The approved original version of this thesis is available in print at TU Wien Bibliothek.

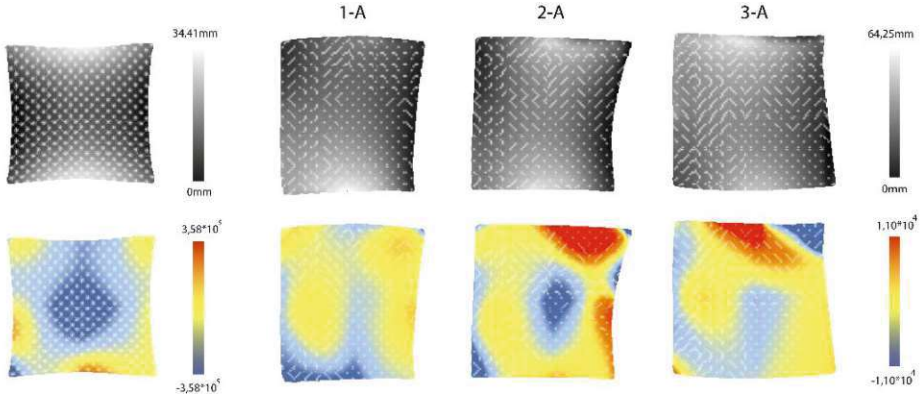

Figure 86: left: initial evaluation of the tile A, right: evaluation of tile A in order of attachment - top: z-displacement evaluation of point cloud, bottom: Gaussian curvature analysis of N.U.R.B.S. surface

Significant changes are evident when comparing the initial evaluation of the central tile A in terms of z-displacement and Gaussian curvature (figure 86, left) to the evaluation during the attachment process, from 1-A = 3 connected tiles to 3-A = 5 connected tiles (figure 86, right). This emphasizes the flexibility and adaptability of the material system presented in this thesis, which can be adjusted through various combinations.

When comparing the edges of the central tile before and after combination (figure 87), the previously mentioned changes are visible, but more prominent are the shifts in the tile's orientation due to the interpolation with the surrounding tiles. This evaluation also reveals that there are no kinks in the edges or other issues resulting from the tiling process.

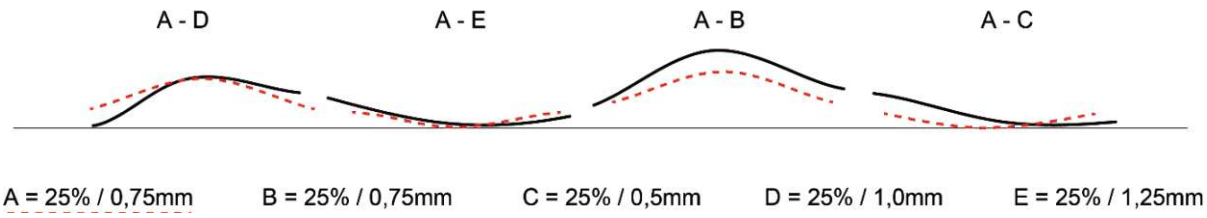

Figure 87: multiple edge combination – diagram of adjacent curves before and after combination

Die approbierte gedruckte Originalversion dieser Diplomarbeit ist an der TU Wien Bibliothek verfügbar
The approved original version of this thesis is available in print at TU Wien Bibliothek.

5.2.1. Case study surface 3x3

After the initial testing of combination parameters, which were still focused on individual tiles, the attention was shifted to exploring the possibilities of tiled surface fabrication. The first experimental surface, designed to consist of a 3 x 3 grid of tiles, was restricted to the combination method of "opposing edges", as described in chapter 5.1, and a single set of tile fabrication parameters, detailed in table 11. The goal was to demonstrate that, using this limited set of parameters, a double curved surface could be fabricated, thereby partially validating the broader concept of using active textiles as tiles for creating double curved surfaces. In figure 88 a preview of the assembled surface is portrayed.

Table 11: fabrication parameters of tiles used for the 3x3 surface

Fabric	stretch X = Y = 72mm, 25%
Border	180mm x 180mm, 7.5mm wide, 0.75mm high

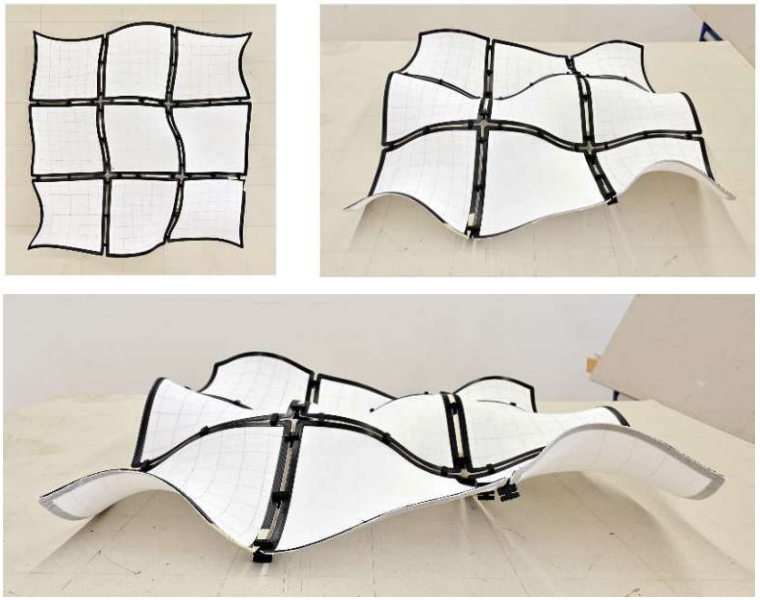

Figure 88: preview of assambled 3x3 surface

Die approbierte gedruckte Originalversion dieser Diplomarbeit ist an der TU Wien Bibliothek verfügbar
The approved original version of this thesis is available in print at TU Wien Bibliothek.

The result of this process was an undulating double curved surface with peaks and valleys, appearing to tile within a single plane. In the plan view, a consistent deformation of the grid is clearly visible, reflecting the overall surface geometry. To assess the geometry of this surface in a similar way to the previous experiments, the scanning method using a 6-axis collaborative robot, as previously described, was employed for the first time.

The z-displacement (figure 89, left) and Gaussian curvature analysis (figure 89, right) clearly illustrate the undulating behavior of the surface. The corresponding light and dark areas in the greyscale image represent the high (light) and low (dark) points of the surface, which correlate with areas of positive (red) and negative (blue) curvature. At the exposed edges of the surface, both evaluations show a loss in regularity due to the reduced control over these unattached edges.

This effect is as well illustrated by the extracted edges of the surface in figure 90, with the inner edges b and c in both directions showing smooth transitions between peaks and valleys in contrast to for example edge a in X direction

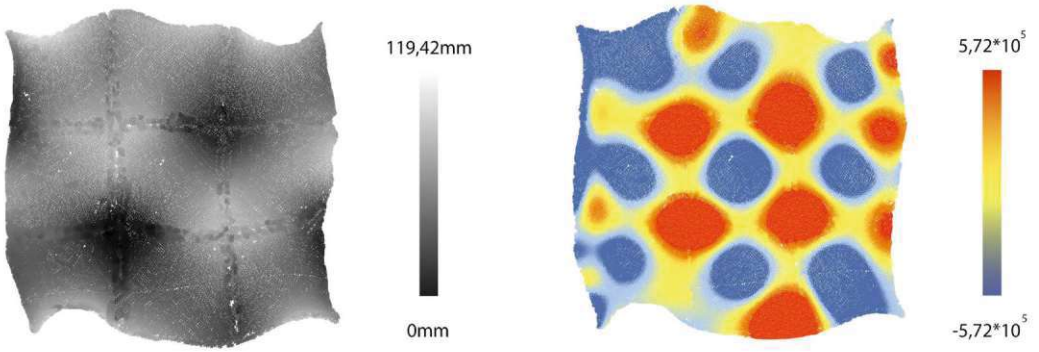

Figure 89: evaluation 3x3 surface - left: z-displacement evaluation of point cloud, right: Gaussian curvature analysis of N.U.R.B.S. surface

.

Die approbierte gedruckte Originalversion dieser Diplomarbeit ist an der TU Wien Bibliothek verfügbar
The approved original version of this thesis is available in print at TU Wien Bibliothek.

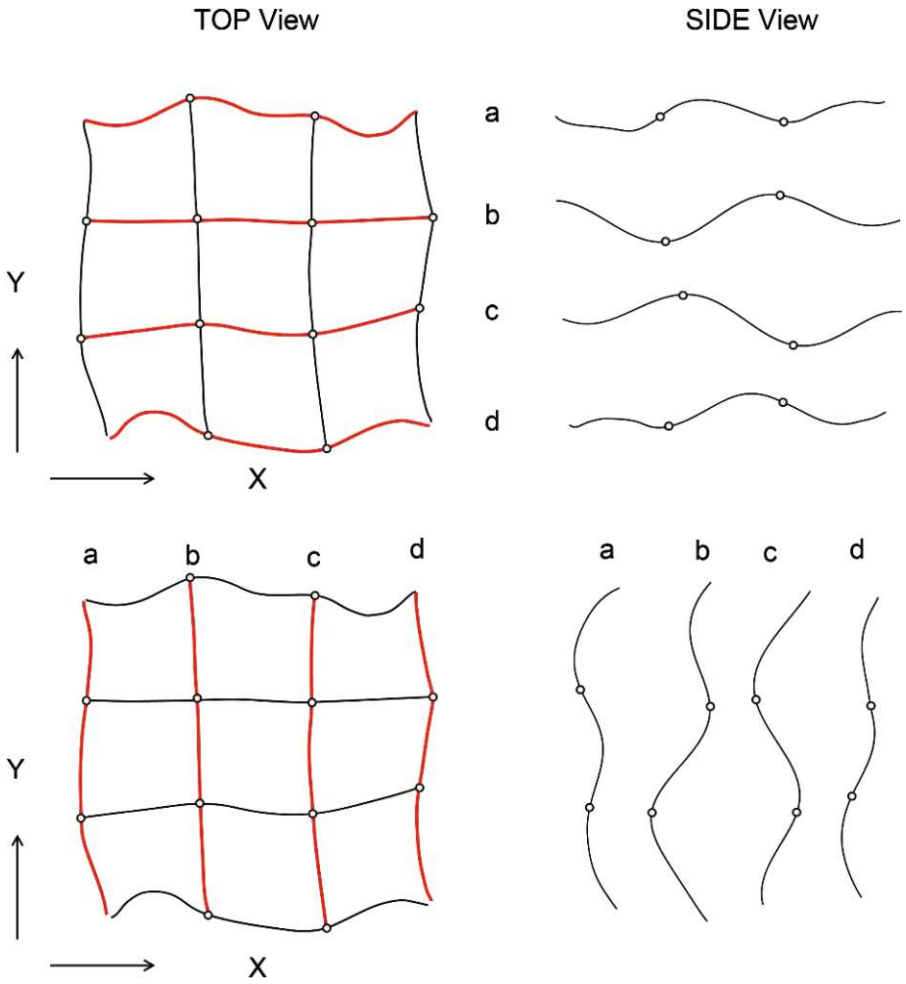

Figure 90: 3x3 surface – evaluation of combined edges of the surface

Die approbierte gedruckte Originalversion dieser Diplomarbeit ist an der TU Wien Bibliothek verfügbar
The approved original version of this thesis is available in print at TU Wien Bibliothek.

Figure 91: finished 3x3 surface on custom built display

Die approbierte gedruckte Originalversion dieser Diplomarbeit ist an der TU Wien Bibliothek verfügbar
The approved original version of this thesis is available in print at TU Wien Bibliothek.

5.2.2. Case study surface 4x4

After confirming that active textile tiles can be used to tile double curved surfaces, the next step was to investigate whether the regular undulating behavior of the 3x3 case study surface could be resolved. To achieve this, a broader range of tiles and both combination methods established in 5.1. were employed to create a surface with longer arches spanning across multiple tiles. Additionally, the overall grid size was expanded by one tile in each direction, aiming for a 4x4 surface. The parameters of the individual tiles used to create this model are detailed in table 12.

Table 12: detailed list of fabrication parameters corresponding to letters in figure 92

A	uniform	0.75mm / 25%
B	2-dia hinge	0.75mm / 25%
C	uniform	0.75mm / 25%
D	3 hinges	0.75mm / 25%
E	non-u printing	Height: a = 0.5mm, b = 0.9mm, c = 1.3mm
F	uniform	1.0mm / 25%
G	uniform	1.0mm / 25%
H	uniform	1.0mm / 25%
I	uniform	0.75mm / 30%
J	uniform	1.2mm / 30%
K	1 hinge	0.75mm / 25%
L	uniform	0.75mm / 25%
M	uniform	1.2mm / 25%
N	uniform	0.75mm / 30%
O	nun-u printing	Height: a = 0.5mm, b = 0.9mm, c = 1.3mm
P	4 hinges	0.75mm / 25%

Die approbierte gedruckte Originalversion dieser Diplomarbeit ist an der TU Wien Bibliothek verfügbar
The approved original version of this thesis is available in print at TU Wien Bibliothek.

Figure 92: preview of assembled 4x4 surface

Die approbierte gedruckte Originalversion dieser Diplomarbeit ist an der TU Wien Bibliothek verfügbar
The approved original version of this thesis is available in print at TU Wien Bibliothek.

Figure 92 shows the resulting surface, featuring a prominent arch that spans all four tiles in X direction, from tile M to tile P, with further two arches spanning 3 tiles, one in X direction from tile B to D and in Y direction from tile D to L. The innovative aspect of this combination method was the incorporation of tiles with hinges to create a “crease line,” where the surface slightly folded in. This, in conjunction with the other methods, helped disrupt the regular behavior of the material system used.

The z-displacement analysis (figure 93, left) and, more notably, the Gaussian curvature analysis (figure 93, right) confirm the observations drawn from the initial images of the 4x4 surface in figure 92. In the upper section, the analysis reveals the system's characteristic undulating behavior, with corresponding areas of positive (red) and negative (blue) curvature. However, from the middle part, encompassing tiles E to H, to the lower end of the surface, including tiles M to P, the color-graded map transitions, reflecting the previously mentioned longer-spanning arch with relatively lower curvature compared to the undulations.

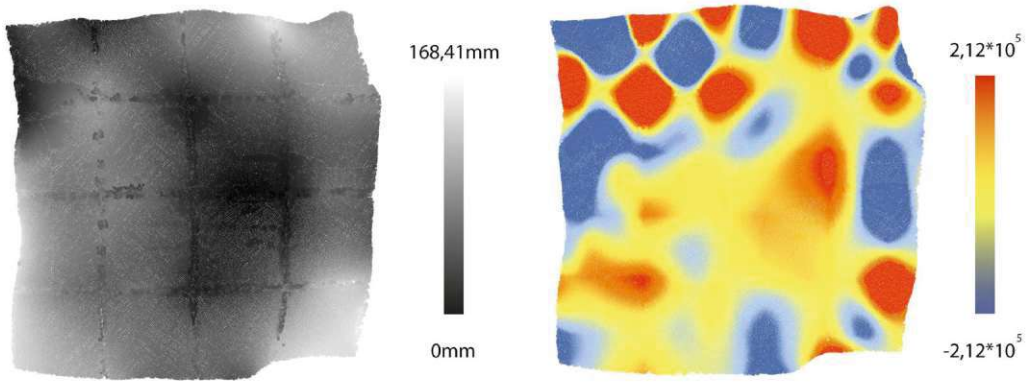

Figure 93: evaluation of the 4x4 surface - left: z-displacement evaluation of point cloud, right: Gaussian curvature analysis of N.U.R.B.S. surface

Die approbierte gedruckte Originalversion dieser Diplomarbeit ist an der TU Wien Bibliothek verfügbar
The approved original version of this thesis is available in print at TU Wien Bibliothek.

The extracted curves (figure 94) emphasize the significant variation within the surface, showcasing multiple changes in both the magnitude and direction of curvature, particularly as well along edges corresponding to single tiles (figure 94, edges d and e in Y direction). This further demonstrates that the design potential of the proposed material system extends beyond regular undulating surfaces and warrants additional exploration. However, a limitation observed in this example is the recurring loss of control over the exposed edges of the surface.

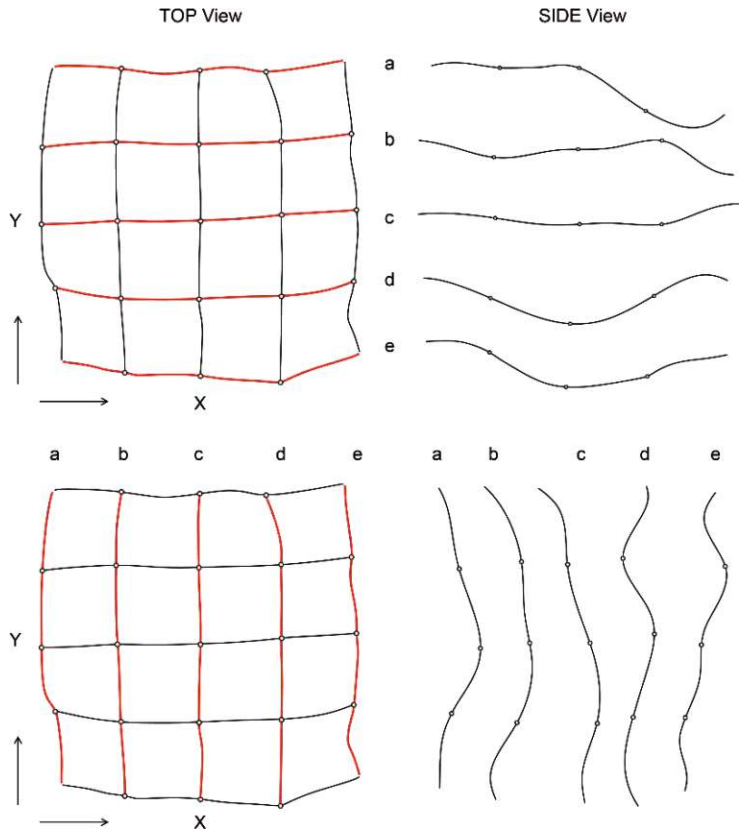

Figure 94: 4x4 surface – evaluation of combined edges of the surface

Die approbierte gedruckte Originalversion dieser Diplomarbeit ist an der TU Wien Bibliothek verfügbar
The approved original version of this thesis is available in print at TU Wien Bibliothek.

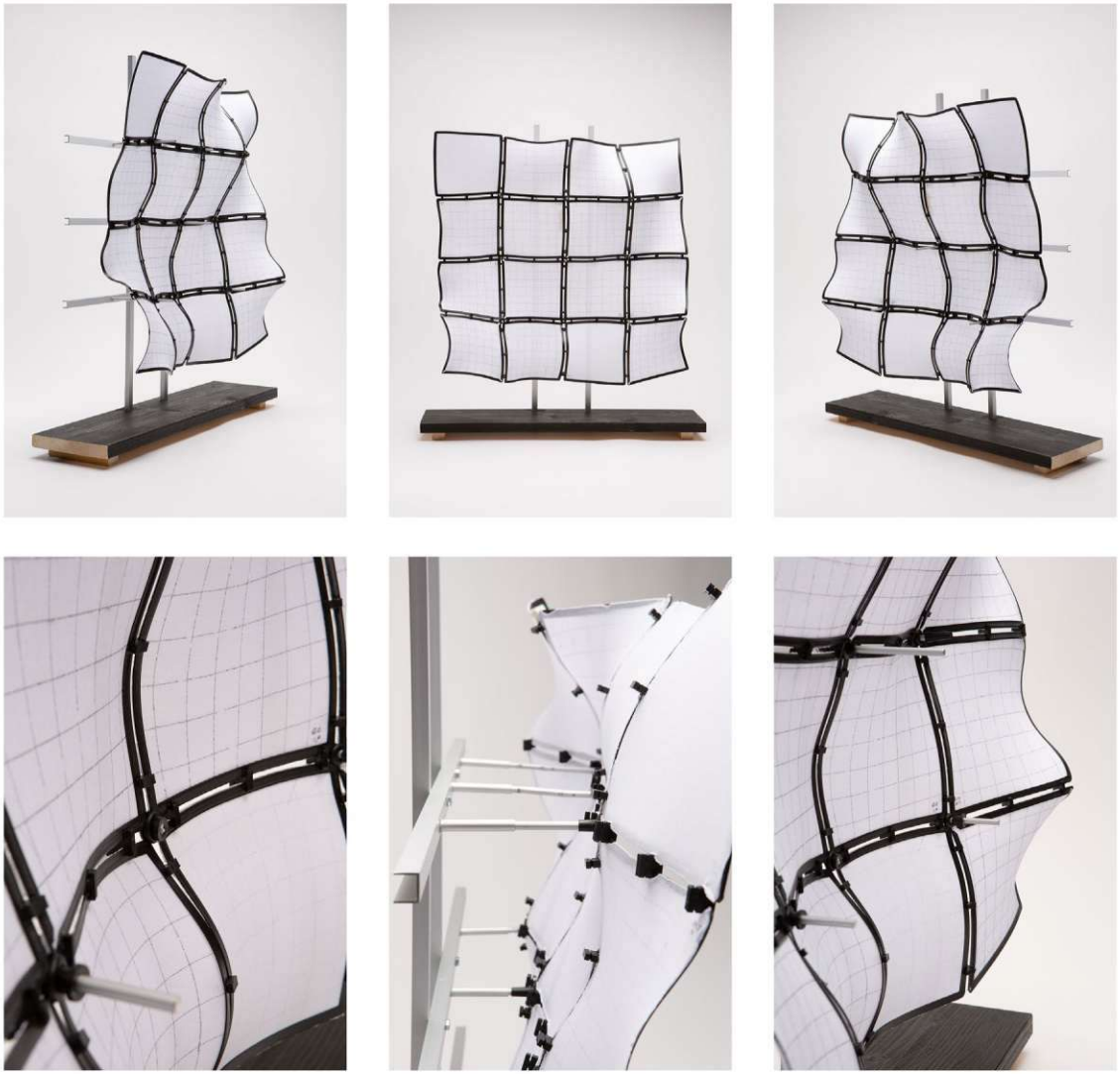

Figure 95: finished 4x4 surface on custom built display

Die approbierte gedruckte Originalversion dieser Diplomarbeit ist an der TU Wien Bibliothek verfügbar
The approved original version of this thesis is available in print at TU Wien Bibliothek.

5.2.3. Double layer

Another approach for testing multiple edge combinations involved the creation of a double layer structure, where two uniform tiles were stacked on top of each other and combined at all four edges. This method allowed for exploration of the procedures outlined in section 5.1., including the combination of tiles with different fabrication parameters, either aligned with “matching edges” or “opposing edges”. It was assumed that the previously established principles regarding surface and edge curvature apply to this approach as well, and that the creation of a "sandwich" system would provide added structural rigidity. This method was briefly tested as proof of concept, using two uniform tiles with the same parameters as tile A in the earlier combination test, as detailed in tables 10. The test involved combinations of “matching edges”, as shown in the two left images of figure 96, and “opposing edges”, as shown in the two right images.

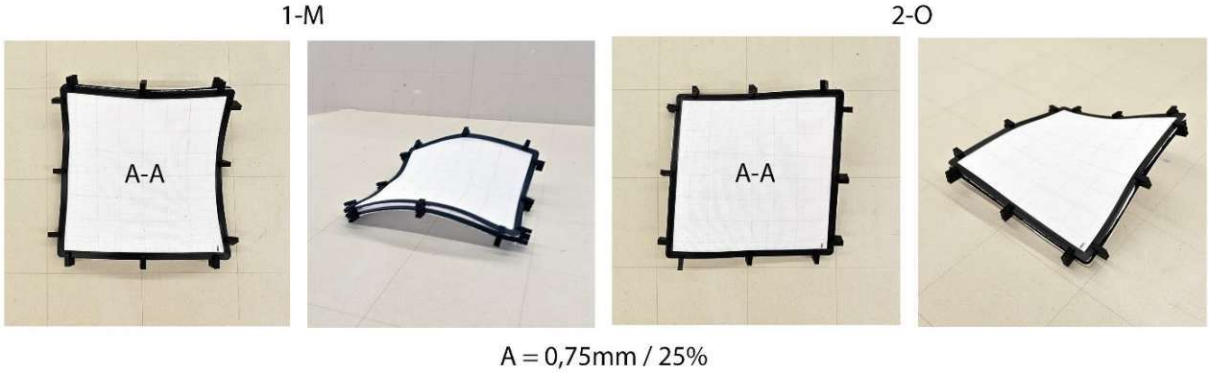

Figure 96: matrix of double layer structure test

The "stacking" of tiles proved to be just as feasible as side-by-side combinations, yielding similar results in terms of activation and "response" of the individual tiles, as shown in figure 96. Additionally, it confirmed the assumption that stacking could enhance structural rigidity. A comparison of the z-displacement (figure 97, top) and Gaussian curvature analysis (figure 97, bottom) for a single uniform tile (figure 97, A) and the double layer structure made up of two tiles with the same parameters (figure 97, 1-M) showed similar outcomes, with the exception of the upper boundary of the z-displacement, which differed due to the increased thickness.

Die approbierte gedruckte Originalversion dieser Diplomarbeit ist an der TU Wien Bibliothek verfügbar
The approved original version of this thesis is available in print at TU Wien Bibliothek.

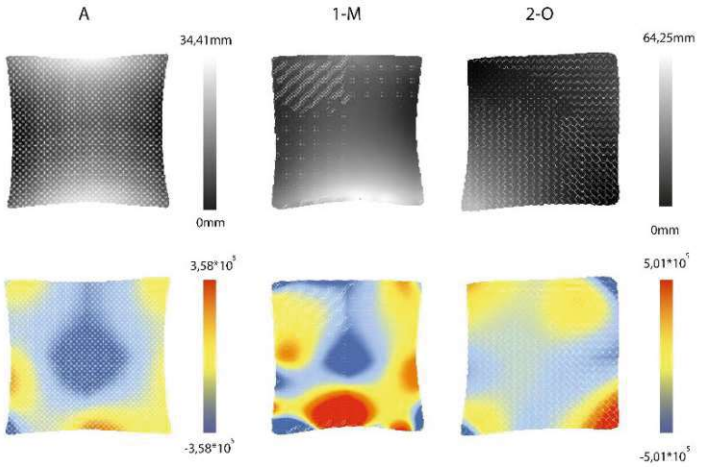

Figure 97: double layer structure test, left: single tile, right: double layer with B matching edge and C opposing edge combination - top: z-displacement evaluation of point cloud, bottom: Gaussian curvature analysis of N.U.R.B.S. surface

Edge analysis (figure 98) shows distinct behaviors for the two different combination methods described in chapter 5.1, with system 1-M still showing similarities with the initial edge curvatures of single tile A. At test 2-O the edges start to have inflection points similar to the tile with two diagonal hinges as illustrated in chapter 4.3., figure 70.

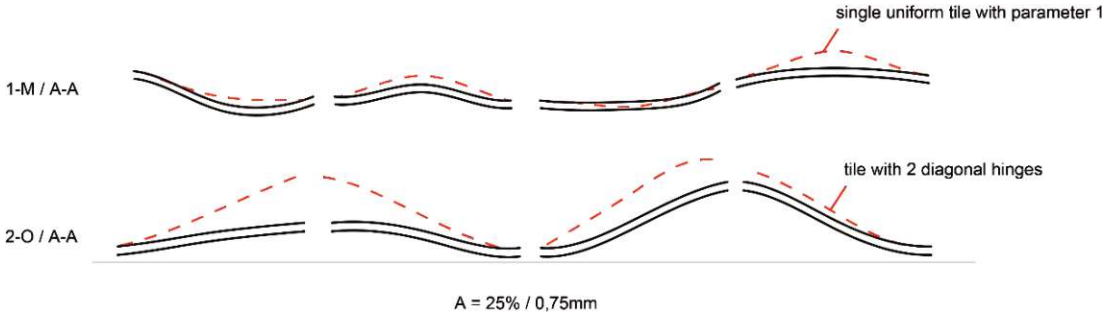

Figure 98: double layer – edge evaluation, top: matching edges, bottom: opposing edges combined

Die approbierte gedruckte Originalversion dieser Diplomarbeit ist an der TU Wien Bibliothek verfügbar
The approved original version of this thesis is available in print at TU Wien Bibliothek.

Die approbierte gedruckte Originalversion dieser Diplomarbeit ist an der TU Wien Bibliothek verfügbar
The approved original version of this thesis is available in print at TU Wien Bibliothek.

6. Design exploration

To test the assumption that tiled surfaces made from active textile are not constrained to grids with few parts like the previously shown 3x3 or 4x4 structures, an attempt was made to fabricate a larger surface. This experiment focused on examining how the induced control over the edge curvature of individual tiles translated to the control over an overall tiled surface geometry and how it evolved as the number of combined tiles increases.

Unlike the previous experiments in sections 5.2.1 and 5.2.2, where already prefabricated tiles were arranged and the resulting geometry analyzed post-fabrication, this approach began with a digitally designed surface. The designed geometry served as a reference, and the physical model was constructed to align with this target shape using carefully selected tiles. This method not only evaluated the scalability and geometric possibilities of double curved surfaces created with this material system but also validated the knowledge gained in earlier experiments by testing the ability to reproduce a desired surface geometry.

Die approbierte gedruckte Originalversion dieser Diplomarbeit ist an der TU Wien Bibliothek verfügbar
The approved original version of this thesis is available in print at TU Wien Bibliothek.

6.1. Digital design

The geometry of the designed digital surface drew on insights from the test surfaces developed in sections 5.2.1 and 5.2.2 (figure 99), which provided an understanding of the relationship between tile parameters, resulting surfaces, and achievable geometries. Key findings, such as inducing undulation (figure 99, left side) through the method of “opposing edges” and creating long continuous curves (figure 99, right side) by canceling curvature or strategically placing hinges, were applied to design an independent surface.

The design process involved a continuous feedback loop (figure 100) between manual adjustments of the target surface in the Rhinoceros 3D modeling environment and parametric modeling in Grasshopper 3D. This iterative process ensured the desired shape was adapted to meet the material system’s constraints. One of the main challenges was adhering to the requirement that only square tiles of a specific size, each with an edge length of 180 mm, could be used. This necessitated post-processing and modifications to the modeled input to generate a feasible approximation through tile subdivision.

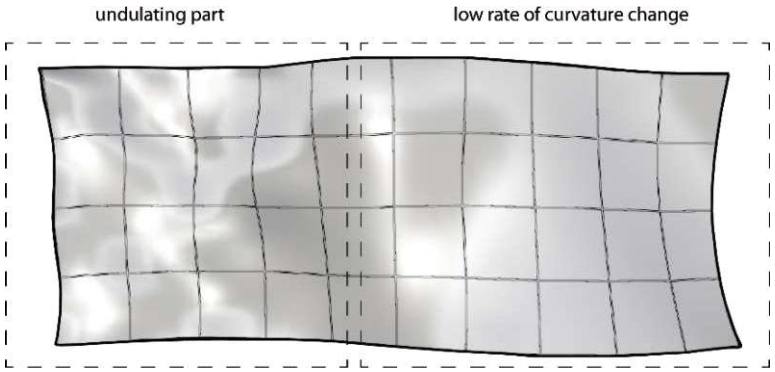

Figure 99: designed surface - highlighted areas with connection to case study surfaces

Die approbierte gedruckte Originalversion dieser Diplomarbeit ist an der TU Wien Bibliothek verfügbar
The approved original version of this thesis is available in print at TU Wien Bibliothek.

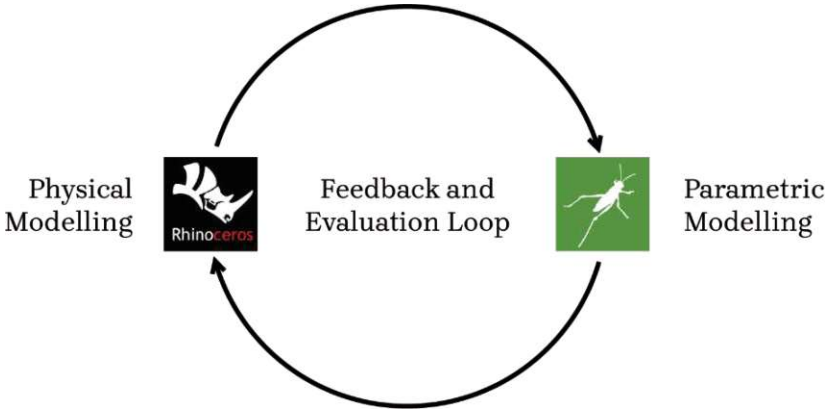

Figure 100: simplification of the digital design process

The design process began by determining the overall dimensions of the final model. A bounding box measuring 180 cm x 50 cm x 80 cm (length, width, height) was created in Rhinoceros 3D which could accommodate a 4x10 tile grid (figure 101, top left). This size was chosen as it balanced production time, manageability, and proof-of-concept requirements. The initial geometry outline was defined by drawing a set of curves along the four sides of the box (figure 101, top right). Using the Rhinoceros 3D tool “Surface from Edge Curves”, a corresponding double curved surface was generated (figure 101, mid left), forming the base for further shape refinements. To align with the dimensions of the fabricated tiles, the surface edges were divided into 180 mm segments in the Grasshopper 3D environment. Connecting these points generated a curve network using the Grasshopper 3D component “Curve on Surface” (figure 101, mid right). These curves were baked and further refined by manipulating control points to develop the desired geometry, particularly for creating the undulating part (figure 101, bottom left). The final network of curves was then used to recreate the surface, as shown in figure (101, bottom right).

Die approbierte gedruckte Originalversion dieser Diplomarbeit ist an der TU Wien Bibliothek verfügbar
The approved original version of this thesis is available in print at TU Wien Bibliothek.

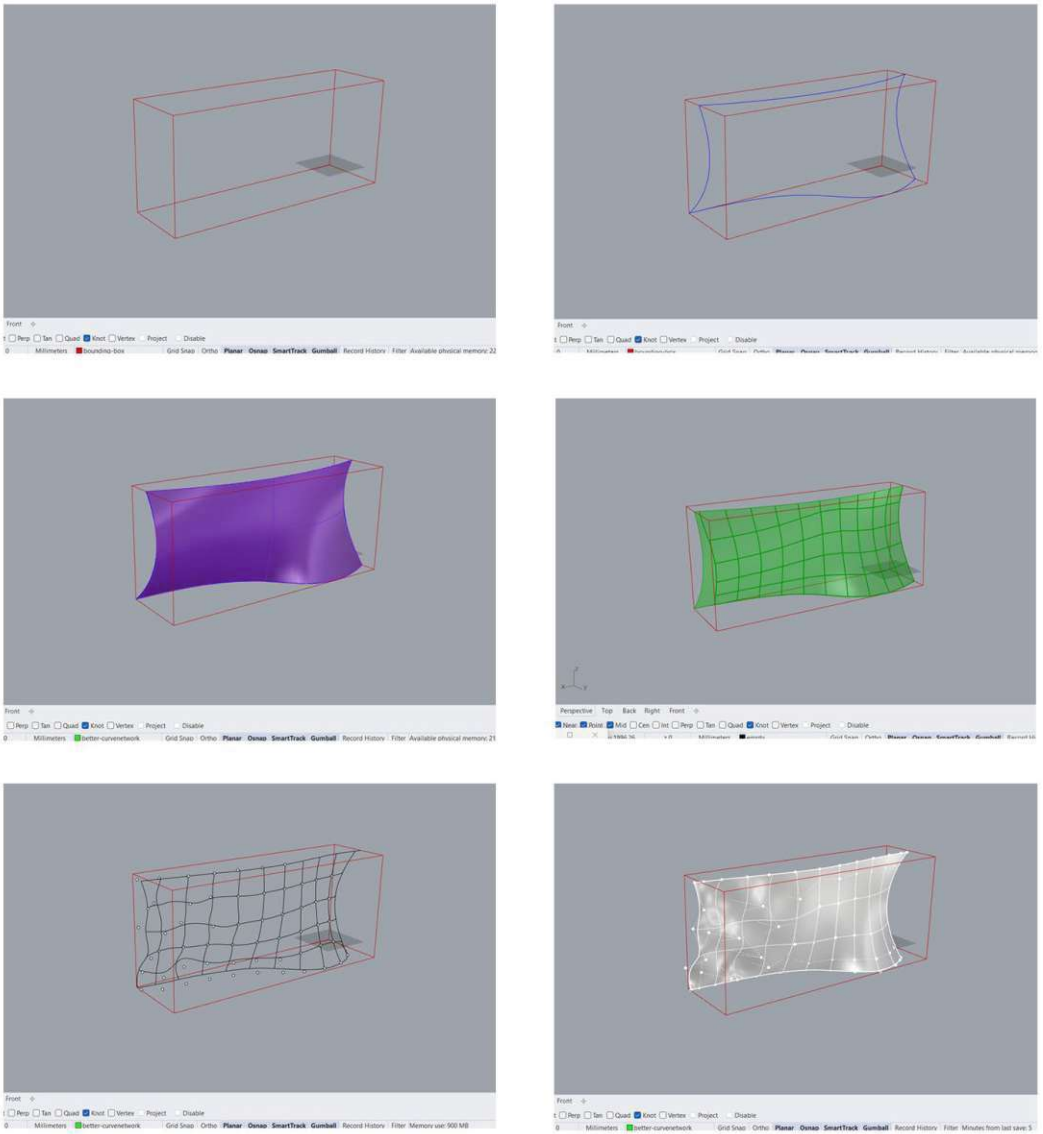

Figure 101: matrix of digital design process No. 1

Die approbierte gedruckte Originalversion dieser Diplomarbeit ist an der TU Wien Bibliothek verfügbar
The approved original version of this thesis is available in print at TU Wien Bibliothek.

This process was repeated several times until the surface suited the before mentioned aspects and the design was satisfying. As a further step, a small optimization routine in the Grasshopper 3D environment was developed with the goal of keeping the surface dividable through a curve network with individual curve lengths of multiples of 180 mm (figure 102, top left). This was achieved by using the length of the curve segments as the fitness for the “Galapagos Solver” in Grasshopper 3D and sliders that could manipulate the position of the surface control points as the genomes. Through this operation the surface could slightly change and adapt to better suit the fabrication parameters. This process was again repeated several times which led to the final design of the double curved surface and produced the correct sub-division simultaneously (figure 102).

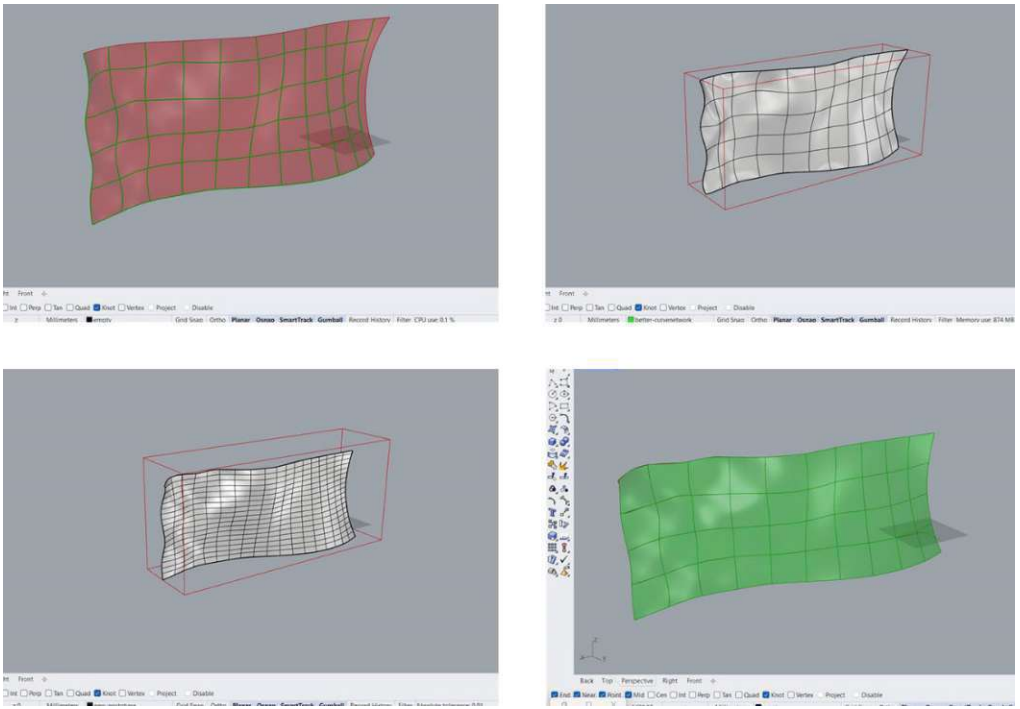

Figure 102: matrix of digital design process No. 2

Die approbierte gedruckte Originalversion dieser Diplomarbeit ist an der TU Wien Bibliothek verfügbar
The approved original version of this thesis is available in print at TU Wien Bibliothek.

The design now consisted of a grid of 4x10 individual surfaces which were again baked into Rhino (figure 103, top right). There the individual tiles were extruded and a suitable structure for fixing and displaying the fabricated pieces was designed. This step concluded the digital design process for the surface-study (figure 103, bottom).

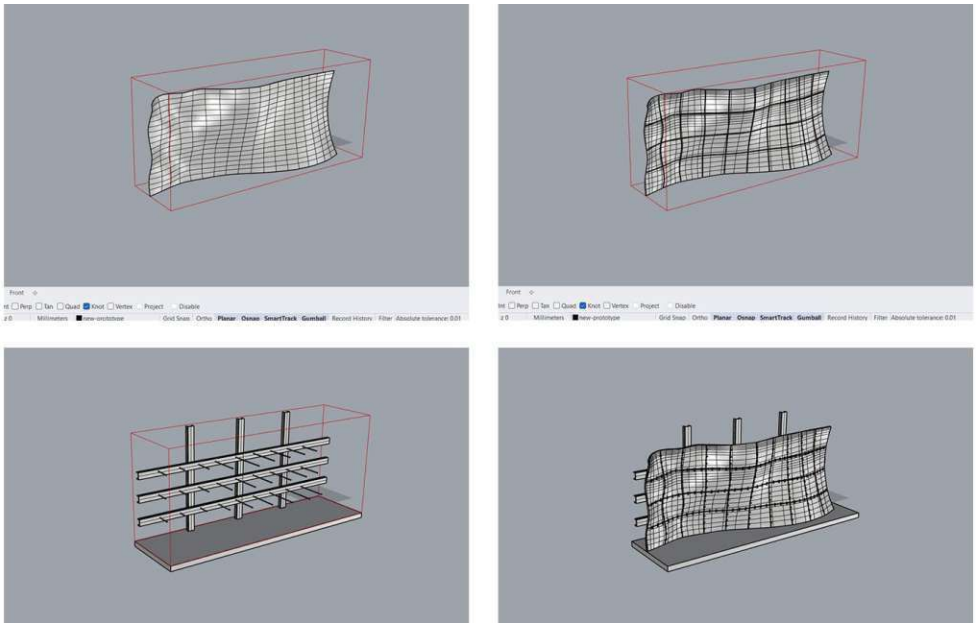

Figure 103: matrix of digital design process No. 3

Additionally, the digitally designed double curved surface was analyzed using the same methods applied to the physically fabricated tiles and surfaces. A greyscale image represent the z-displacement (figure 105, left), while a color-graded map depicts the Gaussian curvature analysis (figure 105, right). Especially the Gaussian curvature analysis highlights the two distinct parts, left the undulating grid with great amount of change in curvature and right a drastic decline in amount of curvature change, of the designed surface.

Die approbierte gedruckte Originalversion dieser Diplomarbeit ist an der TU Wien Bibliothek verfügbar
The approved original version of this thesis is available in print at TU Wien Bibliothek.

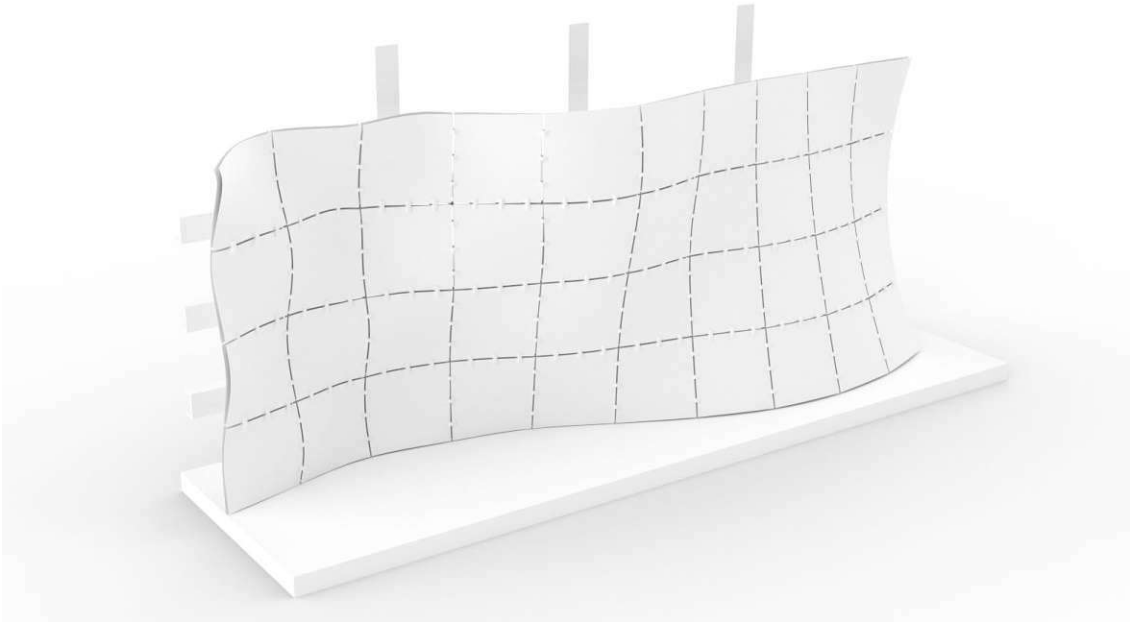

Figure 104: final digital design of the design exploration model

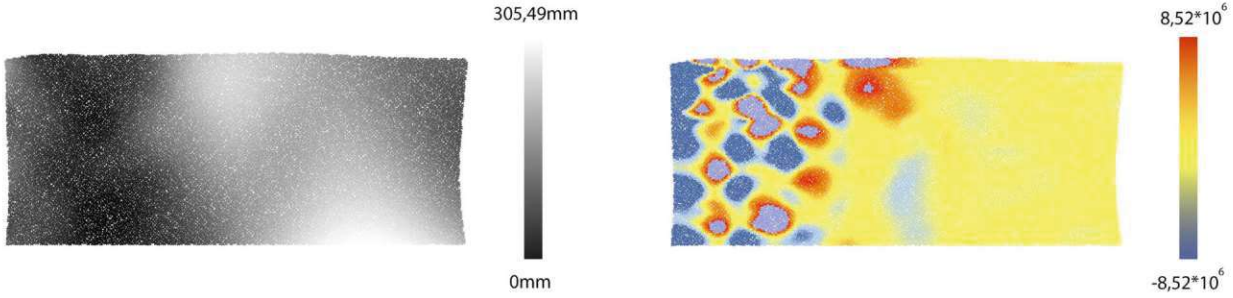

Figure 105: design exploration surface - left: z-displacement evaluation of point cloud, right: Gaussian curvature analysis of N.U.R.B.S. surface

Die approbierte gedruckte Originalversion dieser Diplomarbeit ist an der TU Wien Bibliothek verfügbar
The approved original version of this thesis is available in print at TU Wien Bibliothek.

6.2. Fabrication

The fabrication of the tiled surface was carried out in two steps. First, specific sets of fabrication parameters and tile orientations were assigned to the individual pieces to achieve the desired geometry using active textile components. Only then could the actual fabrication of the tiles commence, following the developed plan.

6.2.1. Parameter assessment

Certain fabrication parameters and orientations were assigned to the 40 individual tiles. This was done by evaluating individual tile edge curvatures complemented with an estimation on the interplay between two connected edges and the influence on overall tile geometry through adjacent tiles as illustrated in figure 106. This process relied on the knowledge gained during the material experiments on individual tile fabrication parameters as well as the combination studies.

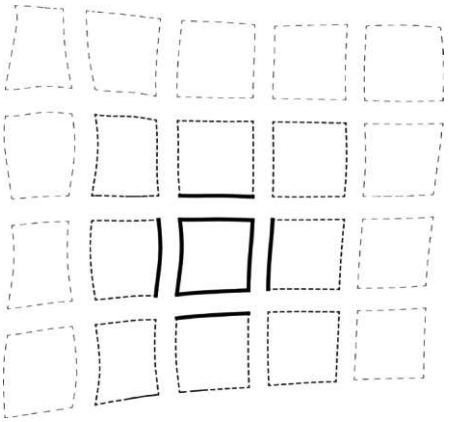

Figure 106: considerations for assigning fabrication parameters, direct effect (bold black) to low influence (light)

The evaluation process categorized the pieces into families of tiles based on the fabrication parameters outlined in the material experiments in chapter 4. The families are represented using a green, red, and blue color scheme (figure 107) to provide an overview of the tile-family distribution across the surface and are grouped under letters U, N, and H in a detailed fabrication parameter layout. To convey the distinct properties of the tiles, a system of lines and symbols is employed, as shown in figure 108.

Die approbierte gedruckte Originalversion dieser Diplomarbeit ist an der TU Wien Bibliothek verfügbar
The approved original version of this thesis is available in print at TU Wien Bibliothek.

The 3D printed boundary height of the tiles is indicated by line thickness in the diagram, ranging from 0.5 mm (represented by the thinnest line) to 1.25 mm (depicted by the thickest line). Uniform tiles are outlined with frames of uniform thickness, while the edges with larger cross-sections in non-uniform boundary thickness are specifically highlighted. Hinges are represented by triangles pointing to the designated corners.

- Uniform tiles (green, U) – corresponding to chapter 4.1
    - Tiles with uniform pre-stretching and uniform boundary cross-section
    - Used for undulating pattern and as “fill-in”
    - Pre-stretching: 25%
    - Boundary heights: 0,5 mm, 0,75 mm, 1,0 mm, 1,25 mm
    - 11 pieces
- Non-uniform printing thickness (red, N) – corresponding to chapter 4.2.2
    - Tiles with uniform pre-stretching and non-uniform printing thickness
    - Edgewise variations, no sub-division of edges
    - Used where curvature in one direction was predominant and for tiles with low curvature (e.g. edges)
    - Pre-stretching: 25%
    - Boundary heights: 3 categories
        - 3 Edges 0,75 mm, 1 Edge 1 mm
        - 2 Edges 0,75 mm, 2 Edges 1 mm
        - 1 Edge 0,75 mm, 3 Edges 1 mm / 1,25 mm
        - 25 pieces
- Hinges (blue, H) – corresponding to chapter 4.3
    - Tiles with uniform pre-stretching and printing thickness with hinges
    - Placement of two opposing hinges was used
    - Used to introduce rapid changes in curvature
    - Pre-stretching: 25%
    - Boundary height: 0,75 mm
    - 4 pieces

Die approbierte gedruckte Originalversion dieser Diplomarbeit ist an der TU Wien Bibliothek verfügbar
The approved original version of this thesis is available in print at TU Wien Bibliothek.

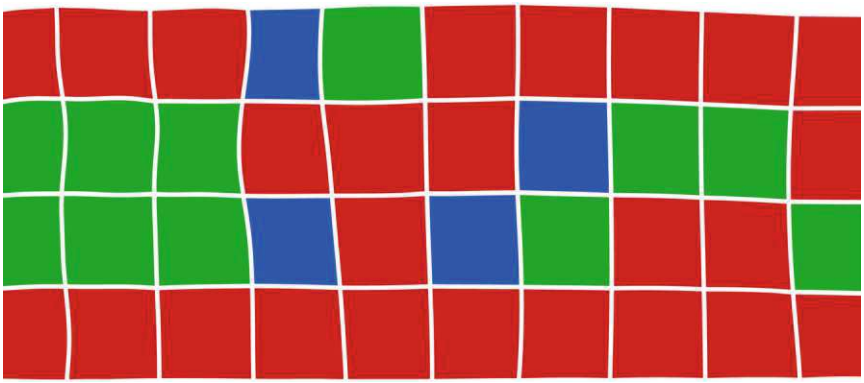

Figure 107: color graded map - overview of parameter families assigned to the tiles of the digital surface

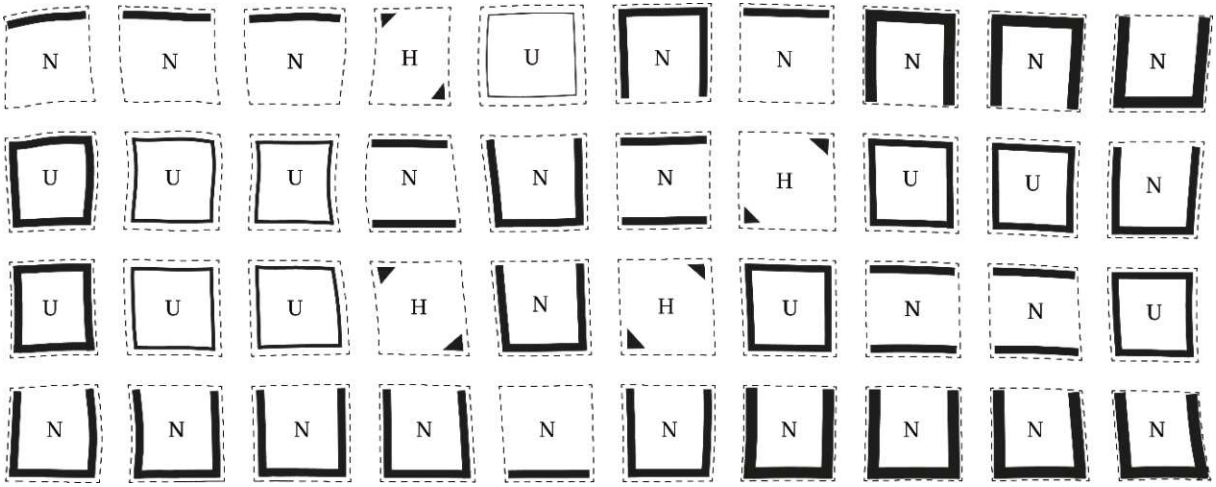

Figure 108: detailed map of fabrication parameters of each tile

Die approbierte gedruckte Originalversion dieser Diplomarbeit ist an der TU Wien Bibliothek verfügbar
The approved original version of this thesis is available in print at TU Wien Bibliothek.

Tile orientation

The orientation of individual pieces played a crucial role in either "canceling out" unintended edge curvature or amplifying the inherent curvature. When applied across multiple tiles, this approach enabled the creation of the desired undulating pattern. However, in areas with lower curvature or minimal curvature variation, this method had a reduced effect. A color-graded map is again utilized to visualize the directionality of the combined tiles (figure 109). In figure 110 the orientation of tiles is illustrated in more detail with dashed and continuous lines referring to edges curved in the same direction. Therefore, two adjacent tiles with a dashed line on the corresponding edge signals the “matching edge” method. Tiles with hinges are again depicted as in figure 108.

- Matching edges (magenta, M)
    - More prominent in low curvature areas and with non-uniform printing thickness tiles

- Opposing edges (orange, O)
    - Clearly focused on the undulating part of the surface and with uniform tiles

- Hinges (blue, H)
    - Placement of hinges establishes “crease lines” were curvature changes rapidly

Die approbierte gedruckte Originalversion dieser Diplomarbeit ist an der TU Wien Bibliothek verfügbar
The approved original version of this thesis is available in print at TU Wien Bibliothek.

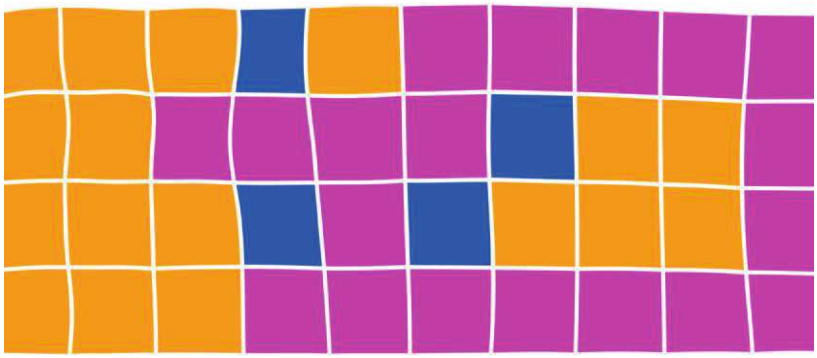

Figure 109: color graded map - overview of assigned orientation to the tiles of the digital surface

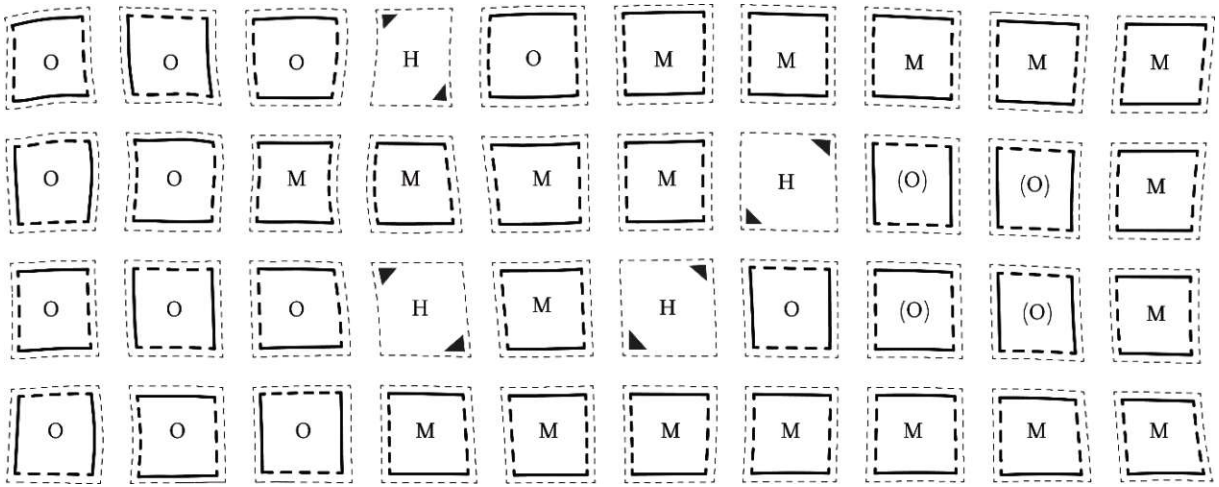

Figure 110: detailed map of the orientation of tiles according to the direction of edges of their neighbors

Die approbierte gedruckte Originalversion dieser Diplomarbeit ist an der TU Wien Bibliothek verfügbar
The approved original version of this thesis is available in print at TU Wien Bibliothek.

6.2.2. Tile fabrication

With the parameters for the individual tiles and the overall surface established, fabrication commenced (figure 111).

Figure 111: working place at the modelbuilding workshop at the TU Wien

Die approbierte gedruckte Originalversion dieser Diplomarbeit ist an der TU Wien Bibliothek verfügbar
The approved original version of this thesis is available in print at TU Wien Bibliothek.

Initially, the jersey fabric was measured and cut into strips of size 350 mm in width and 1500 mm in length. (figure 112, top). These strips were then further processed into 300 mm x 300 mm squares using a laser cutter (figure 112, bottom). This served as the starting point for tile fabrication, with the individual steps depicted in figure 113. The total estimated printing time for 40 tiles was approximately 50 hours, excluding the time required for clamping, pre-stretching, and releasing the fabric. The same procedures described in the material exploration (chapter 3) were consistently applied throughout the process.

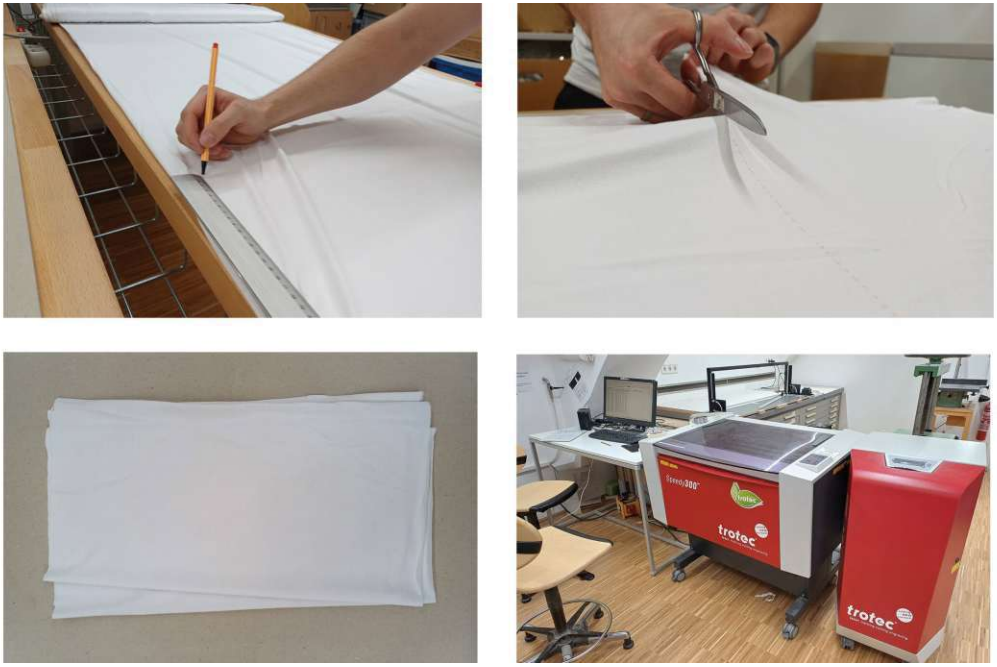

Figure 112: fabrication steps of individual tiles – textile preparation

Die approbierte gedruckte Originalversion dieser Diplomarbeit ist an der TU Wien Bibliothek verfügbar
The approved original version of this thesis is available in print at TU Wien Bibliothek.

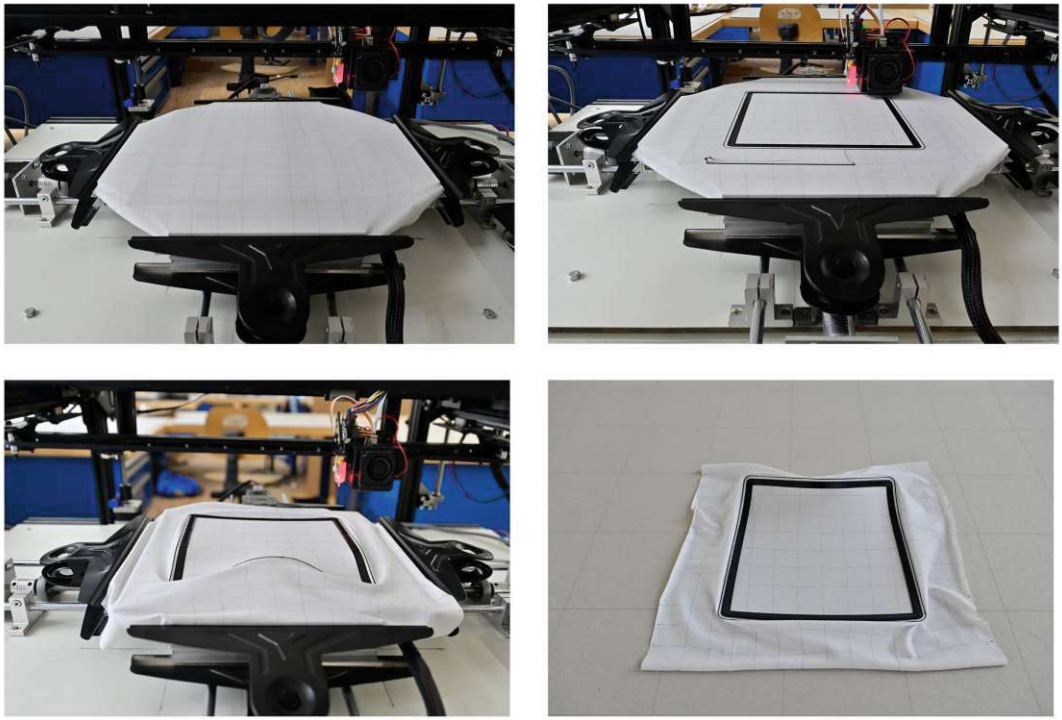

Figure 113: fabrication steps of individual tiles – actual 4D printing

Die approbierte gedruckte Originalversion dieser Diplomarbeit ist an der TU Wien Bibliothek verfügbar
The approved original version of this thesis is available in print at TU Wien Bibliothek.

The tiles for the left, undulating part of the surface (see figure 99) were printed first. After completing an initial 4x3 grid, the assembly of these 12 tiles began simultaneously with the ongoing printing process.

Figure 114 illustrates this process of attaching/tiling the surface from the initial 4x3 grid to the full surface. The approach of assembling while still printing allowed for verification of the estimated tile parameters and helped reduce the overall surface fabrication time.

To combine the individual tiles, custom-designed connections were 3D printed using a Bambu Carbon X1 printer and PLA filament. Three of these joints were placed at each edge, as shown in figure 114, top left, resulting in a total of 198 pieces. Prior to permanently securing these connections with glue, paper tape was used to hold the tiles in place and prevent movement.

Due to the geometry of the designed surface, further assembly was carried out on the prefabricated stand (figure 114, third row). Rubber rings were placed at the corner points of the tiles (figure 114, second row) to support the transition from the surface to the aluminum rods of the substructure. From this point, vertical strips of four tiles were joined together on the table before being attached to the already mounted surface.

The total printing time was 58 hours and 36 minutes, including fabric handling and the reprinting of four tiles.

Die approbierte gedruckte Originalversion dieser Diplomarbeit ist an der TU Wien Bibliothek verfügbar
The approved original version of this thesis is available in print at TU Wien Bibliothek.

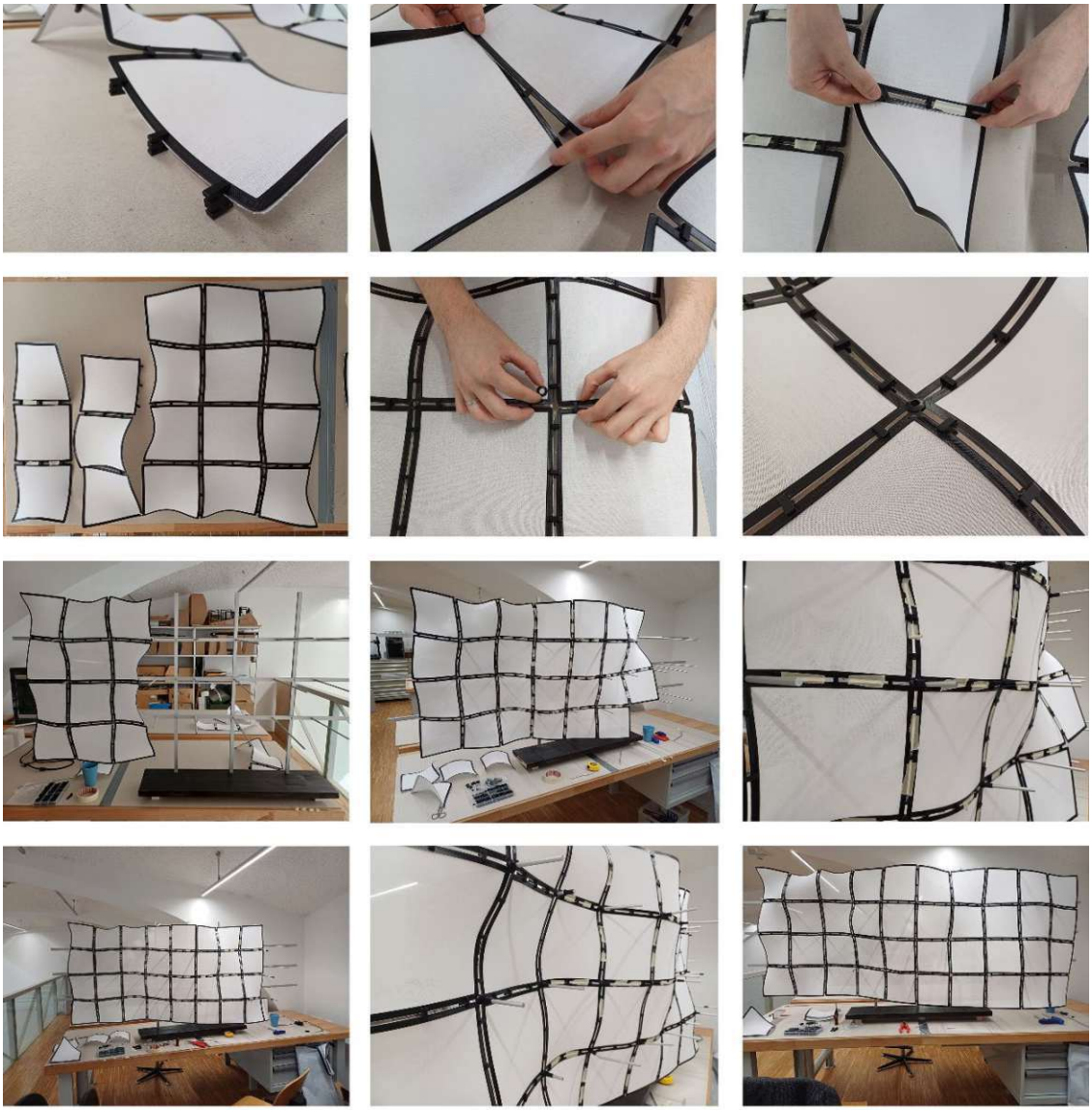

Figure 114: assembly process of design exploration model

Die approbierte gedruckte Originalversion dieser Diplomarbeit ist an der TU Wien Bibliothek verfügbar
The approved original version of this thesis is available in print at TU Wien Bibliothek.

Figure 115: final design exploration model No. 1

Die approbierte gedruckte Originalversion dieser Diplomarbeit ist an der TU Wien Bibliothek verfügbar
The approved original version of this thesis is available in print at TU Wien Bibliothek.

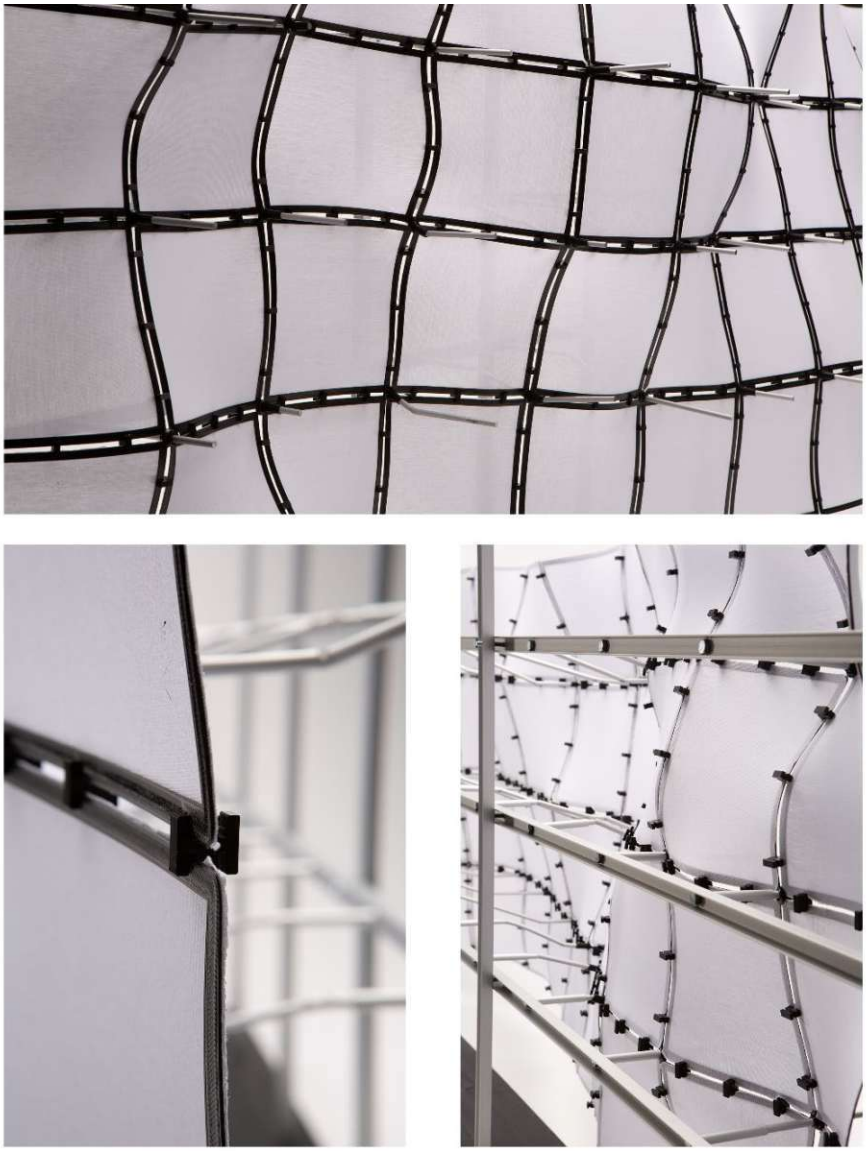

Figure 116: final design exploration model No. 2

Die approbierte gedruckte Originalversion dieser Diplomarbeit ist an der TU Wien Bibliothek verfügbar
The approved original version of this thesis is available in print at TU Wien Bibliothek.

6.3. Evaluation

The evaluation process for the surface study model followed the procedure outlined in chapter 5, utilizing a 6-axis collaborative robot for surface scanning. In addition to the direct recreation of the fabricated geometry using a N.U.R.B.S. surface from the point cloud (figure 119), a recreation of the surface was also performed by lofting the edges of the assembled model (figure 120). The z-displacement, presented as a greyscale image, demonstrates strong similarities across all three surfaces (figures 118, left / 119, left / 120, left), with a noticeable variation of 39.93 mm at the top boundary. The Gaussian curvature analysis (figures 118, right / 119, right / 120, right) provides a deeper evaluation, revealing overall similarities between the three surfaces but highlighting deviations in both the undulating and less curved areas. Notably, in figure (119, right), which uses the direct point cloud data, the fabricated surface still shows slight undulation in the top-right corner.

Figure 117 evaluates the overall deviation between surfaces. The N.U.R.B.S. surface generated from the point clouds and the digitally designed surface depicted in figure (117, left), as well as the loft surface created from the edge curves and the digitally designed surface (figure 117, right) emphasize the previously mentioned issue of unattached edges at the surface boundary, as discussed in sections 5.2.1 and 5.2.2, with the greatest deviation occurring along the left edge of the surfaces.

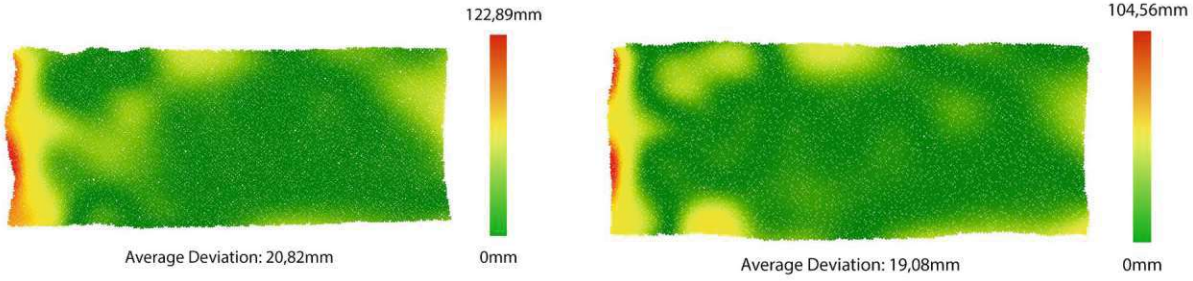

Figure 117: fabricated surface deviation from designed surface – left: surface from point cloud, right: surface from edge curves

Die approbierte gedruckte Originalversion dieser Diplomarbeit ist an der TU Wien Bibliothek verfügbar
The approved original version of this thesis is available in print at TU Wien Bibliothek.

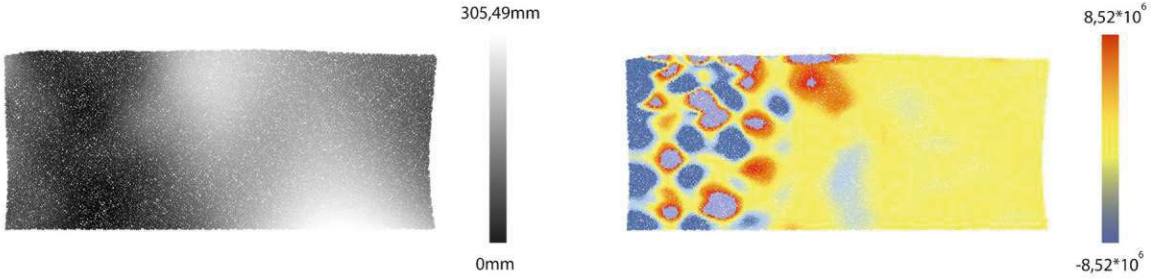

Figure 118: digitally designed surface - left: z-displacement evaluation of point cloud, right: Gaussian curvature analysis of N.U.R.B.S. surface

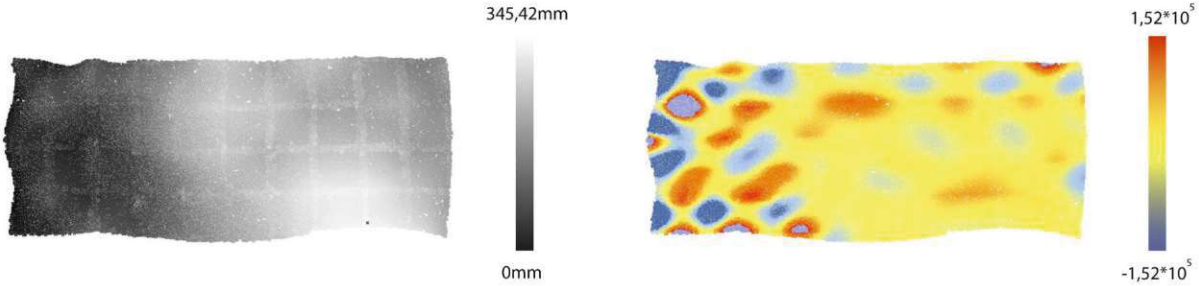

Figure 119: fabricated surface from point cloud - left: z-displacement evaluation of point cloud, right: Gaussian curvature analysis of N.U.R.B.S. surface

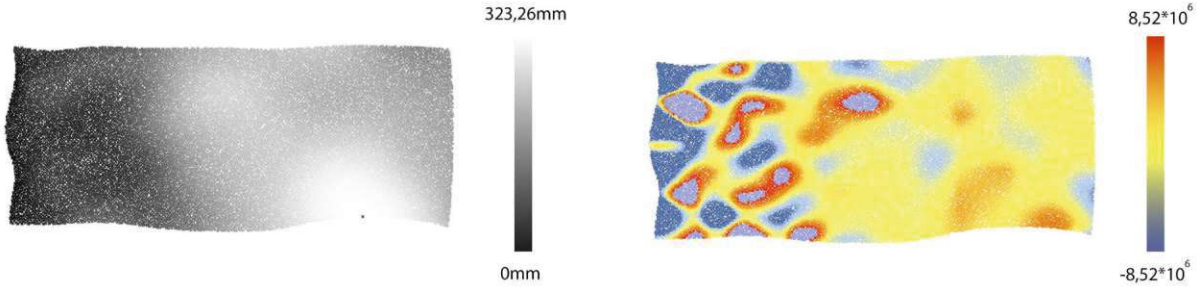

Figure 120: fabricated surface from edge curves - left: z-displacement evaluation of point cloud, right: Gaussian curvature analysis of N.U.R.B.S. surface

Die approbierte gedruckte Originalversion dieser Diplomarbeit ist an der TU Wien Bibliothek verfügbar
The approved original version of this thesis is available in print at TU Wien Bibliothek.

The evaluation of the extracted edges from the fabricated surface confirms this observation, with the maximum deviation occurring at the left undulating section when compared to the designed surface. Otherwise, the curves in the X-direction (figure 121) display similar curvature directions with only minimal deviations. However, when examining the curves in the Y-direction (figure 122), the deviations become more pronounced, particularly where slight undulating patterns persist while the designed surface maintains a consistent curvature. Edges g and h in figure 122 serve as key examples of this behavior.

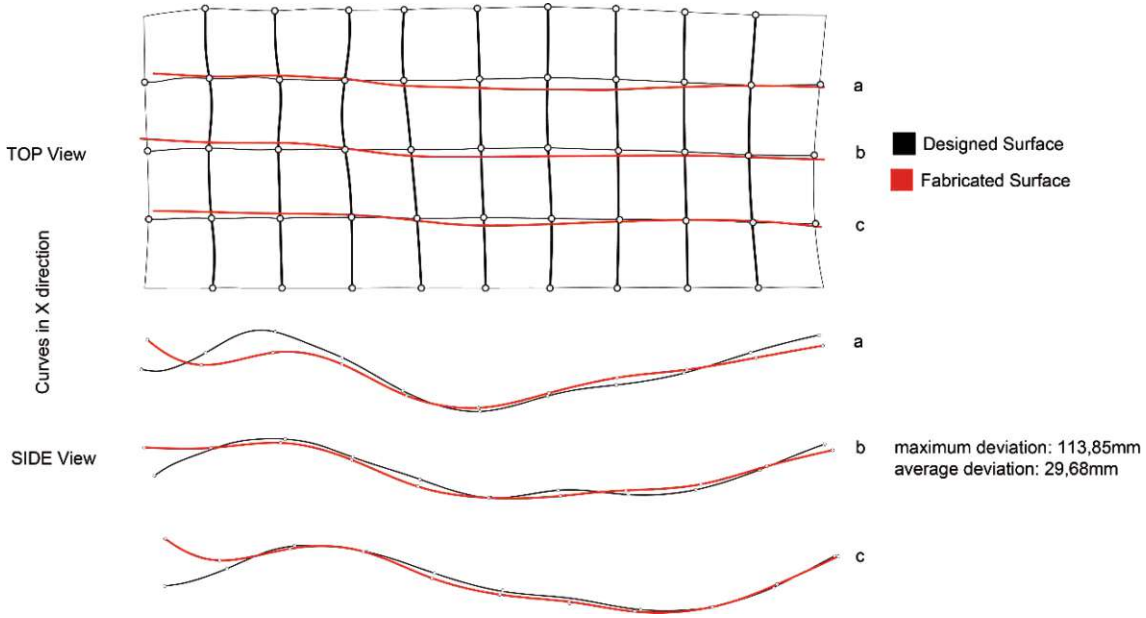

Figure 121: design exploration – evaluation of extracted edges – X-direction

Die approbierte gedruckte Originalversion dieser Diplomarbeit ist an der TU Wien Bibliothek verfügbar
The approved original version of this thesis is available in print at TU Wien Bibliothek.

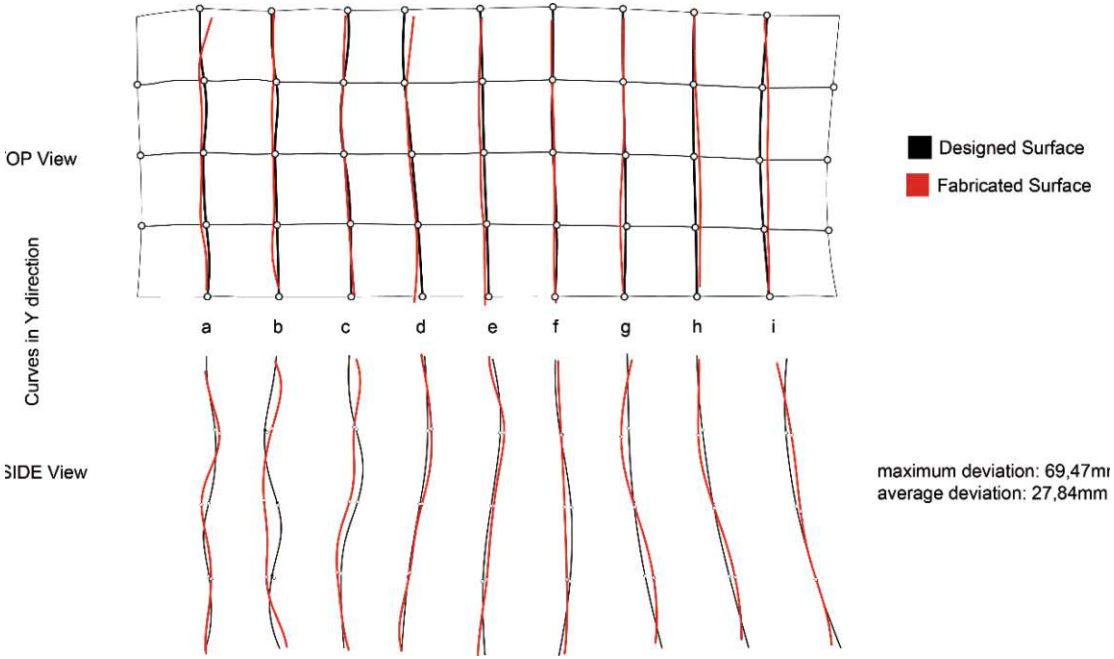

Figure 122: design exploration – evaluation of extracted edges – Y-direction

Die approbierte gedruckte Originalversion dieser Diplomarbeit ist an der TU Wien Bibliothek verfügbar
The approved original version of this thesis is available in print at TU Wien Bibliothek.

Die approbierte gedruckte Originalversion dieser Diplomarbeit ist an der TU Wien Bibliothek verfügbar
The approved original version of this thesis is available in print at TU Wien Bibliothek.

7. Conclusion

This chapter summarizes the conclusions drawn from the material, unit and tiling explorations, discussing the observed parameters and insights gained to enable control over the geometry and edge curvature of active textiles. Furthermore, it evaluates the statement that active textile components can be effectively utilized to create tiled surfaces.

The application of findings from chapters 4 and 5 in efforts to replicate a digitally designed surface is assessed, with a discussion on curvature control in larger tiled surfaces. Finally, the chapter concludes by outlining the limitations of the current study and suggesting directions for future research

Die approbierte gedruckte Originalversion dieser Diplomarbeit ist an der TU Wien Bibliothek verfügbar
The approved original version of this thesis is available in print at TU Wien Bibliothek.

Unit and tiling exploration

The fabrication methods outlined in chapter 4 demonstrate promising results in controlling edge curvature in the produced tiles and highlight a notable variety of achievable geometries. Using the proposed fabrication setup, uniform stretching with linear actuators and clamps has proven to be a reliable and repeatable production method. By maintaining uniform pre-stretching and printing thickness (chapter 4.1), a controlled gradation in the resulting tile curvature can be achieved by varying one of these parameters. This variation is constrained by the inherent properties of the chosen textile, which limits the degree of pre-stretching, and by the achievable layer height of the 3D printing setup. However, these limitations did not pose significant challenges during the production of tiled surfaces.

Modifications to the fabrication methods described in chapters 4.2 and 4.3 significantly expand the range of geometries that can be produced using active textile tiles. The non-uniform stretching approach shows potential for improving control over edge curvatures, but the pointwise clamping mechanism currently represents the weakest aspect of the setup in terms of repeatability, control, and efficiency. Interestingly, the experiments on tiled surfaces revealed no critical need for non-uniformly stretched tiles, as other methods effectively addressed similar requirements. For instance, employing non-uniform printing thickness at the tile boundaries circumvents the downsides of non-uniform stretching, leveraging the repeatability of uniform stretching and linear clamping while enabling more refined control over edge curvature. The incorporation of hinges offered limited control over the resulting geometrical features of the tiles, yet the tiling explorations confirmed their value in the fabrication repertoire. Hinges allow for local curvature changes by introducing "crease lines," adding versatility to the material system.

The thesis successfully verified the core hypothesis that active textiles can be used to create tiled double curved surfaces. The flexibility of the proposed material system proved instrumental, particularly with the "opposing edges" combination method introduced in chapter 5.1. This method became crucial for fabricating tiled surfaces that remain in one plane, leveraging the material's inherent adaptability. Recognizing the orientation of adjacent tiles as a critical parameter for tiling surfaces of active textiles was essential for fabricating tiled surfaces. Case study surfaces produced in sections 5.2.1 and 5.2.2 exhibited uniform activation across the entire surface, highlighting a

Die approbierte gedruckte Originalversion dieser Diplomarbeit ist an der TU Wien Bibliothek verfügbar
The approved original version of this thesis is available in print at TU Wien Bibliothek.

strong interdependence between individual tiles and the global surface system. While the overall curvature appeared well-controlled, a notable issue emerged at the exposed edges where tiles lacked further connections, this was particularly evident with the designed display. A double layer system is hypothesized to mitigate this issue by increasing system rigidity, though further investigation is needed to confirm this assumption.

Design exploration

As outlined in chapter 6, the primary objective was to validate the concept of tiled surfaces using active textiles and assess the scalability of curvature control across larger areas. This goal was achieved through the conducted test, which produced results consistent with those in sub-chapters 5.2.1 and 5.2.2, with again reduced control over the tiles at the surface edges. Trying a top-down process with a digitally designed surface to be replicated was a way to see if the gathered knowledge from all previously conducted experiments can be applied. It became clear that the collected data is somewhat subjective and not universally applicable, as much of the understanding stemmed from tacit knowledge acquired through hands-on experimentation with the material system. Nevertheless, the proposed system demonstrates a fast and intuitive method for fabricating (or replicating) double curved tiled surfaces. While precision was not a primary goal, the accuracy of the recreated surface was encouraging, suggesting that this process merits further exploration.

Although general statements regarding the proposed system can be made, at present, the findings are specific to the materials and fabrication parameters used in this research. Further investigations are necessary to expand the applicability and refine the process. Furthermore, while the flexibility of the proposed system is a significant advantage, it may also pose challenges for future applications, highlighting the need for further research into improving rigidity as a key area of focus as described in “Further Steps”.

Die approbierte gedruckte Originalversion dieser Diplomarbeit ist an der TU Wien Bibliothek verfügbar
The approved original version of this thesis is available in print at TU Wien Bibliothek.

Limitations

The limitations of the material system, briefly discussed in the previous section, are partially linked to constraints in the structure, timeframe, and methodology of the presented work. Advancing from initial material experiments to tiled surfaces required focusing on a single material combination and a fixed tile geometry. As a result, the findings are specific to the fabric and PLA used, with only square tiles being analyzed. Additionally, the limited sample size of material experiments was influenced by time constraints.

The methods used to collect and process data for evaluating the fabricated tiles and surfaces also have limitations, particularly in terms of accuracy and the volume of data obtained. For example, extending the evaluation process to include measurements of the actual forces used to pre-stretch the textile or residual forces stored in activated tiles could provide more comprehensive insights. Such data could potentially be adapted for use with other textiles or membranes.

Finally, the design-to-fabrication workflow relies partly on tacit knowledge gained through material experimentation. Further evaluation is needed to convert this subjective knowledge into objective data, enabling more efficient and reproducible fabrication of desired double curved surfaces.

Die approbierte gedruckte Originalversion dieser Diplomarbeit ist an der TU Wien Bibliothek verfügbar
The approved original version of this thesis is available in print at TU Wien Bibliothek.

Further steps

Future research opportunities can be categorized into two areas: a) the digital realm and b) the physical realm.

On the digital side, further investigation is needed into the process of translating a digitally designed surface into specific fabrication parameters. This could involve developing evaluation, simulation, and optimization routines to reliably predict the behavior of the global surface system and automatically generate appropriate fabrication parameters. Additionally, continued exploration of the material system could provide the data necessary to advance these digital processes.

On the physical side, research into alternative material combinations, double layer systems, or treatments such as tile coatings could address the flexibility challenges of the current system, offering solutions for enhancing rigidity and broadening its potential applications. Exploring variations in tile geometries could also expand the design possibilities, enabling more diverse and complex surface configurations.

Die approbierte gedruckte Originalversion dieser Diplomarbeit ist an der TU Wien Bibliothek verfügbar
The approved original version of this thesis is available in print at TU Wien Bibliothek.

Die approbierte gedruckte Originalversion dieser Diplomarbeit ist an der TU Wien Bibliothek verfügbar
The approved original version of this thesis is available in print at TU Wien Bibliothek.

References

Die approbierte gedruckte Originalversion dieser Diplomarbeit ist an der TU Wien Bibliothek verfügbar
The approved original version of this thesis is available in print at TU Wien Bibliothek.

Adriaenssens, S., Block, P., Veenendaal, D., & Williams, C. (2014). *Shell Structures for Architecture: Form Finding and Optimization.* Routledge.

Aldawood, F. K. (2023). A Comprehensive Review of 4D Printing: State of the Arts, Opportunities, and Challenges. *actuators.*

Aldinger, L., Margariti, G., Körner, A., Suzuki, S., & Knippers, J. (2018). Tailoring Self-Formation fabrication and simulation of membrane-actuated stiffness gradient composites. *IASS Symposium.* Boston.

AMA: architectural membraneassociation. (2024, 11 17).

Andreoletti, A., & Rzezonka, A. (2016). Designing with Matter: From Programmable Materials to Processual Things. *CITAR Journal.*

Berdos, Y., Agkathidis, A., & Brown, A. (2020). Architectural hybrid material composites: computationally enabled techniques to control form generation. *Architectural Science Review.*

Bhagat, P. H., & Gursoy, B. (2022). Stretch-3D Print-Release: Formal descriptions of shape-change in 3D printed shapes on stretched fabric. *eCAADe.*

Casta˜neda, E., Lauret, B., Lirola, J., & Ovando, G. (2015). Free-form architectural envelopes: Digital processes opportunities of industrial production at a reasonable price. *Journal of Facade Design and Engineering.*

Chilton, J. (2010). Heinz Isler's Infinite Spectrum: Form-Finding in Desig. *Architectural Design, 80*(4), 64-71.

Enriquea, L., Cepaitisb, P., Ordóñezc, D., & Pilesd, C. (2016). CASTonCAST: Architectural freeform shapes from precast stackable components. *VLC arquitectura.*

Fassade aus Sonnensegeln mit integrierter Illumination. (2014, Dezember 08). *Detail.*

Die approbierte gedruckte Originalversion dieser Diplomarbeit ist an der TU Wien Bibliothek verfügbar
The approved original version of this thesis is available in print at TU Wien Bibliothek.

flickr. (n.d.). Retrieved 11 21, 2024, from https://www.flickr.com/photos/monicaandlydia/3966312923

Fu, J. (2019, August 13). *Linked in*. Retrieved from https://www.linkedin.com/pulse/types-working-principle-membrane-structure-judy-fu

Gengnagel, C. (2005). *Mobile Membrankonstruktionen, Schriftenreihe des Lehrstuhls für Tragwerksplanung*. München.

Interdesign. (n.d.). Retrieved 11 17, 2024, from https://interdesign.co.id/products-services/intrino-stretch-membrane/

Janbaz, S., Hedayati, R., & Zadpoor, A. (2016). Programming the shape-shifting of flat soft matter: from self-rolling/self-twisting materials to self-folding origami. *Mater. Horiz.*

Jourdan, D., Skouras, M., Vouga, E., & Bousseau, A. (2020). Printing-on-fabric meta-material for self-shaping architectural models. *Advances in Architectural Geometry*.

Kima, K., Sonb, K., Kimb, E.-D., & Kima, S. (2015). Current trends and future directions of free-form building technology. *Architectural Science Review*.

Koch, H. C., Schmelzeisen, D., & Gries, T. (2021). 4D Textiles Made by Additive Manufacturing on Pre-Stressed Textiles—An Overview. *actuators*.

Lettner, S., Palma, M., & Baseta, E. (2024). Towards the control of doubly curved active textiles through graded pre-stretching and 3D printing. *Proceedings of the IASS 2024 Symposium*. Zürich.

Liu, Y., Genzer, J., & Dickey, M. (2016). "2D or not 2D": Shape-programming polymer sheets. *Prog. Polym. Sci.*

Mamou-Mani, A. (2021). *Mamou-Mani*. Retrieved 11 17, 2024, from https://mamou-mani.com/project/orange-hq-woodenwaves/

Manen, T. v., Janbaz, S., & Zadpoor, A. (2018). Programming the shape-shifting of flat soft matter. *Mater. Today*.

Die approbierte gedruckte Originalversion dieser Diplomarbeit ist an der TU Wien Bibliothek verfügbar
The approved original version of this thesis is available in print at TU Wien Bibliothek.

Mitchell, A., Lafont, U., Hołyńska, M., & Semprimoschnig, C. (2018). Additive manufacturing — A review of 4D printing and future applications. *Additive Manufacturing*.

Modes, C., & Warner, M. (2016). Shape-programmable MATERIALS. *Phys. Today*.

Momeni, F., Hassani.N, S. M., Liu, X., & Ni, J. (2017). A review of 4D printing. *Materials and Design*.

Nam, S., & Pei, E. (2019). A taxonomy of shape-changing behavior for 4D printed parts using shape-memory polymers. *Progr. Addit. Manuf.* .

nedcam : shaping technology. (n.d.). Retrieved 11 16, 2024, from https://nedcam.com/produkte-und-dienstleistungen/cnc-fraesen/?lang=de

Olbrechts, B. (2023, Januar 31). On-demand digital sheet forming. *sirris: innovation forward*.

Palma, M. (2024, Juli 01). ,rs_gh. , Juli 01, 2024. *Zenodo*.

Pastor, L. A., Lauret, B., Vergara, E. C., & Aguirregabiria, D. D. (2012). Free-Form Architectural Facade Panels: An Overview of available Massproduction. *International Conference on Construction and Building Research*. Velncia.

Pei, E., & Loh, G. (2018). Technological considerations for 4D printing: An overview. *Prog. Addit. Manuf.*

PERI. (n.d.). Retrieved 11 16, 2024, from https://www.peri.at/produkte/freiformschalungen.html#vorteile

Pottmann, H., Asperl, A., Hofer, M., & Kilian, A. (2010). *Architectural Geometry*. Springer & Bentley Institute Press.

Puza, F., & Lienkamp, K. (2022). 3D printing of polymer hydrogels - from basic techniques to programmable actuation. *Adv. Funct. Mater.*

Raun, C., & Kirkegaard, P. H. (2015). Adaptive mould - A cost-effective mould system linking design and manufacturing of double-curved GFRC panels. *GRC*. Dubai.

Scalet, G. (2024). Programmable materials: Current trends, challenges, and perspectives. *Applied Materials Today*.

Die approbierte gedruckte Originalversion dieser Diplomarbeit ist an der TU Wien Bibliothek verfügbar
The approved original version of this thesis is available in print at TU Wien Bibliothek.

Schipper, R., & Janssen, B. (2011). Manufacturing double-curved elements in precast concrete using a flexible mould: First experimental results. *fib Symposium.* Prague.

Scott System. (n.d.). Retrieved 11 16, 2024, from https://www.scottsystem.com/formwork/manufacturing/

Self-Assembly Lab. (n.d.). Retrieved 11 13, 2024, from https://selfassemblylab.mit.edu/active-shoes

Sitotaw, D. B., Ahrendt, D., Kyosev, Y., & Kabish, A. K. (2020). Additive manufacturing and textiles—state-of-the-art. *Applied Sciences.*

Tamke, M., Baranovskaya, Y. S., Monteiro, F., Lienhard, J., Magna, R. L., & Thomsen, M. R. (2020). Computational knit – design and fabrication systems for textile structures with customised and graded CNC knitted fabrics. *Architectural Engineering and Design Management.*

Tibbits, S. (2021). *Things Fall Together : a guide to the new materials revolution.* Princeton: Princeton University Press.

Tibert, A. G., & Pellegrino, S. (2011). Review of Form-Finding Methods for Tensegrity Structures. *International Journal of Space Structures, 26*(3), 241-255.

Vivanco, T., Valencia, A., & Yuan, P. F. (2020). 4D Printing: Computational mechanical design of Bi-Dimensional 3D-Printed patterns over tensioned textiles for low-energy three-dimensional volumes. *CAADRIA.*

TU WIEN Bibliothek Your knowledge hub
Die approbierte gedruckte Originalversion dieser Diplomarbeit ist an der TU Wien Bibliothek verfügbar
The approved original version of this thesis is available in print at TU Wien Bibliothek.

Die approbierte gedruckte Originalversion dieser Diplomarbeit ist an der TU Wien Bibliothek verfügbar
The approved original version of this thesis is available in print at TU Wien Bibliothek.

Bibliography

Die approbierte gedruckte Originalversion dieser Diplomarbeit ist an der TU Wien Bibliothek verfügbar
The approved original version of this thesis is available in print at TU Wien Bibliothek.

Figure 1: active textile fabrication procedure as developed by the Self-Assembly Lab at MIT (Self-Assembly Lab, n.d.) 10
Figure 2: diagram of the developed fabrication procedure 12
Figure 3: tangent (t) in point (p) on curve (c) 17
Figure 4: Osculating circle in point (p)on curve (c) with radius (r) 18
Figure 5: vertices of curve (c) 19
Figure 6: inflection point (p) of curve (c) 19
Figure 7: control points of curve (c) highlighted 20
Figure 8: Gaussian curvature analysis illustrated as color graded map 21
Figure 9: Peri – double curved formwork system for concrete structures (PERI,) 24
Figure 10: 3D milling process for a mold made from a block of foam (nedcam : shaping technology, n.d.), (Scott System, n.d.) 25
Figure 11: left: digital sheet forming (Olbrechts, 2023), middle: corian forming process (Pastor, Lauret, Vergara, & Aguirregabiria, 2012), right: 2D milled plywood sheets (Mamou-Mani, 2021) 26
Figure 12: left: membrane and sub-structure (Fu, 2019), middle: interior ceiling design (Interdesign, n.d.), Right: Membranes used as building facade (Fassade aus Sonnensegeln mit integrierter Illumination, 2014) 27
Figure 13: fabrication principle of ADAPA mold (Raun & Kirkegaard, 2015) 28
Figure 14: left: stacks created with the CASTonCAST method, right: fabricated surface (Enriquea, Cepaitisb, Ordóñezc, & Pilesd, 2016) 29
Figure 15: project Isoropia using flexible textiles to generate a double curved structure (Tamke, et al., 2020) 30
Figure 16: illustration of basic principle behind programmable materials. 32
Figure 17: types of programmable materials, left: self-transformation, right: self-assembly (Self-Assembly Lab, n.d.) 33
Figure 18: matrix of deformation types in shape changing materials. (Scalet, 2024) 35
Figure 19: shape-changing system created with a 4D printing process at MIT. (Self-Assembly Lab, n.d.) 36
Figure 20: illustration of shape change in active textiles (Vivanco, Valencia, & Yuan, 2020) 38
Figure 21: fabrication process of active textiles in prior research (Koch, Schmelzeisen, & Gries, 2021) 40

Die approbierte gedruckte Originalversion dieser Diplomarbeit ist an der TU Wien Bibliothek verfügbar
The approved original version of this thesis is available in print at TU Wien Bibliothek.

Figure 22: rapid prototyping of shell structures with active textiles (Jourdan, Skouras, Vouga, & Bousseau, 2020) 42
Figure 23: shift in material system for large scale tests (Aldinger, Margariti, Körner, Suzuki, & Knippers, 2018) 42
Figure 24: top: individual tile, bottom: tiled surface exploration 44
Figure 25: diagram of initial fabrication technique used to produce active textile tiles 47
Figure 26: manual pre-stretching with tape used for clamping 48
Figure 27: left: parchment making technique (flickr, n.d.) right: inspired wooden frame for textile pre-stretching 48
Figure 28: using a FDM 3D printer with a pre-stretched piece of fabric fixed to the print bed 49
Figure 29: resulting pieces from the initial fabrication process 49
Figure 30: digital model of custom printing rig 50
Figure 31: left: first iteration of a baseplate for numerically controlled textile pre-stretching, right: layout of electronics used to control the amount of pre-stretching 52
Figure 32: digital model, left: custom-built base plate, right: 3D printing set-up 52
Figure 33: illustration of the individual parts of the printing system 54
Figure 34: left: programs used to modify the printer firmware, right: actual electronic components 55
Figure 35: left: revised version of ground plate added to the fabrication set-up, right: full view of custom hardware 57
Figure 36: left: pointwise clamping mechanism with individual pins, right: linear clamping mechanism 57
Figure 37: completed custom-built fabrication set-up at the modelbuilding workshop 58
Figure 38: diagram of fabrication workflow from digital input to physical output 59
Figure 39: fabrication workflow: stretch – 3D print – release and post-printing procedure 60
Figure 40: preparation of fabric pieces for printing 64
Figure 41: 3D printing filament used for all experiments 64
Figure 42: left: static scanning procedure with Intel RealSense L515 LiDAR camera, right: point cloud generated in the Grasshopper environment 66
Figure 43: evaluation routine, focused on the aspect of digital point cloud processing 66
Figure 44: visualization of uniform pre-stretching and linear clamping. 67
Figure 45: resulting tiles with increasing amounts of stretching. 68

Die approbierte gedruckte Originalversion dieser Diplomarbeit ist an der TU Wien Bibliothek verfügbar
The approved original version of this thesis is available in print at TU Wien Bibliothek.

Figure 46: resulting tiles with increasing 3D printed boundary height and 25% pre-stretching. 69
Figure 47: matrix of all fabricated tiles with parameters tested in sub-chapter 4.1. 70
Figure 48: variable parameters of pre-stretching - top: z-displacement evaluation of point cloud, bottom: Gaussian curvature analysis of N.U.R.B.S. surface 71
Figure 49: variable parameters of 3D printed boundary height - top: z-displacement evaluation of point cloud, bottom: Gaussian curvature analysis of N.U.R.B.S. surface 72
Figure 50: edge evaluation - top: tiles with changing amount of pre-stretching, bottom: tiles with increase in 3D printed boundary thickness 73
Figure 51: graph mapping curvature of the evaluated tile edge to the fabrication parameters 74
Figure 52: graph mapping z-displacement of the evaluated tile edge to the fabrication parameters 74
Figure 53: three corresponding tiles marked in figure 47 - top: z-displacement evaluation of point cloud, bottom: Gaussian curvature analysis of N.U.R.B.S. surface 75
Figure 54: edge evaluation of the three corresponding tiles marked in figure 47 75
Figure 55: resulting tiles - uniform pre-stretching (25%) and uniform boundary cross sections 76
Figure 56: repeatability test - uniform stretching and uniform printing thickness – top: z-displacement evaluation of point cloud, bottom: Gaussian curvature analysis of N.U.R.B.S. surface 77
Figure 57: repeatability test - analysis of edges 77
Figure 58: visualization of non-uniform pre-stretching and pointwise clamping 79
Figure 59: produced tiles – non-uniform pre-stretching top: repeatability test, bottom: test with variable pre-stretching parameter and resulting curvature 79
Figure 60: repeatability test – non-uniform pre-stretching– top: z-displacement evaluation of point cloud, bottom: Gaussian curvature analysis of N.U.R.B.S. surface 80
Figure 61: variable parameter of pre-stretching – non-uniform pre-stretching– top: z-displacement evaluation of point cloud, bottom: Gaussian curvature analysis of N.U.R.B.S. surface 81
Figure 62: non-uniform pre-stretching - left: edge analysis, right: graph mapping curvature to amount of pre-stretch 81
Figure 63: visualization of non-uniform boundary cross section 82
Figure 64: produced tiles – non-uniform boundary cross section, top: repeatability test, bottom: test with variable boundary cross section parameter and resulting curvature 83

Die approbierte gedruckte Originalversion dieser Diplomarbeit ist an der TU Wien Bibliothek verfügbar
The approved original version of this thesis is available in print at TU Wien Bibliothek.

Figure 65: repeatability test – non-uniform boundary cross section – top: z-displacement evaluation of point cloud, bottom: Gaussian curvature analysis of N.U.R.B.S. surface 84
Figure 66: variable parameter of boundary cross section – non-uniform boundary cross section– top: z-displacement evaluation of point cloud, bottom: Gaussian curvature analysis of N.U.R.B.S. surface 84
Figure 67: non-uniform boundary cross section - top: analysis of edges, bottom: graph mapping curvature to cross section thickness 85
Figure 68: hinge design in Rhinoceros 3D 86
Figure 69: different hinge-designs tested for function 88
Figure 70: resulting tiles - different hinge placements - adding 1 – 4 hinges 88
Figure 71: different hinge placements– top: z-displacement evaluation of point cloud, bottom: Gaussian curvature analysis of N.U.R.B.S. surface 89
Figure 72: different hinge placements - diagram of direction of edge curvature in relation to one another 90
Figure 73: scanning procedure with Intel RealSense L515 LiDAR camera and the aid of a 6-axis collaborative robot 93
Figure 74: matrix of combination tests done on one edge 95
Figure 75: matrix of subset of combination test: matching edges 96
Figure 76: matching edges – combinations - top: z-displacement evaluation of point cloud, bottom: Gaussian curvature analysis of N.U.R.B.S. surface 97
Figure 77: matching edges combinations – diagram of adjacent curves and shared edge curves 98
Figure 78: matching edges combinations – graph of curvature at high point of section curves 98
Figure 79: matrix of subset of combination test: opposing edges 100
Figure 80: opposing edges – combinations - top: z-displacement evaluation of point cloud, bottom: Gaussian curvature analysis of N.U.R.B.S. surface 100
Figure 81: opposing edges combinations – diagram of adjacent curves and shared edge curves 101
Figure 82: opposing edges combinations – graph of curvature at high point of section curves 101
Figure 83: collage of further connected tiles – left: opposing edges, right: matching edges 102
Figure 84: matrix of combination test done on multiple edges 104
Figure 85: order of attachment – multiple edge test 104
Figure 86: left: initial evaluation of the tile A, right: evaluation of tile A in order of attachment - top: z-displacement evaluation of point cloud, bottom: Gaussian curvature analysis of N.U.R.B.S. surface 105

Die approbierte gedruckte Originalversion dieser Diplomarbeit ist an der TU Wien Bibliothek verfügbar
The approved original version of this thesis is available in print at TU Wien Bibliothek.

Figure 87: multiple edge combination – diagram of adjacent curves before and after combination 105
Figure 88: preview of assambled 3x3 surface 106
Figure 89: evaluation 3x3 surface - left: z-displacement evaluation of point cloud, right: Gaussian curvature analysis of N.U.R.B.S. surface 107
Figure 90: 3x3 surface – evaluation of combined edges of the surface 108
Figure 91: finished 3x3 surface on custom built display 109
Figure 92: preview of assembled 4x4 surface 111
Figure 93: evaluation of the 4x4 surface - left: z-displacement evaluation of point cloud, right: Gaussian curvature analysis of N.U.R.B.S. surface 112
Figure 94: 4x4 surface – evaluation of combined edges of the surface 113
Figure 95: finished 4x4 surface on custom built display 114
Figure 96: matrix of double layer structure test 115
Figure 97: double layer structure test, left: single tile, right: double layer with B matching edge and C opposing edge combination - top: z-displacement evaluation of point cloud, bottom: Gaussian curvature analysis of N.U.R.B.S. surface 116
Figure 98: double layer – edge evaluation, top: matching edges, bottom: opposing edges combined 116
Figure 99: designed surface - highlighted areas with connection to case study surfaces 119
Figure 100: simplification of the digital design process 120
Figure 101: matrix of digital design process No. 1 121
Figure 102: matrix of digital design process No. 2 122
Figure 103: matrix of digital design process No. 3 123
Figure 104: final digital design of the design exploration model 124
Figure 105: design exploration surface - left: z-displacement evaluation of point cloud, right: Gaussian curvature analysis of N.U.R.B.S. surface 124
Figure 106: considerations for assigning fabrication parameters, direct effect (bold black) to low influence (light) 125
Figure 107: color graded map - overview of parameter families assigned to the tiles of the digital surface 127
Figure 108: detailed map of fabrication parameters of each tile 127
Figure 109: color graded map - overview of assigned orientation to the tiles of the digital surface 129

Die approbierte gedruckte Originalversion dieser Diplomarbeit ist an der TU Wien Bibliothek verfügbar
The approved original version of this thesis is available in print at TU Wien Bibliothek.

Figure 110: detailed map of the orientation of tiles according to the direction of edges of their neighbors 129
Figure 111: working place at the modelbuilding workshop at the TU Wien 130
Figure 112: fabrication steps of individual tiles – textile preparation 131
Figure 113: fabrication steps of individual tiles – actual 4D printing 132
Figure 114: assembly process of design exploration model 134
Figure 115: final design exploration model No. 1 135
Figure 116: final design exploration model No. 2 136
Figure 117: fabricated surface deviation from designed surface – left: surface from point cloud, right: surface from edge curves 137
Figure 118: digitally designed surface - left: z-displacement evaluation of point cloud, right: Gaussian curvature analysis of N.U.R.B.S. surface 138
Figure 119: fabricated surface from point cloud - left: z-displacement evaluation of point cloud, right: Gaussian curvature analysis of N.U.R.B.S. surface 138
Figure 120: fabricated surface from edge curves - left: z-displacement evaluation of point cloud, right: Gaussian curvature analysis of N.U.R.B.S. surface 138
Figure 121: design exploration – evaluation of extracted edges – X-direction 139
Figure 122: design exploration – evaluation of extracted edges – Y-direction 140